マルチスケールモデリング・シミュレーションによる（ナノ）材料強度予測

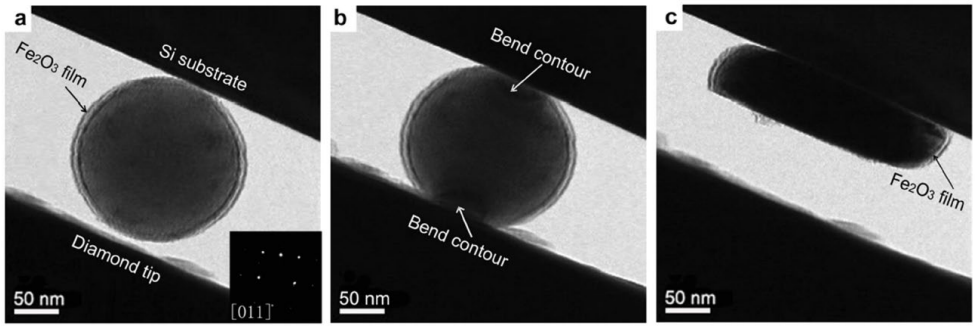

Advanced Materials **27** (2016) 3385

Shigenobu Ogata
(尾方成信）
Graduate School of Engineering Science, Osaka University
（大阪大学　基礎工学研究科）

Theoretical Solid Mechanics Lab.

Graduate School of Engineering Science
Osaka University

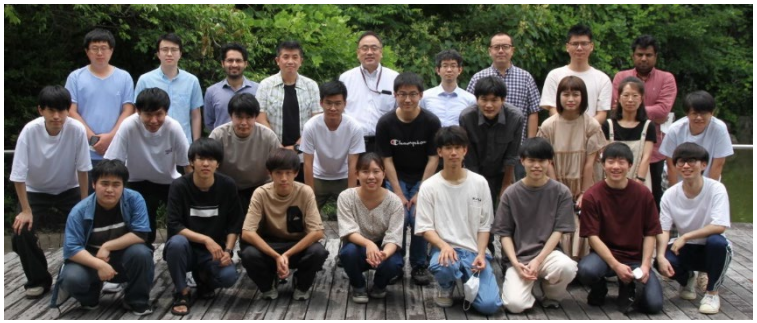

- **M**echanics of **M**aterials
- **M**aterials Science
- **M**ultiscale and **M**ultiphysics **M**odeling
- **M**achine Learning / Data Science

and ... more **M** will come ...??

大阪大学 OSAKA UNIVERSITY

ENGINEERING SCIENCE

Research Activities
- Mechanics of Materials -

TSME Theoretical Solid MEchanics
Ogata Laboratory ▶ Osaka University

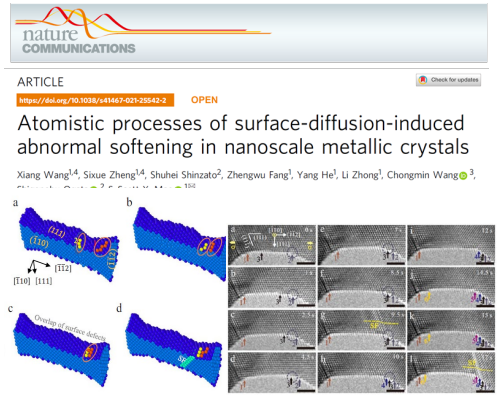

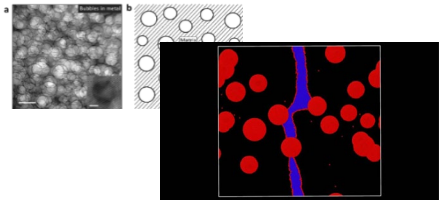

NANO LETTERS

Ming-Shuai Ding, Jun-Ping Du, Liang Wan, Shigenobu Ogata, Lin Tian, Evan Ma, Wei-Zhong Han, Ju Li, and Zhi-Wei Shan, *Nano Letters*, (2016) 4118

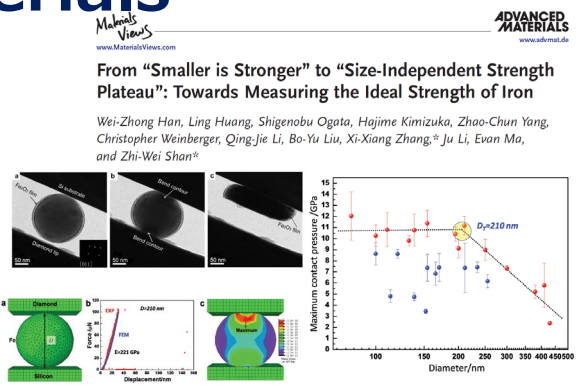

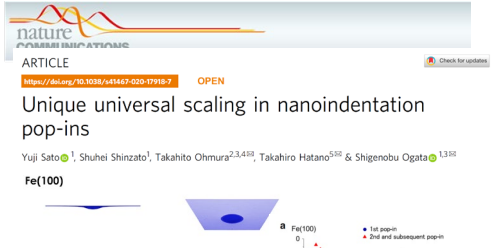

Science AAAS

Ogata et al. Science 2002

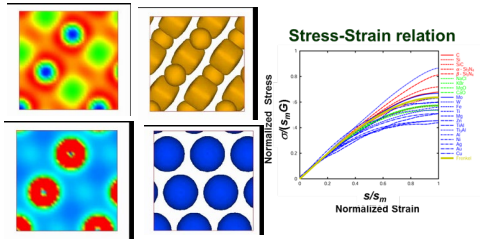

Curious materials deformation behavior at nano- and meso-scales → fundamental understanding → design new materials

TSME Theoretical Solid MEchanics
Ogata Laboratory ▶ Osaka University

Ogata Laboratory | **Osaka University**

Collaborators

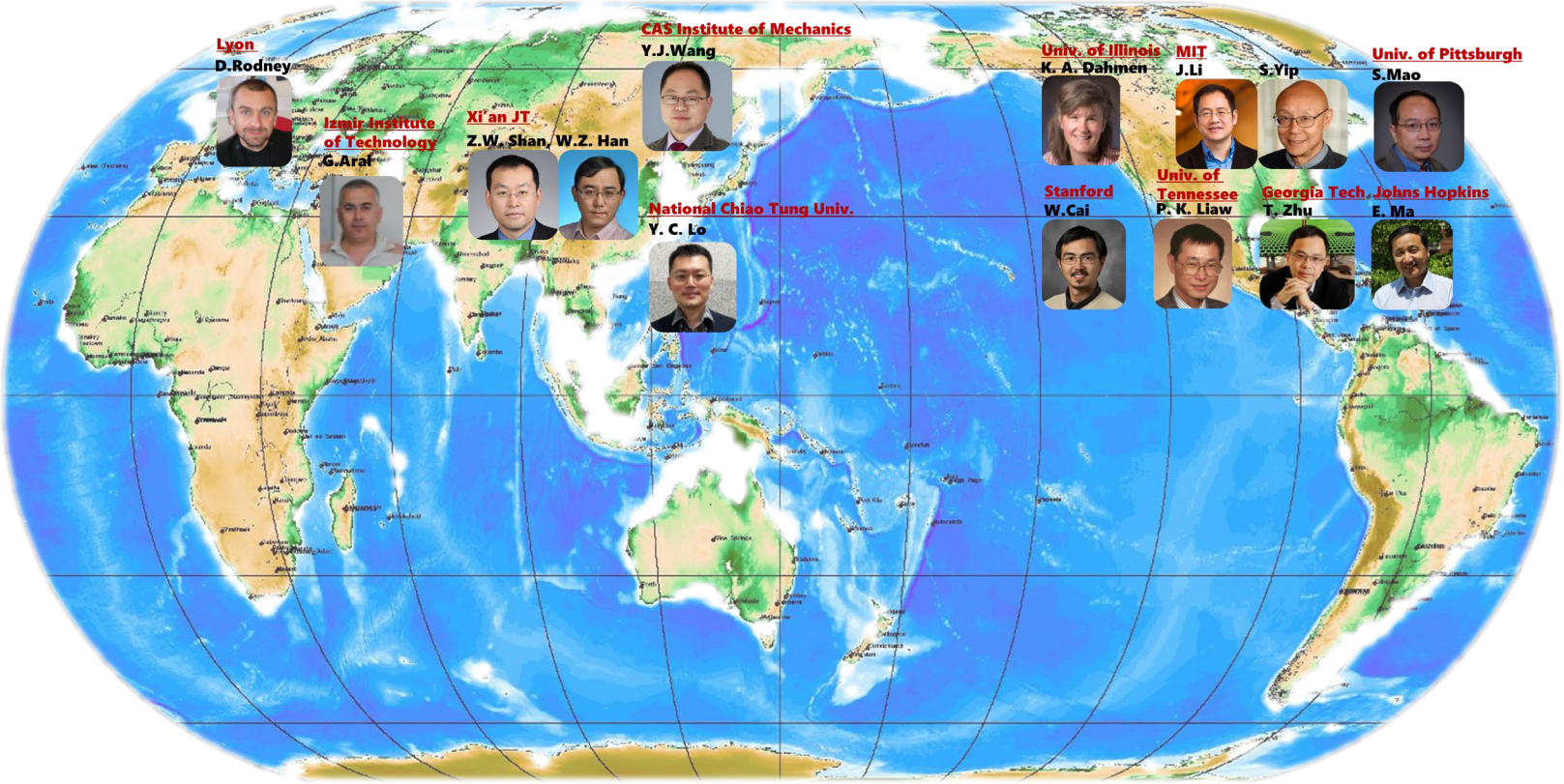

Co-Chairs

Yoji Shibutani
(Osaka Univ.)

Shigenobu Ogata
(Osaka Univ.)

Secretary

General Secretary

Tomotsugu Shimokawa
(Kanazawa Univ.)

内容

- **イントロダクション**　原子論からの材料力学特性のモデリングと材料設計　～マルチスケールの観点から
- **ナノ力学**　原子論からのナノ材料力学の特異性の検討
- **原子論における時間スケール拡張への挑戦**　原子解像度で長時間現象を予測する
- **原子論によるマルチフィジクスへの挑戦**　水素や酸素などの力学特性への影響　～力学・化学・物理
- **材料設計への展開**　強度と延性、靭性を両立した材料設計

原子論からの材料特性・機能の予測と設計

計算材料科学の大きな目標

非経験的材料設計：非経験的予測（シミュレーション）に基づく材料設計

材料・条件

（材料形態）形状　材質　組成　組織　サイズ　欠陥 …

（使用条件）変形速度　温度　力学負荷 …

予測（順問題）

- 経験的予測
- 非経験的予測

設計（逆問題）

- ひらめき
- データ科学

特性・機能

力学的（強度、延性、靭性、疲労強度）

熱的　電気的　化学的　光学的　…

構造材料の原子論からの力学特性予測の難しさ

- 非線形マルチスケール・マルチフィジクス性 -

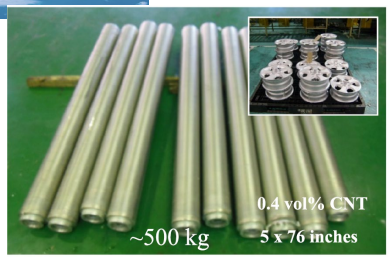

構造材料

非経験的予測・設計が最も難しい材料系

理由

1．時空間マルチスケール性
- ✓ 強いスケール間非線形相関
- ✓ 機能の起源と発現のスケールの違い

2．マルチフィジクス性
- ✓ 多様な物理現象間非線形相関

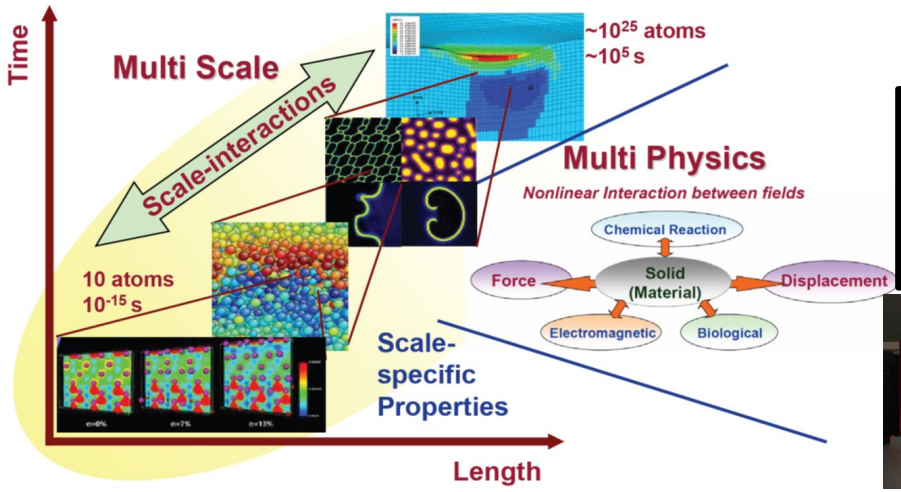

構造材料の予測と設計ができればいかなる材料の予測と設計も可能になるといっても過言ではない！

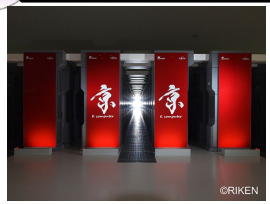

現在どこまで可能になったのか？なにが問題か？

構造材料の原子論からの力学特性予測の難しさ

- 非線形マルチスケール・マルチフィジクス性 -

実は最も基本的な応力ひずみ曲線すら予測できない！

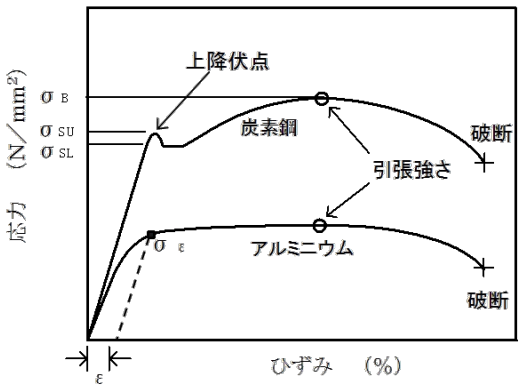

〔応力－ひずみ曲線〕

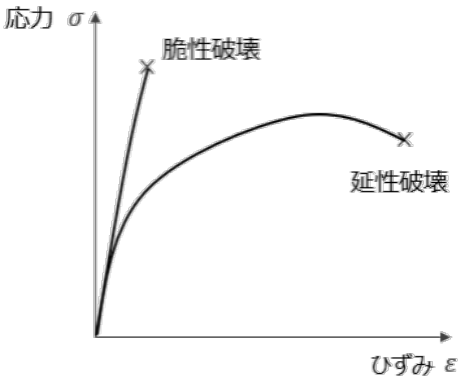

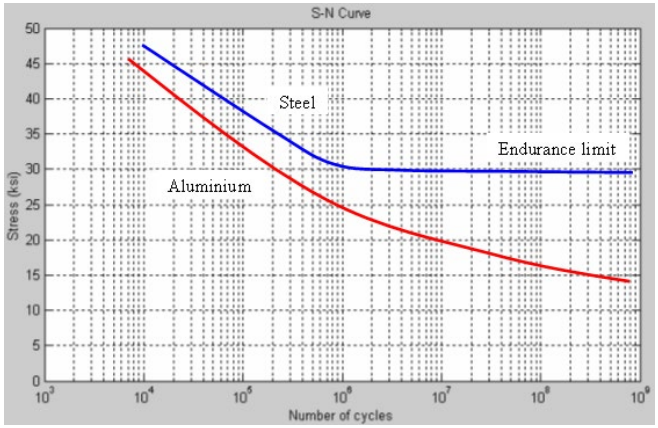

疲労のS-N曲線

（降伏応力より低い繰り返し負荷下でいつ壊れるか）

→全く予測できていない

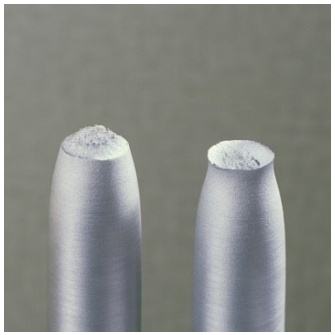

固体材料の振る舞いを実験前になんとか予測したい！！

内容

- **イントロダクション**　原子論からの材料力学特性のモデリングと材料設計　～マルチスケールの観点から
- **ナノ力学**　原子論からのナノ材料力学の特異性の検討
- **原子論における時間スケール拡張への挑戦**　原子解像度で長時間現象を予測する
- **原子論によるマルチフィジクスへの挑戦**　水素や酸素などの力学特性への影響　～力学・化学・物理
- **材料設計への展開**　強度と延性、靭性を両立した材料設計

構造材料のマクロ力学特性の根源
- 強度（変形）や破壊を支配する材料の変形素過程の解析 -

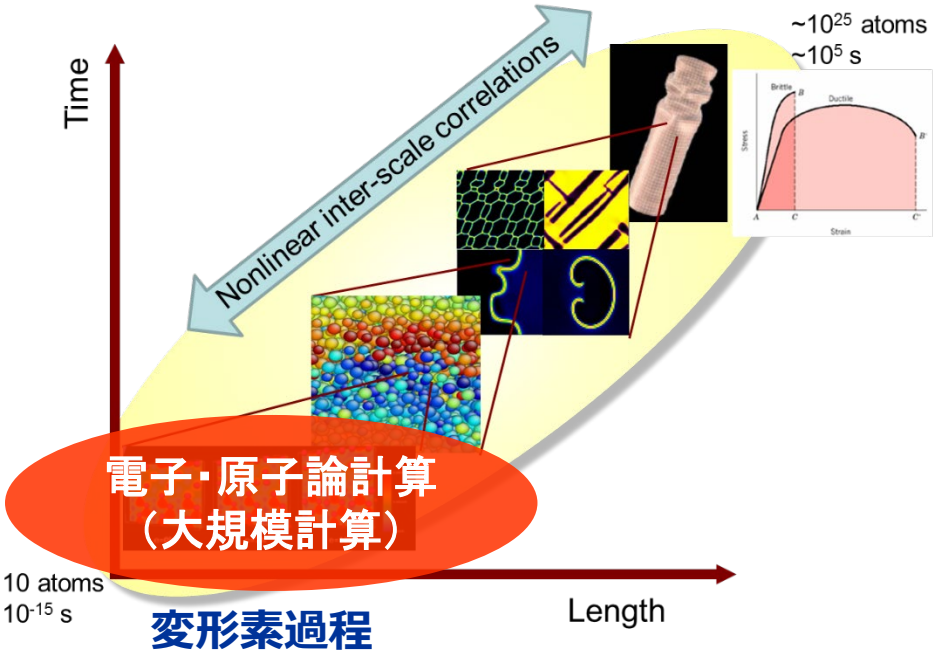

変形素過程の活動

粒内転位核生成（インデンテーション）

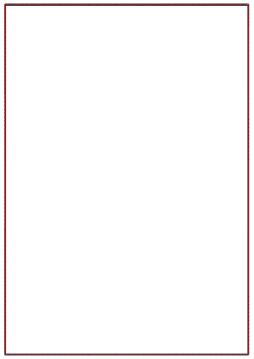

Y.Sato, S.Ogata, Acta Mater. (2022).

粒界転位核生成

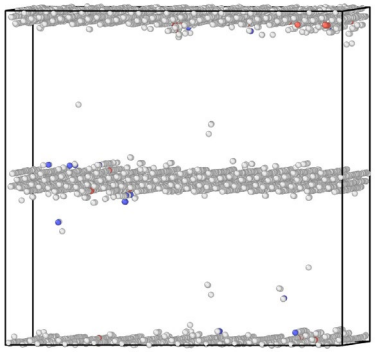

J.-P. Du, S. Ogata, et al., PRB (2016).

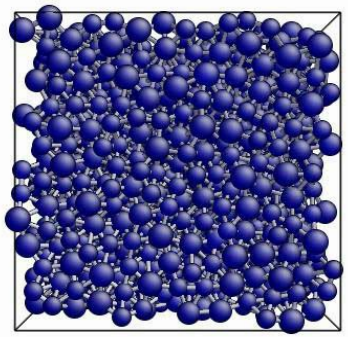

金属ガラス内せん断帯核生成

F.Shimizu, S. Ogata, et al., Mater. Trans. (2007).

◆ 電子・原子論的解析（第一原理計算、分子動力学計算、など）により変形素過程のふるまいを原理原則に基づき非経験的に予測可能

材料による靭性の違いの根源を解明

電子状態計算による応力ひずみ（負荷ー変形）関係および理想強度の予測

Affine tensile and shear deformation tests

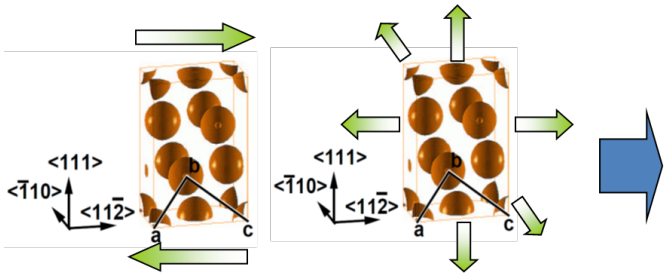

Pure shear deformation test (affine deformation)

Uniform tensile deformation test (affine deformation)

Stress-Strain relation

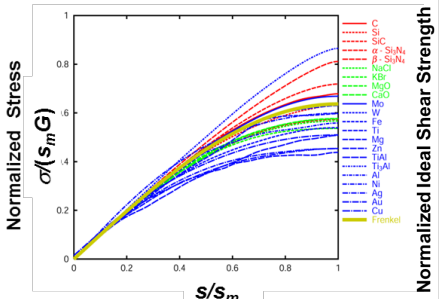

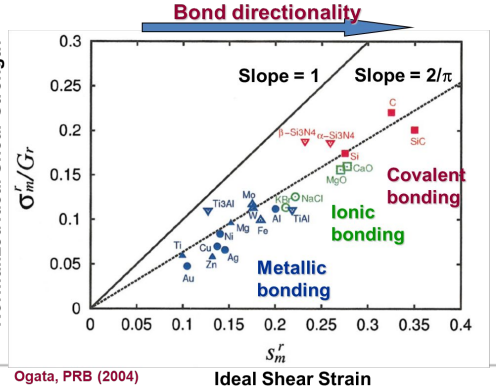

Ogata, PRB (2004)

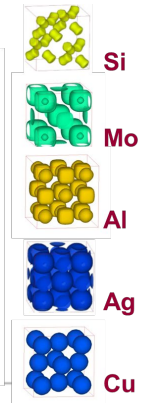

Ogata, Science (2002), PRB (2004)

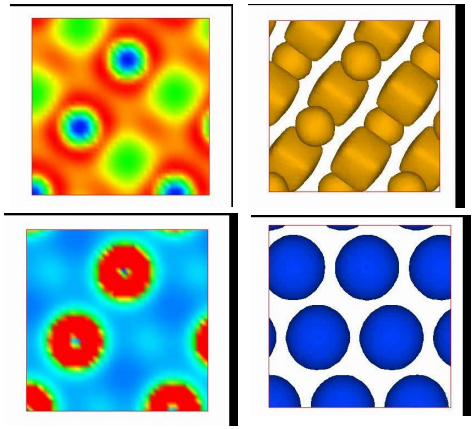

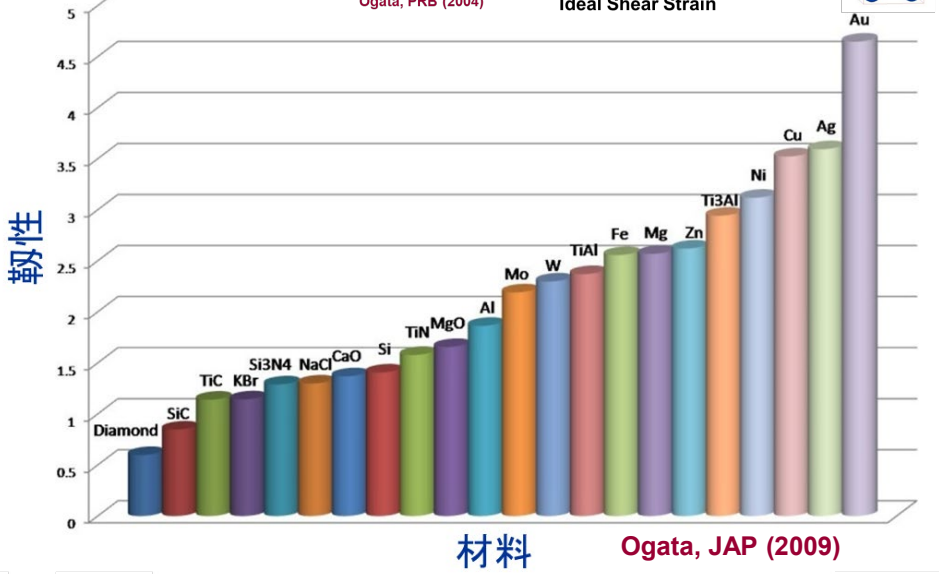

Ogata, JAP (2009)

弾性変形と塑性変形

- **Elastic deformation**
  - The most delocalized

Transition

- **Plastic deformation**
  - Very localized (atomic scale)

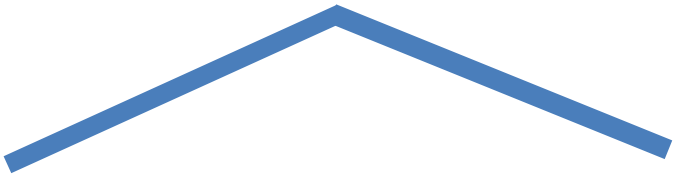

典型的な材料の強度

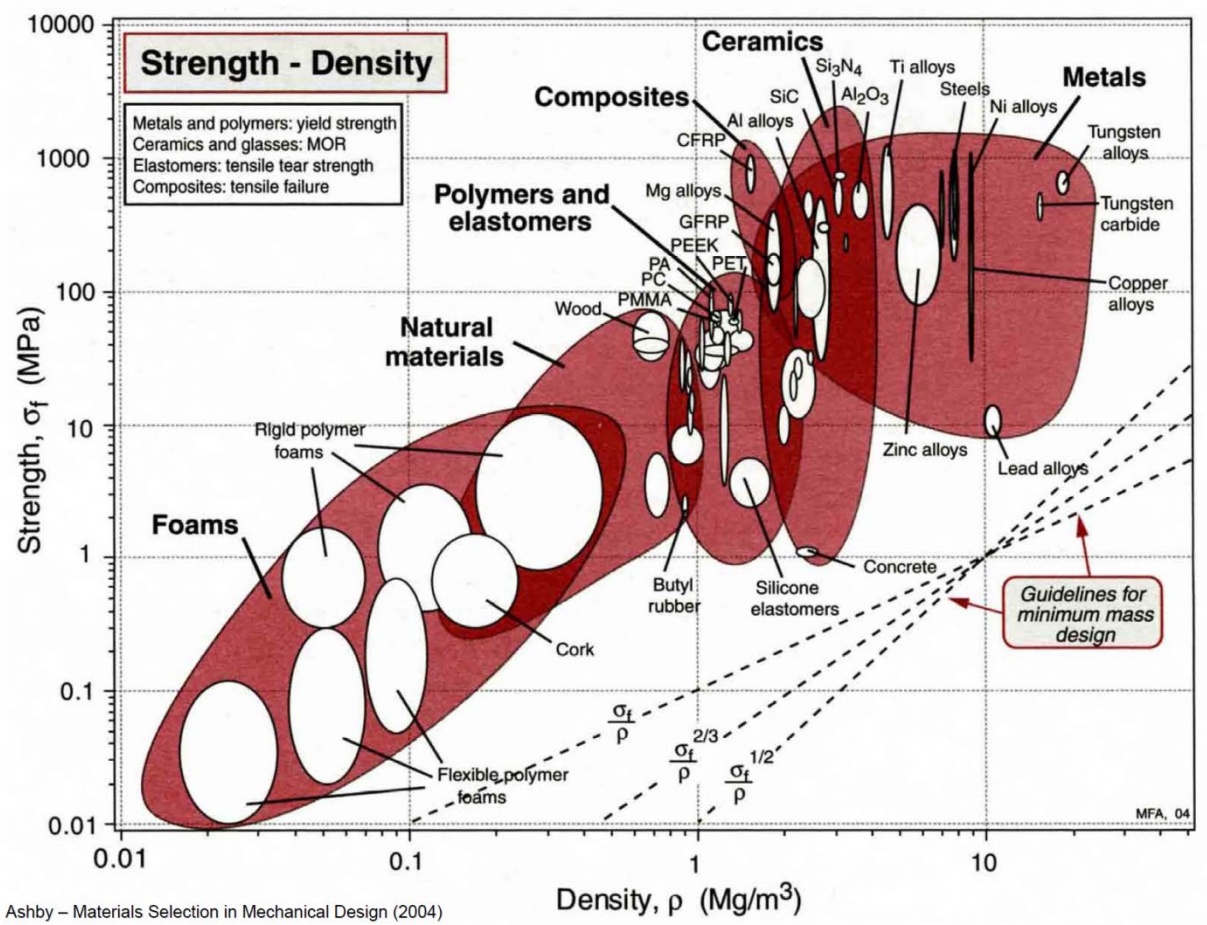

Ashby – Materials Selection in Mechanical Design (2004)

Metals:10MPa～1GPa
Ceramics:1MPa～2GPa
Polymers:1MPa～100MPa

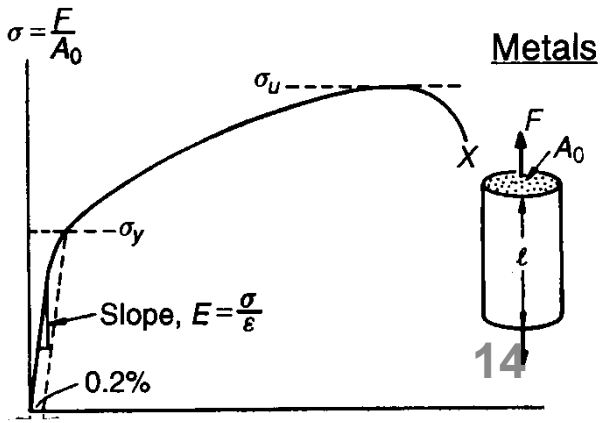

材料強度のサイズ依存性とナノ材料の強度

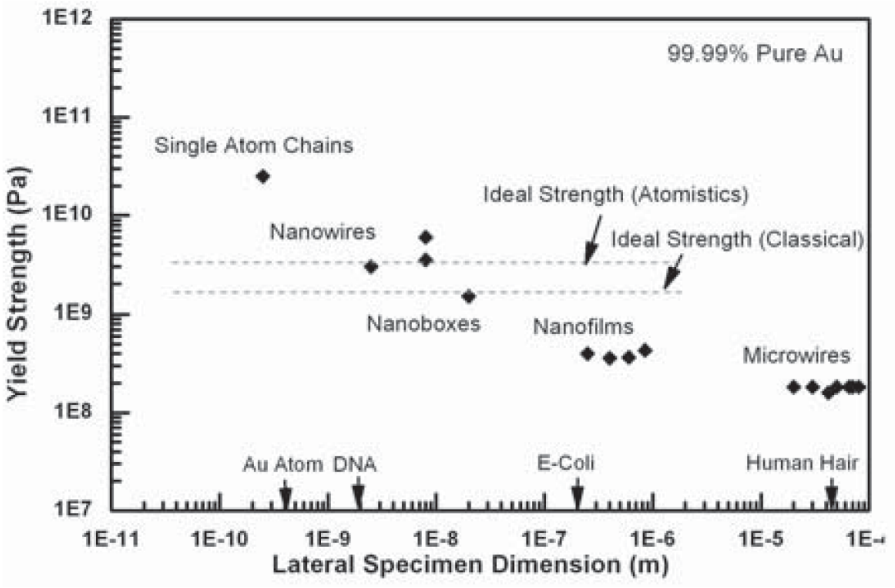

J.R.Greer, Rev.Adv.Mater.Sci. (2006)

Table I. Experimentally Measured Ultra-High Strengths.

Material	Number of Layers or Diameter (nm)	Measured Strength (GPa)	Ideal Strength ~ *E*/10 (GPa)	Reference
CNT	SW	30	100	Falvo et al.[8]
CNT	MW	30	100	Yu et al.[9]
CNT	MW	97–110	100	Peng et al.[10]
WS_2-NT	MW	3.8–16.3	15	Kaplan-Ashiri et al.[11]
ZnO-NW	30	7	14	Wen et al.[12]
Si-NW	100–200	12	17	Hoffmann et al.[13]
Ag-NW	16.5	7.3	8	Wu et al.[14]
Au-NW	40	5.6	8	Wu et al.[15]
Au-NP	300	0.8	8	Greer and Nix[16]
Au-NP	300	1	8	Volkert et al.[17]
Si-NS	20–50	20–50	17	Gerberich et al.[18]
CdS-NS	200–450	2.2	4.6	Shan et al.[19]
Graphene	ML	130	100	Lee et al.[20]

Note: CNT, carbon nanotubes; NT, nanotubes; NW, nanowires; NP, nanopillars; NS, nanospheres; ML, monolayer; SW, single-wall; MW, multi-wall; *E*, Young's modulus.

T.Zhu, J.Li, S.Ogata, S.Yip, MRS Bulletin (2009)

材料強度の組織代表寸法依存性とナノ材料の強度

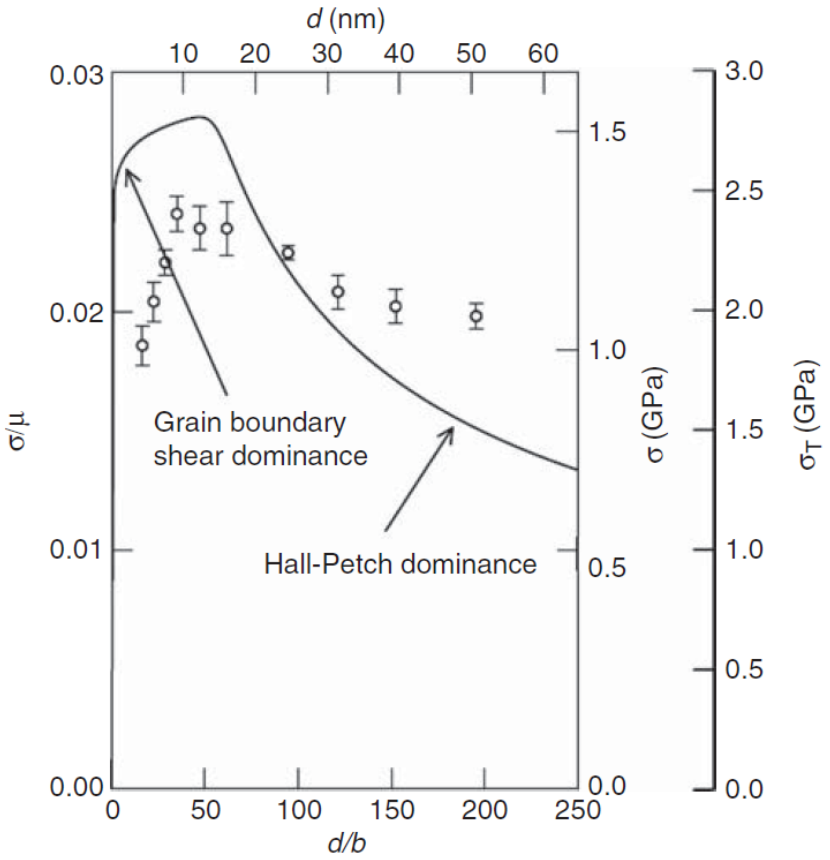

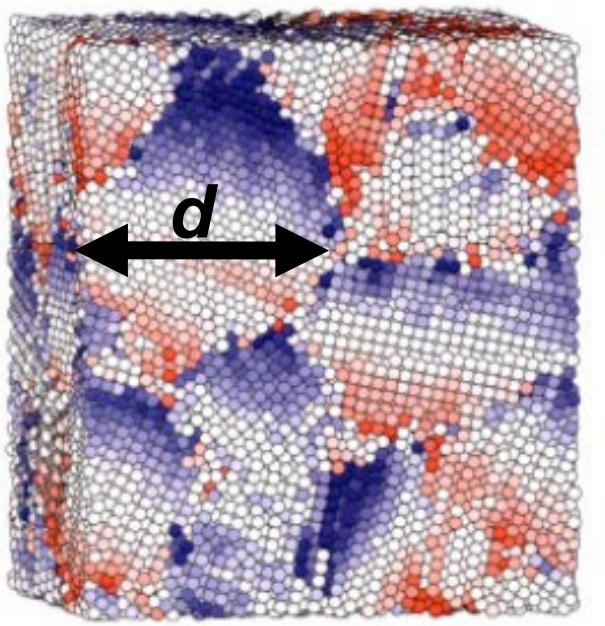

Figure 2. The strongest-size behavior for polycrystalline Cu from the Argon-Yip model[39] (solid line) and molecular dynamics simulations[38] (symbols), where d is the grain size, b is the magnitude of the Burgers vector, σ is the von Mises effective shear stress, σ_T is the tensile flow stress, μ is the shear modulus.

T.Zhu, J.Li, S.Ogata, S.Yip, MRS Bulletin (2009)

変形メカニズムのサイズ依存性

Ti–5 at.% Al single crystal

d=8.0μm　d=1.0μm　d=0.7μm　d=0.4μm

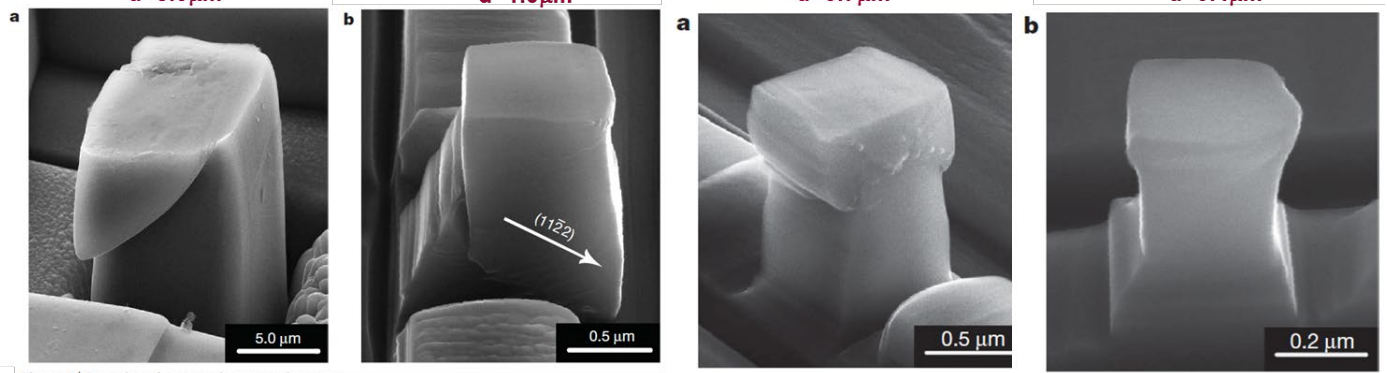

Figure 1 | Scanning electron microscopy images of the deformed micropillars and EBSD pole figure. **a**, $d = 8.0\,\mu m$. **b**, $d = 1.0\,\mu m$. **c**, **d**, EBSD pole figure of the $d = 8.0\,\mu m$ pillar before (**c**) and after (**d**) compression. T_1: $\{11\bar{2}2\}\langle 11\bar{2}3\rangle$ and T_2: $\{10\bar{1}1\}\langle 10\bar{1}2\rangle$ denote the twin type. T_1 and T_2 have misorientation of 64°/<1100> and 57°/<2$\bar{1}\bar{1}$0>, respectively, with respect to the initial orientation. (Half-width 10°; cluster size 5°.)

Twin ⟷ Dislocation

Figure 3 | Electron microscopy images of the tested samples. **a**, **b**, SEM images of the deformed $d = 0.7\,\mu m$ (**a**) and $d = 0.4\,\mu m$ (**b**) pillars. **c**, **d**, Centred dark-field TEM images with diffraction pattern (insets) of the 0.25-μm-diameter pillar before (**c**) and after (**d**) the *in situ* compression test. The beam direction was [0110] and the reflection vector **g** = [0002].

Q.Yu et al., Nature (2010)

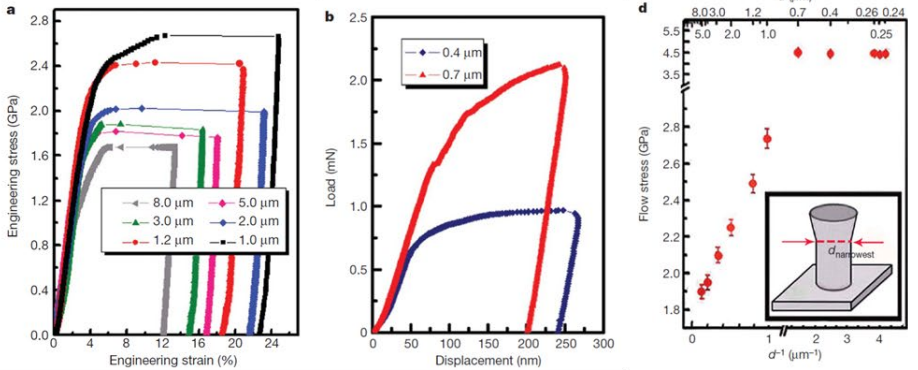

Figure 2 | Mechanical data of the tested samples. **a**, The stress–strain curves of micropillars with decreasing side length, d from 8.0 to 1.0 μm. **b**, The load-displacement curves of submicrometre pillars. **c**, The load-displacement curves of a submicrometre cylindrical pillar with 0.25 μm diameter, in five consecutive load–unload steps during *in situ* testing inside a TEM (see movie in the Supplementary Information). The negative forces at the end of the unloading segments are due to adhesion between diamond tip and the pillars. **d**, Flow stress measured for the pillars versus d. We use the narrowest cross-section $\pi d_{narrowest}^2/4$ to calculate the flow stress. The error bars are two standard deviations.

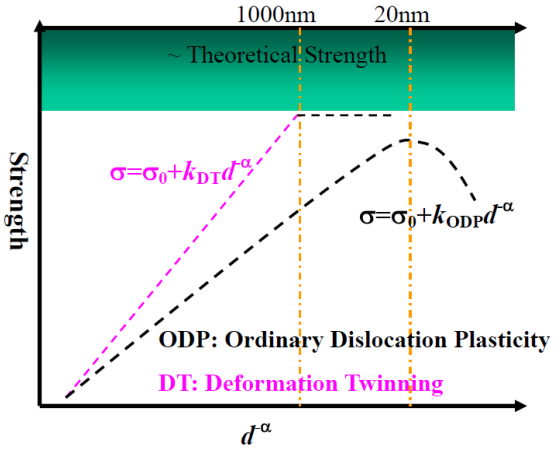

変形メカニズムのサイズ依存性

APPLIED PHYSICS LETTERS **102**, 041902 (2013)

Size-dependent transition of deformation mechanism, and nonlinear elasticity in Ni_3Al nanowires

Yun-Jiang Wang,[1,2,a)] Guo-Jie J. Gao,[1] and Shigenobu Ogata[1,2,b)]
[1]*Department of Mechanical Science and Bioengineering, Graduate School of Engineering Science, Osaka University, Osaka 560-8531, Japan*
[2]*Elements Strategy Initiative for Structural Materials, Kyoto University, Kyoto 606-8501, Japan*

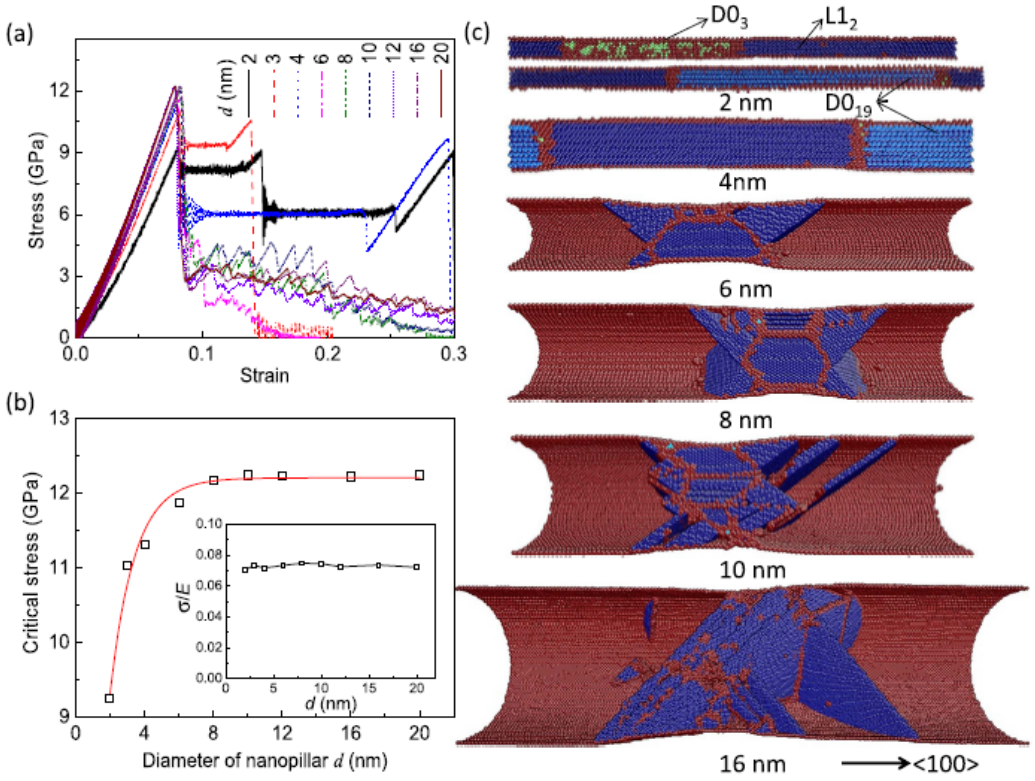

d~2nm（Phase transformation）

Phase transformation
($L1_2$→$D0_3$→$D0_{19}$
FCC → BCC → HCP)

d~8nm（Deformation Twin）

Wang, Gao, Ogata, APL (2013)

ナノ材料の強度
- 鉄微細粒子の圧縮変形および応力場解析 -

Materials Views
www.MaterialsViews.com

ADVANCED MATERIALS
www.advmat.de

From “Smaller is Stronger” to “Size-Independent Strength Plateau”: Towards Measuring the Ideal Strength of Iron

Wei-Zhong Han, Ling Huang, Shigenobu Ogata, Hajime Kimizuka, Zhao-Chun Yang, Christopher Weinberger, Qing-Jie Li, Bo-Yu Liu, Xi-Xiang Zhang, Ju Li, Evan Ma, and Zhi-Wei Shan**

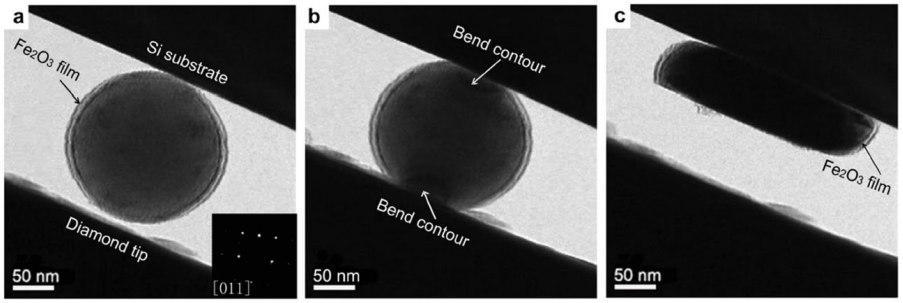

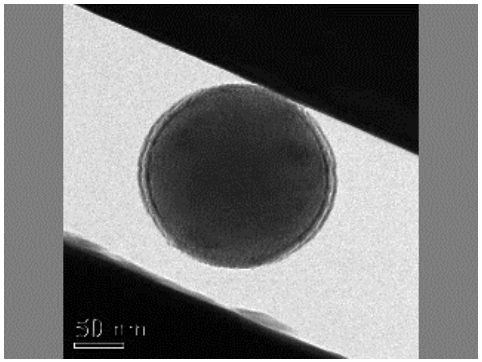

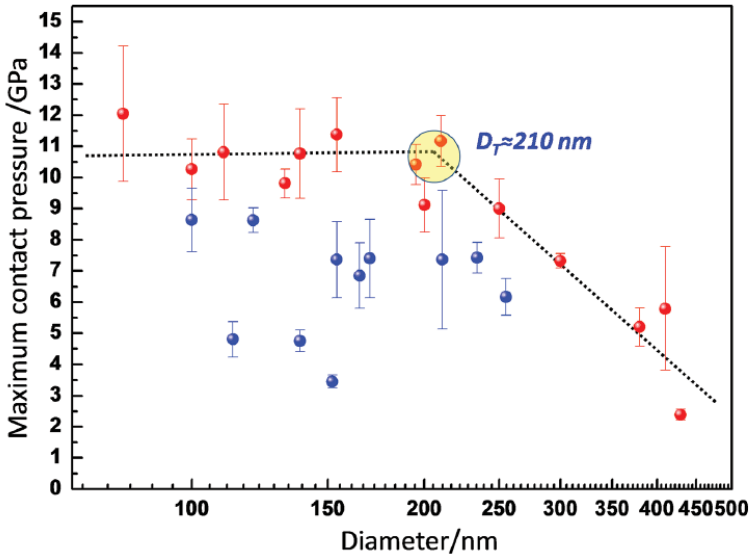

転位発生までを空間マルチスケール解析

（原子構造・原子間相互作用を考慮したFEM）

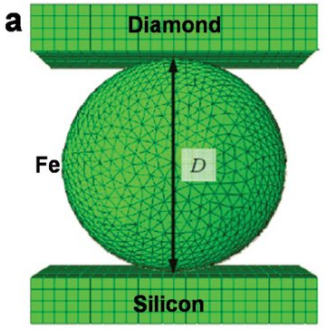

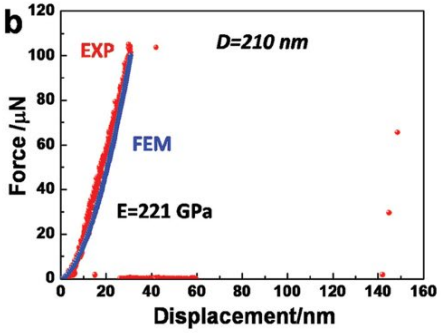

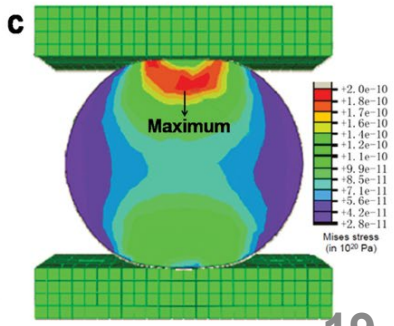

Advanced Materials 27 (2016) 3385

ナノ材料の加工（塑性変形）
- カーボンナノチューブ-

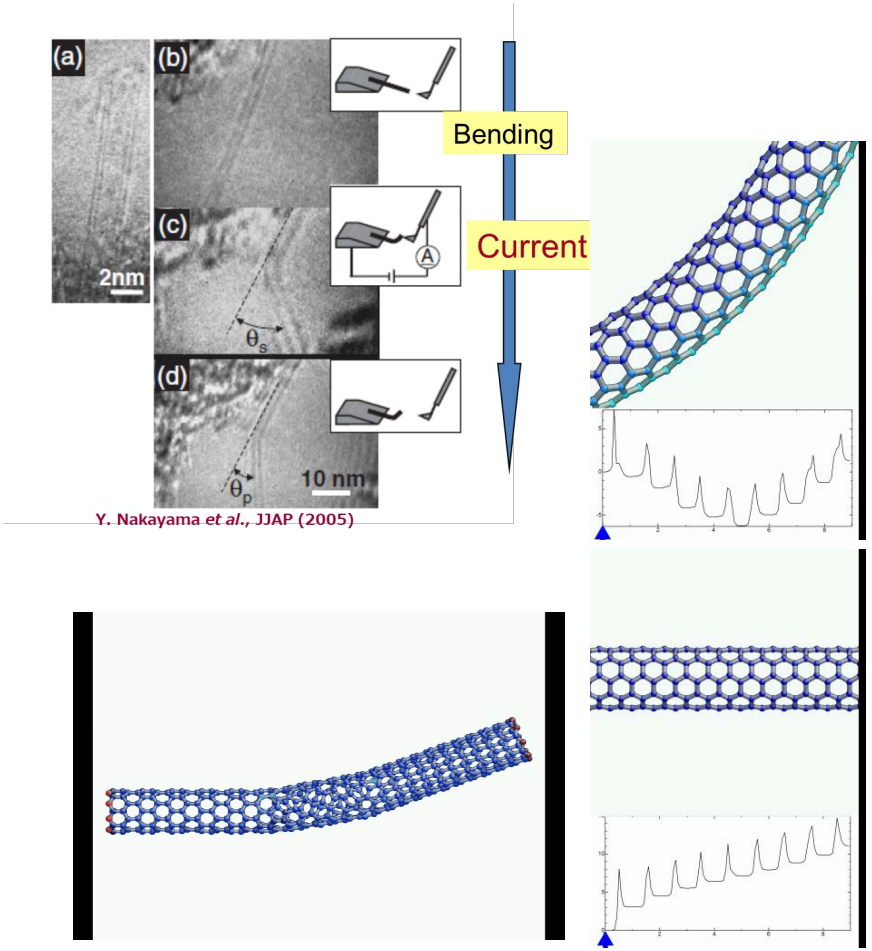

Y. Nakayama *et al.*, JJAP (2005)

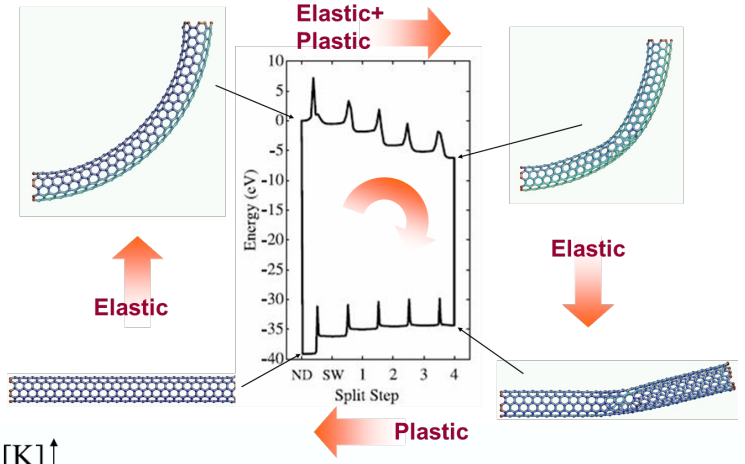

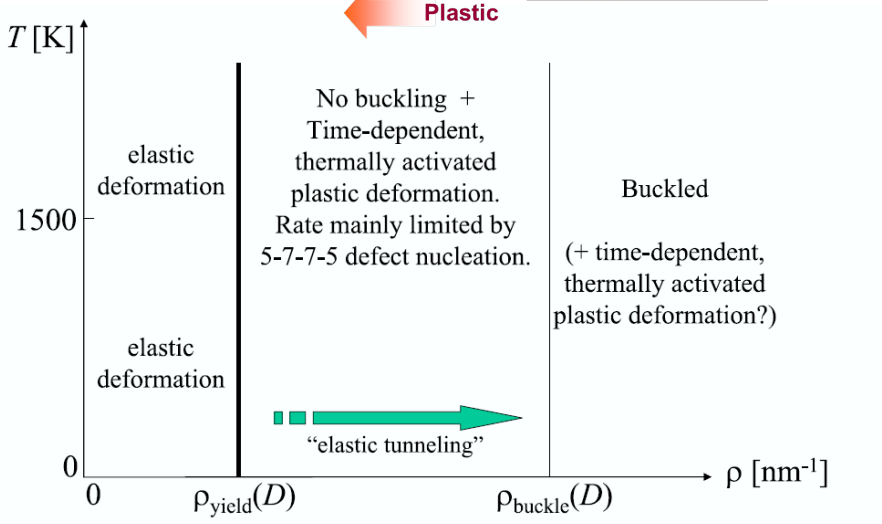

Mori, Ogata, PRB (2006)

ナノ材料の変形
- 応力によるThermomigrationと原子拡散制御 -

nature COMMUNICATIONS

ARTICLE

https://doi.org/10.1038/s41467-019-12416-x OPEN

Controlled growth of single-crystalline metal nanowires via thermomigration across a nanoscale junction

De-Gang Xie[1], Zhi-Yu Nie[1], Shuhei Shinzato[2], Yue-Qing Yang[1], Feng-Xian Liu[3], Shigenobu Ogata[2,4*], Ju Li[1,5*], Evan Ma[1,6] & Zhi-Wei Shan[1*]

NATURE COMMUNICATIONS | (2019)10:4478 | https://doi.org/10.1038/s41467-019-12416-x | www.nature.com/naturecommunications

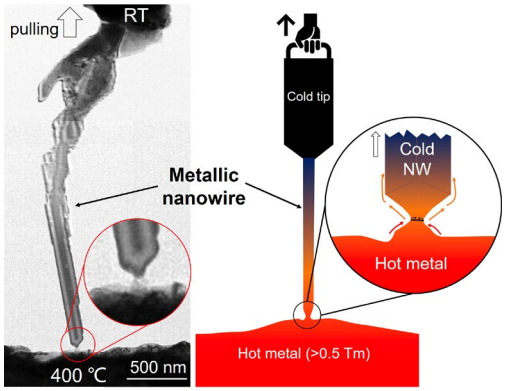

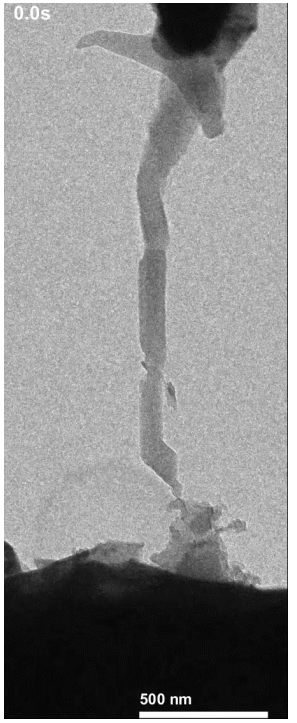

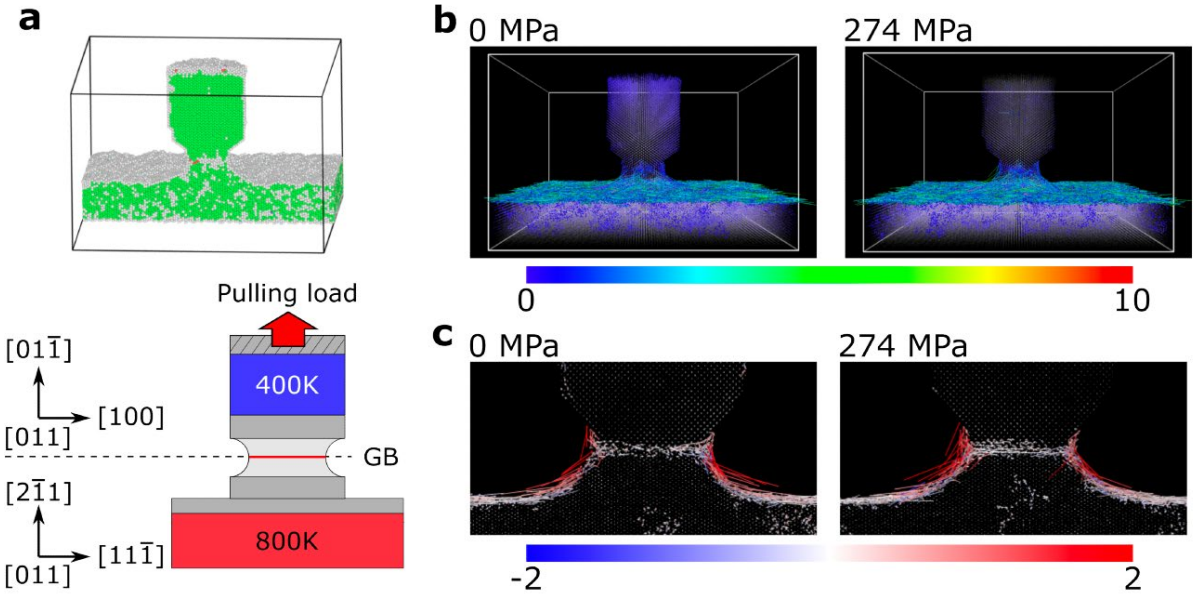

1. 温度勾配による原子拡散 (Thermomigration: entropy production)
2. 粒界への応力負荷による粒界拡散制御

ナノ材料の変形
- 粒界拡散（Coble Creep） -

Stress exponent transition

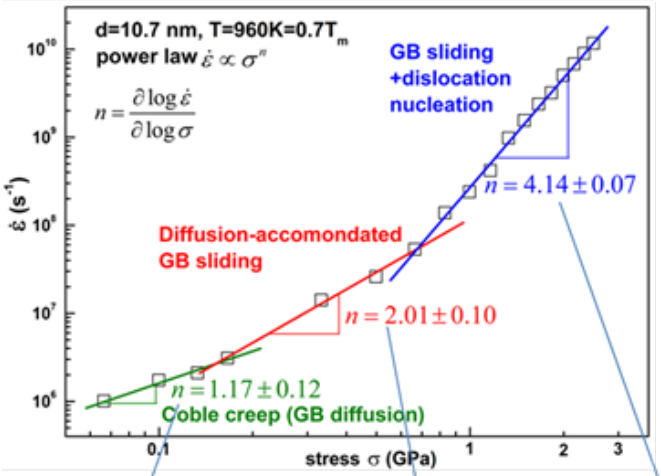

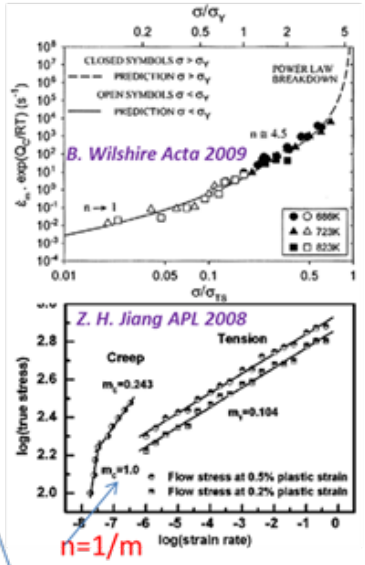

Coarse-grained

Nanoscaled

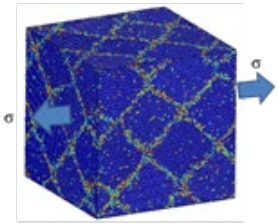

σ(GPa)	T (K)	d (nm)
0.066	720	8
	840	10.7
	960	13.3
	1080	
3.49	1200	16.0

Simulation details:

- Copper with 16 grains
- random grain orientation
- Mishin EAM potential
- NσT ensemble (constant stress)
- Periodic boundary condition

$\dot{\varepsilon}$ strain rate

$$\dot{\varepsilon} = \left(A_C \frac{\delta}{k_B T} \frac{D_{GB}}{d^3} \right) \sigma^1 \qquad \dot{\varepsilon} = \left(\frac{A_{GBS} D_{Gb}}{G} \frac{b}{k_B T} \left(\frac{b}{d} \right)^3 \right) \sigma^2 \qquad \dot{\varepsilon} = \left(A d^{-P} \exp\left(-\frac{\Delta Q}{k_B T} \right) \right) \sigma^{n \geq 4}$$

Coble creep (GB diffusion) | **GB sliding** | **Dislocation Power-law creep**

Wang, Ogata, PRB, (2011)

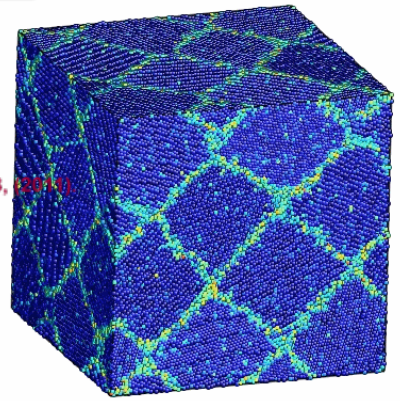

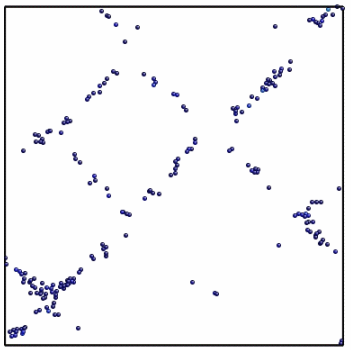

- Y.-J.Wang, S.Ogata, PRB (2011)
- Y.-J.Wang, S.Ogata, PRB (2013)

ナノ材料の靭性制御
- 欠陥による転位運動制御 -

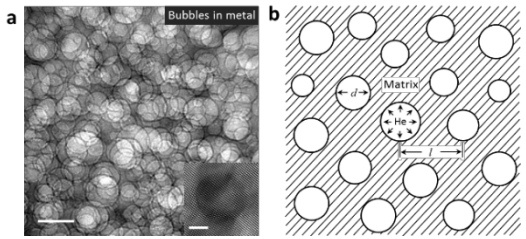

Radiation damage (Cu) (200keV He ion implantation forms 5nm He bubbles)

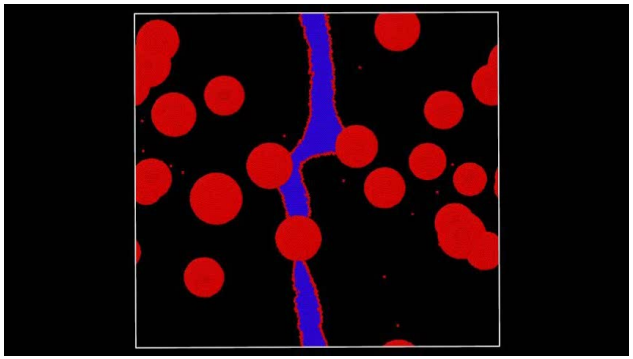

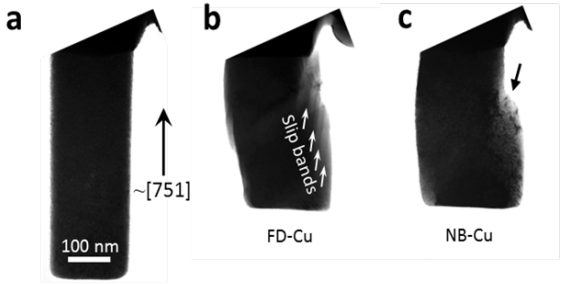

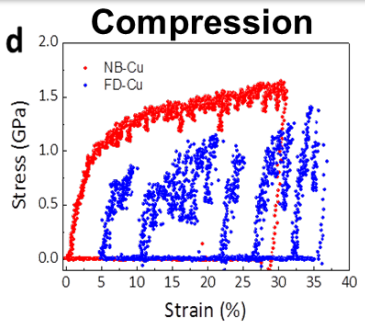

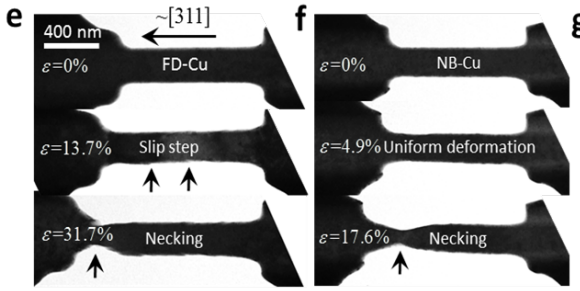

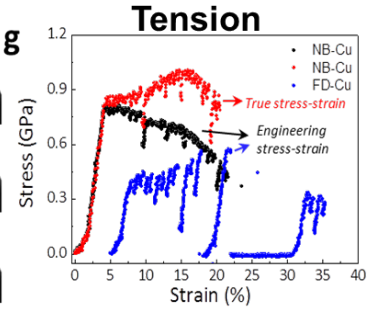

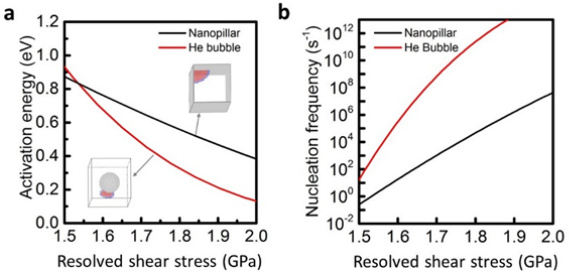

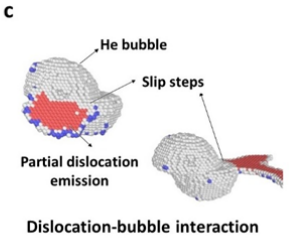

Ming-Shuai Ding, Jun-Ping Du, Liang Wan, Shigenobu Ogata, Lin Tian, Evan Ma, Wei-Zhong Han, Ju Li, and Zhi-Wei Shan, *Nano Letters*, (2016) 4118

NANO LETTERS

金属ガラス材料の変形制御
- rejuvenation による変形能向上 -

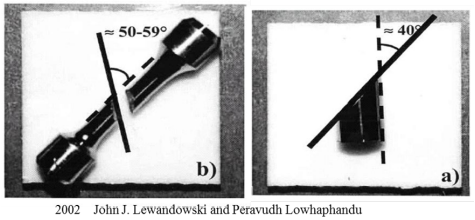

2002 John J. Lewandowski and Peravudh Lowhaphandu

npj nature partner journals
npj Computational Materials

- Masato Wakeda, Junji Saida, Ju Li, Shigenobu Ogata, *Scientific Reports*, 5 (2015), 10545
- Narumasa Miyazaki, Masato Wakeda, Yun-Jiang Wang, Shigenobu Ogata, *npj Computational Materials*, 2 (2016), 16013
- Narumasa Miyazaki, Yi-Chieh Li, Masato Wakeda, Shigenobu Ogata, *Appl. Phys. Lett.*, 109 (2016), 091906

Thermal loading protocol

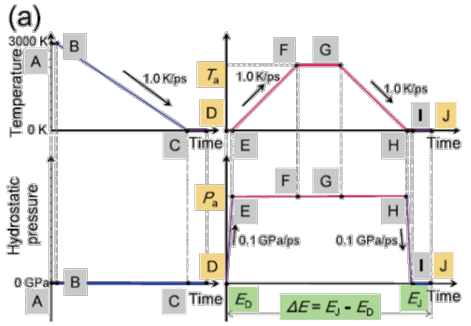

Rejuvenation map

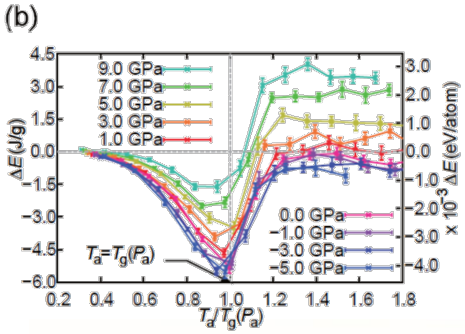

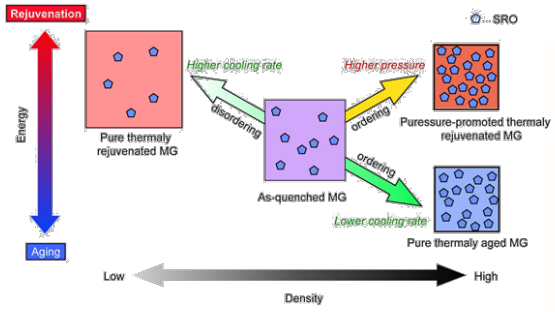

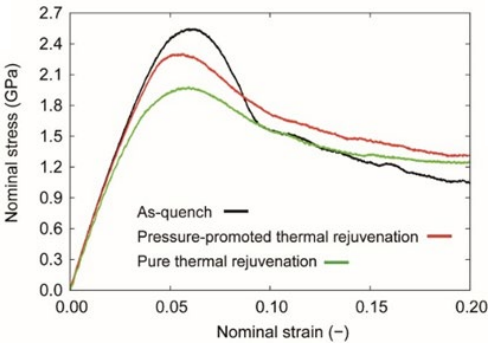

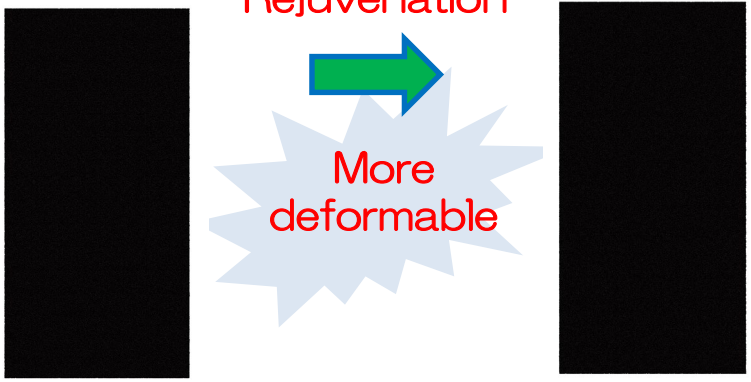

ナノ力学試験の解析
- ナノインデンテーションの温度・押し込み速度依存性予測 -

Atomistically informed multiscale modeling to predict temperature and loading-rate dependencies of first pop-in load

Molecular dynamics (MD) simulation of nanoindentation

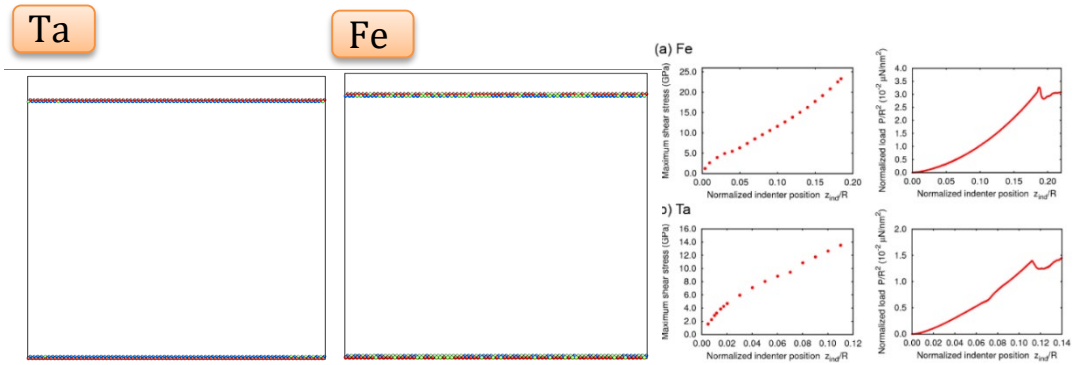

Observe plastic deformation process and obtain local stress state beneath indenter

NEB calculation of dislocation nucleation

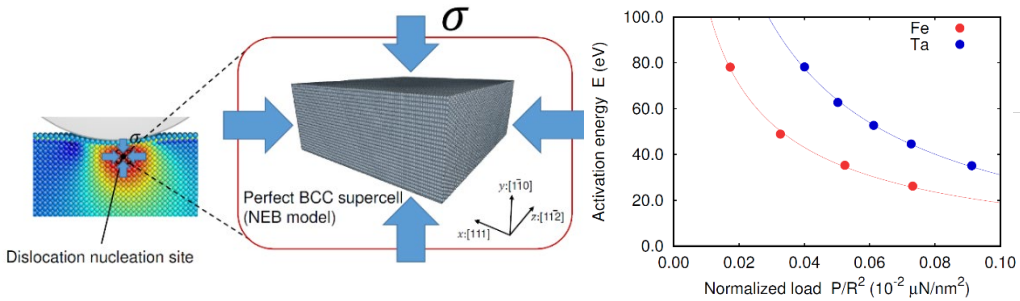

Investigate dislocation nucleation under obtained stress condition

Predicted first pop-in probability

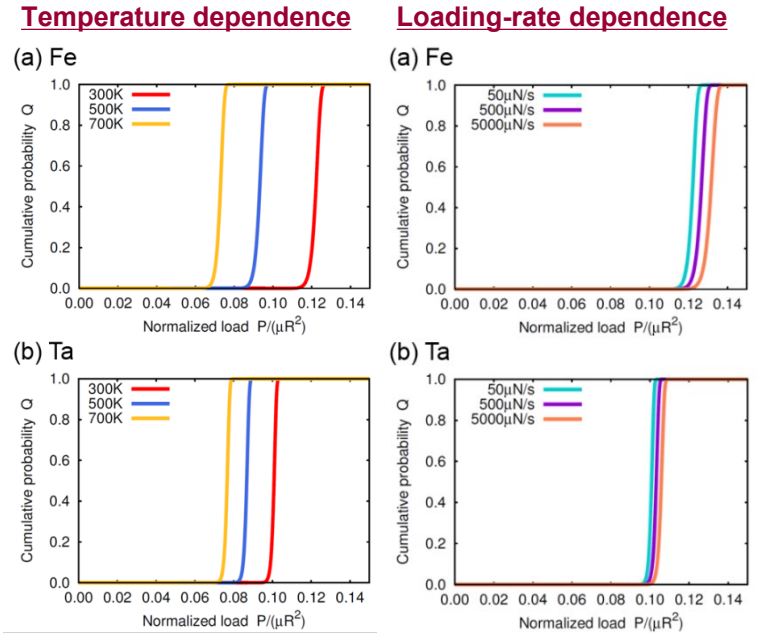

Y. Sato, S. Shinzato, T. Ohmura, S. Ogata
International Journal of Plasticity (2019)
"Atomistic prediction of the temperature- and loading-rate-dependent first pop-in load in nanoindentation"

ナノ力学試験の特異な統計
- ナノインデンテーションが示す特異なスケーリング則 -

nature COMMUNICATIONS

ARTICLE

https://doi.org/10.1038/s41467-020-17918-7 OPEN

Check for updates

Unique universal scaling in nanoindentation pop-ins

Yuji Sato[1], Shuhei Shinzato[1], Takahito Ohmura[2,3,4]✉, Takahiro Hatano[5]✉ & Shigenobu Ogata[1,3]✉

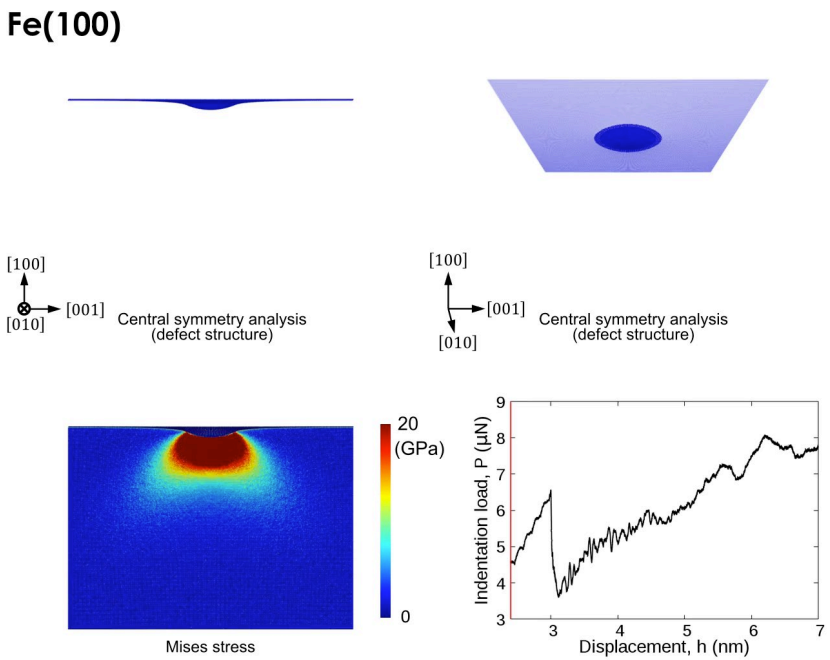

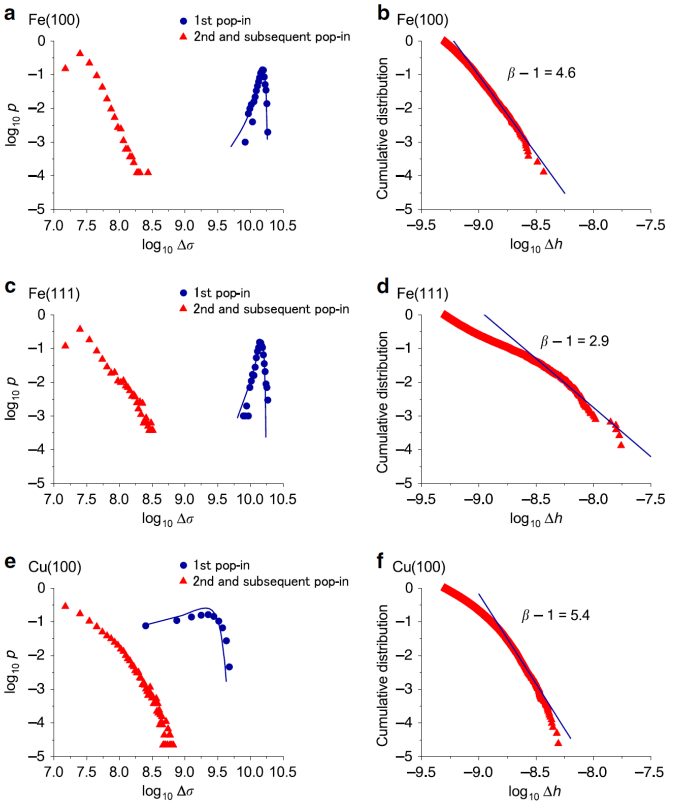

➢ **Y.Sato, S.Shunzato, T.Ohmuda, T.Hatano, S.Ogata, *Nature Communications*, 11 (2020) 4177.**

内容

- **イントロダクション**　原子論からの材料力学特性のモデリングと材料設計　～マルチスケールの観点から
- **ナノ力学**　原子論からのナノ材料力学の特異性の検討
- **原子論における時間スケール拡張への挑戦**
  原子解像度で長時間現象を予測する
- **原子論によるマルチフィジクスへの挑戦**　水素や酸素などの力学特性への影響　～力学・化学・物理
- **材料設計への展開**　強度と延性、靭性を両立した材料設計

原子論からのマクロ力学特性予測
- 空間マルチスケール -

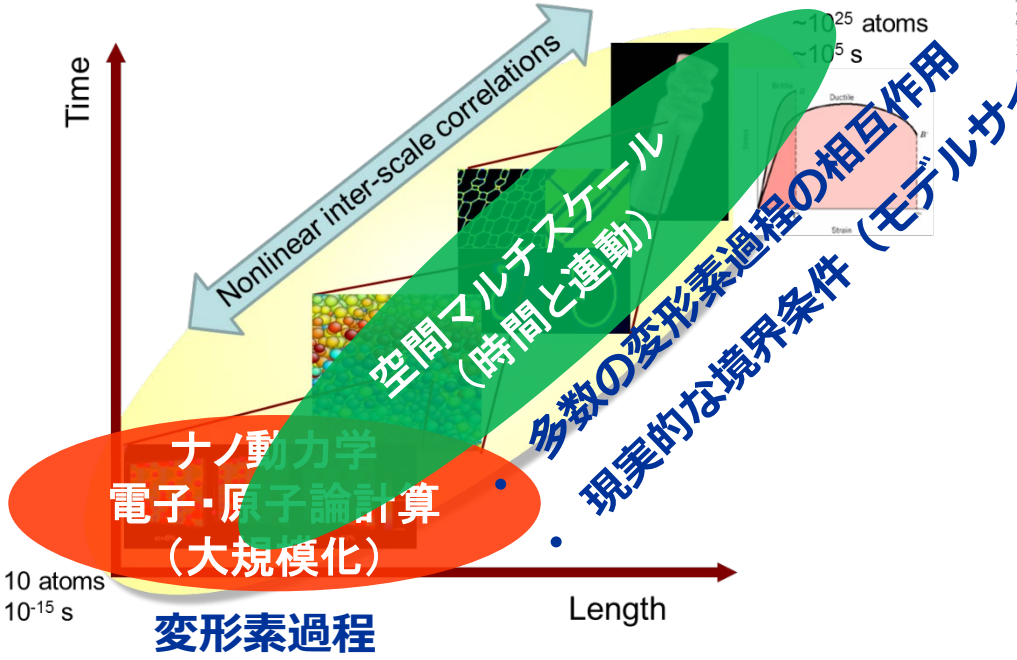

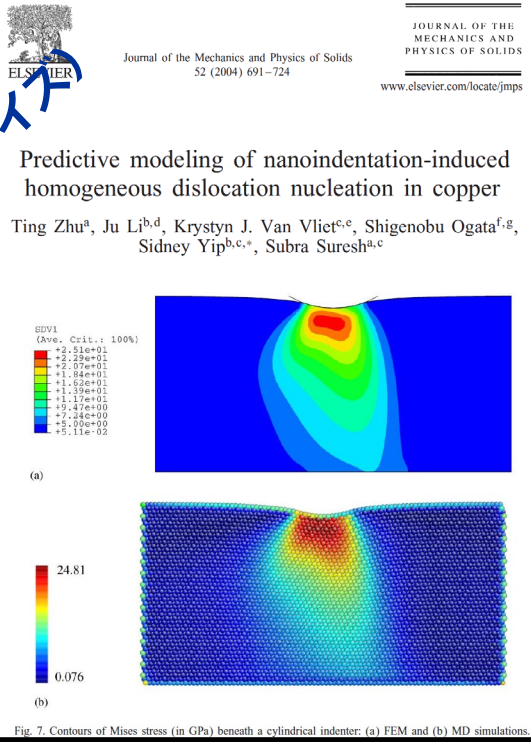

Fig. 7. Contours of Mises stress (in GPa) beneath a cylindrical indenter: (a) FEM and (b) MD simulations.

◆ 原子論的解析をメゾ・マクロに展開する空間マルチスケール解析手法
→ 既に多数提案されている

構造材料極限環境下データ創出のための最先端計算科学手法

空間スケール拡張　機械学習による粗視化モデリング

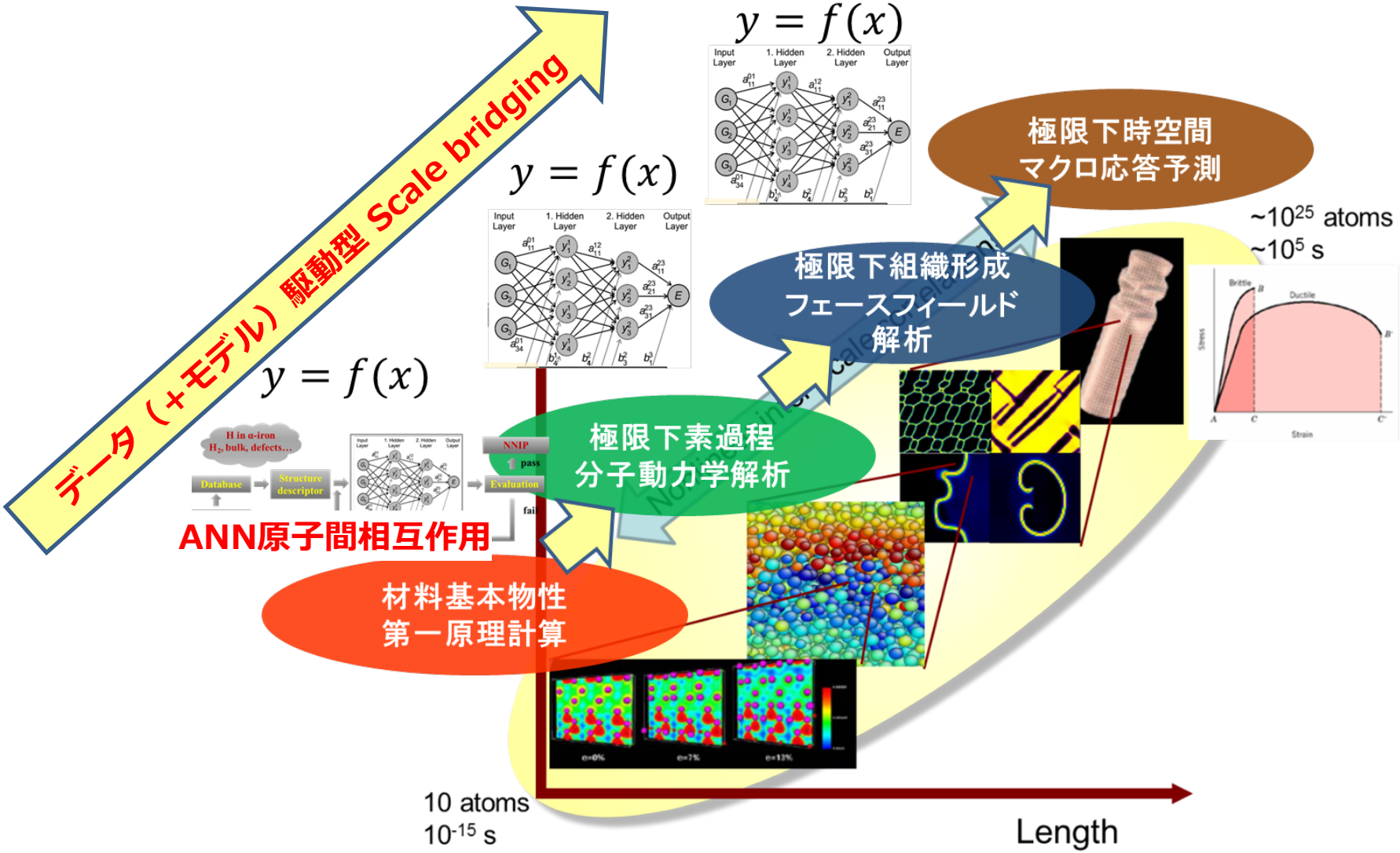

構造材料極限環境下データ創出のための最先端計算科学手法
機械学習原子間相互作用

Model	Transferability / reliability	Computational cost	Typical number of atoms
First-principles (DFT, etc.)	◎	× O(N^3)	1000
Empirical potential function (EAM, etc.)	×	◎ O(N)	100,000,000
Machine Learning Potentials / Deep learning potentials	◎- (Almost same as DFT if well-trained)	◎- O(N) (Little expensive than empirical potential)	10,000,000

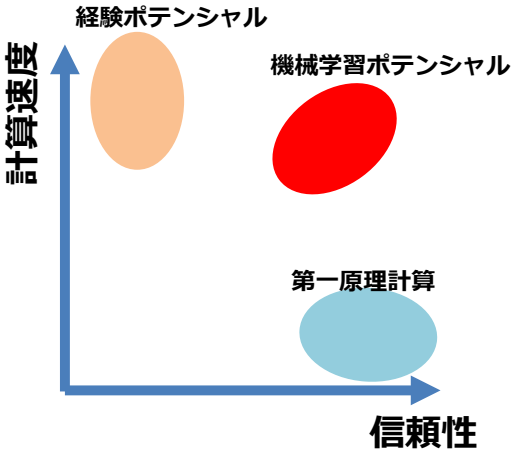

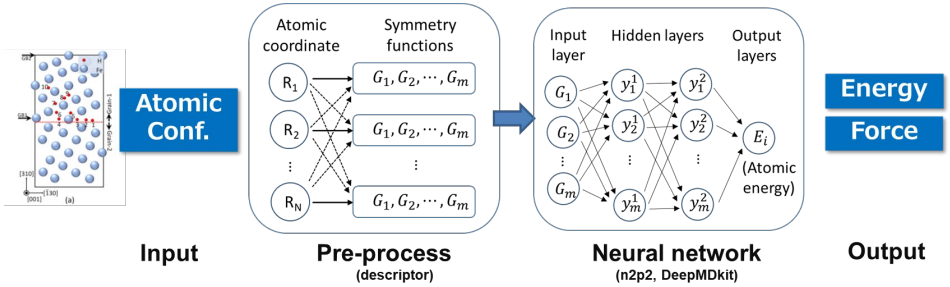

計算速度と信頼性のトレードオフを打破

Machine-learning potential (MLP)

Bayesian Force Field

- Fit the energy/force/stress functions by gaussian process regression
- Predict not only energy but also uncertainty (reliability) of output value
- Hard to fit precisely into training set (intrinsic error by gaussian noise)

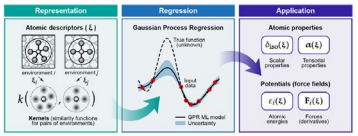

Descriptor-type Neural Network

- Be able to fit precisely into large training set.
- High transferability
- Overfitting may be happened

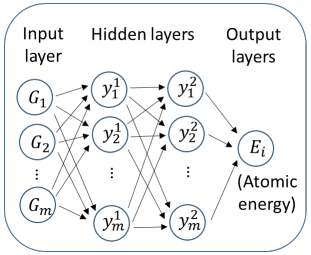

Moment Tensor Potential

- Moment tensors of different ranks are formed by multiplying radial functions by outer products of the position vectors of the neighboring atoms
- Optimal combination of accuracy and computational efficiency
- Less accurate than descriptor-type NN for large training dataset

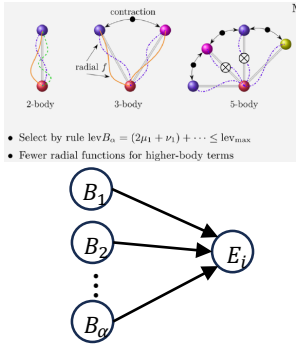

Graph Neural Network Potential

- Structure descriptor is expressed by graph (convolutional) neural network
- Unnecessary to adjust hyperparameters for descriptor
- High computational cost

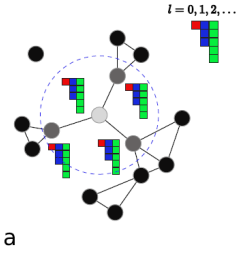

Available codes for training/application of MLP

Bayesian Force Field

- **Gaussian Approximation Potential(GAP/SOAP)**
  (https://libatoms.github.io/GAP/)

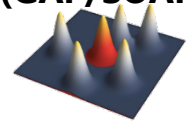

- **FLARE**
  (https://github.com/mir-group/flare)

Descriptor-type Neural Network

- **n2p2**
  (https://github.com/CompPhysVienna/n2p2)
- **ænet**
  (http://ann.atomistic.net)
- **DeePMD-kit***
  (https://docs.deepmodeling.com/projects/deepmd/en/master/)
  *Descriptor is expressed as neural network (DeepPot-SE)

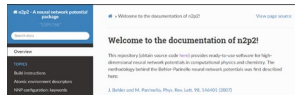

Moment Tensor Potential

- **MLIP package(MLIP-2/MLIP-3)**
  (https://gitlab.com/ashapeev/mlip-2)

Graph Neural Network Potential

- **NequIP**
  (https://github.com/mir-group/nequip)
- **M3GNet**
  (https://github.com/materialsvirtuallab/m3gnet)
- **TeaNet**
  (https://codeocean.com/capsule/4358608/tree/v1)

Fe-C NNP

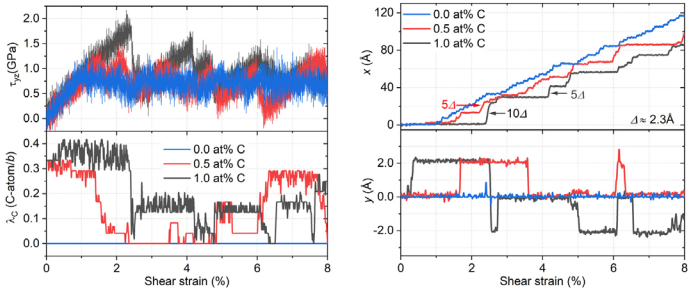

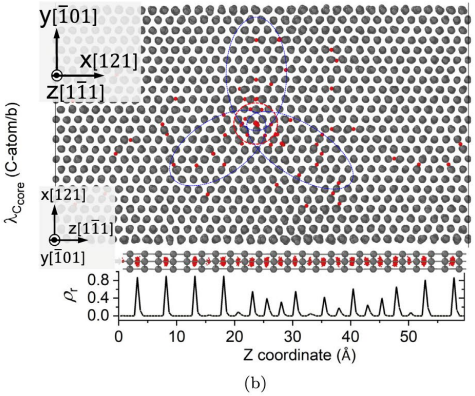

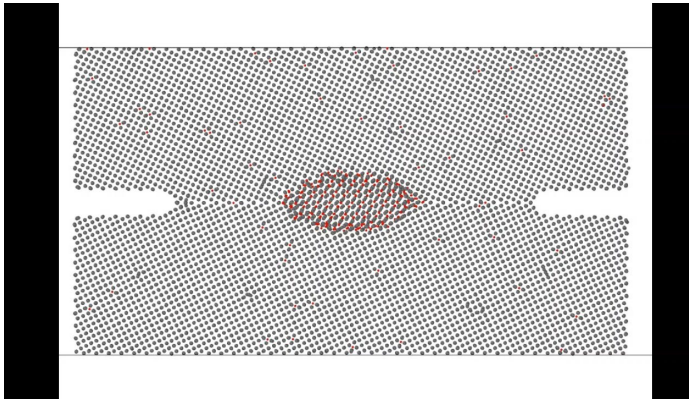

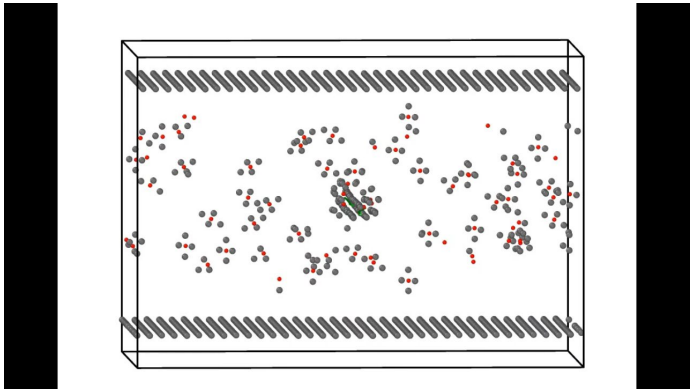

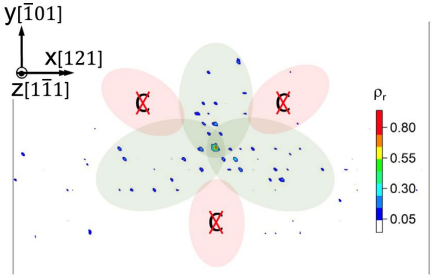

Fan-Shun Meng, et al., Acta Materialia, 281, 120408 (2024)

Ceramics NNP

SrTiO dislocation

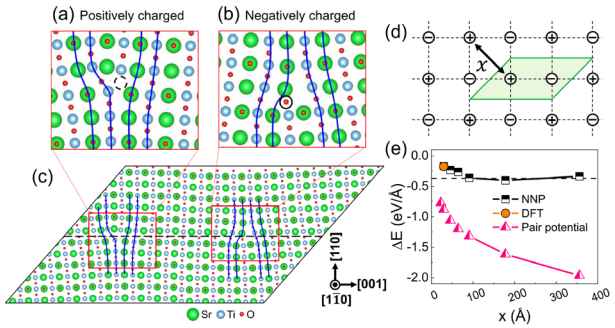

npj | computational materials

Article

Published in partnership with the Shanghai Institute of Ceramics of the Chinese Academy of Sciences

https://doi.org/10.1038/s41524-024-01456-7

Neural network potential for dislocation plasticity in ceramics

GaN nanopillar compression test

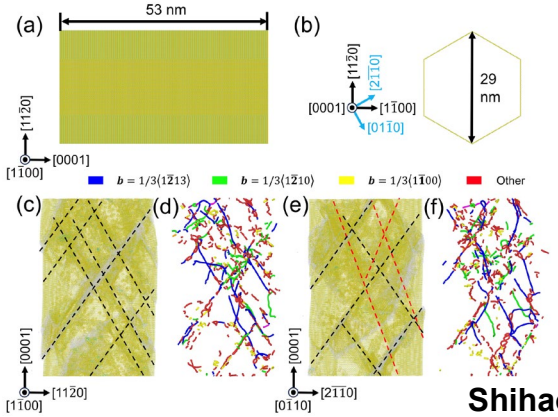

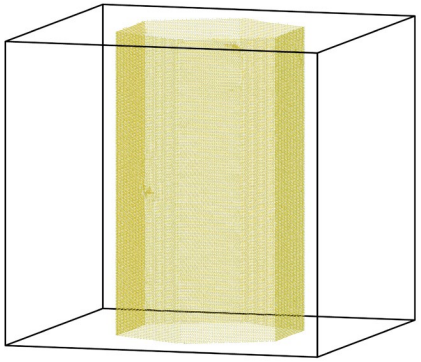

ZnO and GaN nano-indentation test

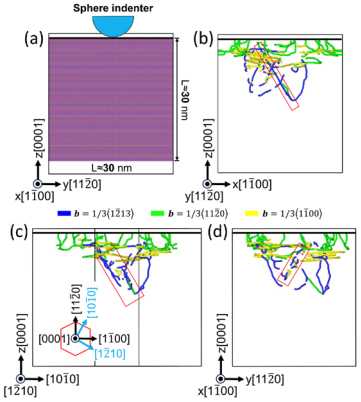

ZnO

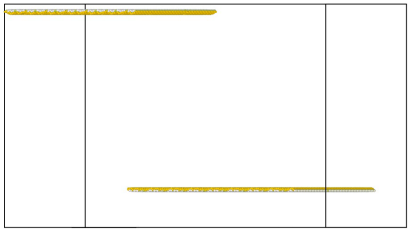

GaN

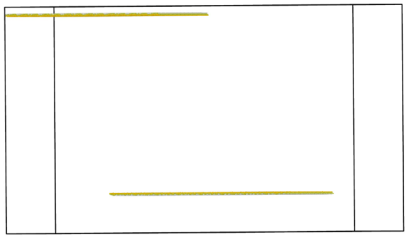

Shihao Zhang, et al., npj computational materials, 10 (2024) 266.

Constructing reliable and highly efficient neural network interatomic potential for Fe-H system

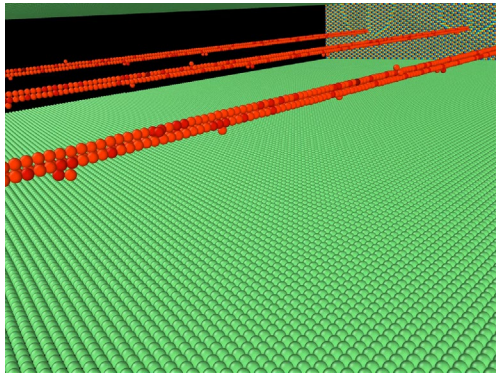

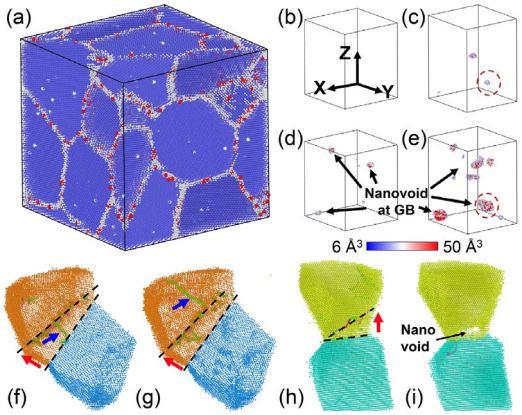

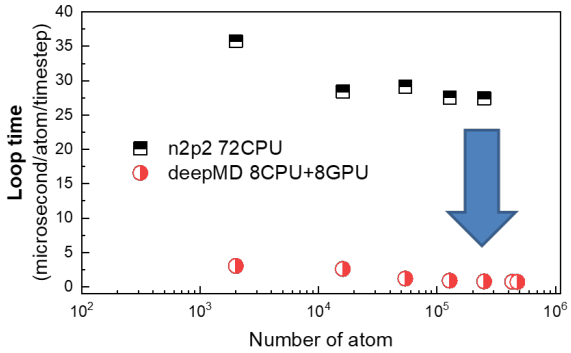

- n2p2 version are available at

  https://github.com/mengfsou/NNIP-FeH

  Fan-Shun Meng, et al., Phys. Rev. Materials, 5, 113606 (2021)

- DeepMD-kit version (GPU acceleration 40x faster) are available at

  Shihao Zhang, et al., Comput. Mater. Sci., 235, 112843 (2024)

原子論からの真のマクロ力学特性予測へ
- 時間マルチスケールへの挑戦 -

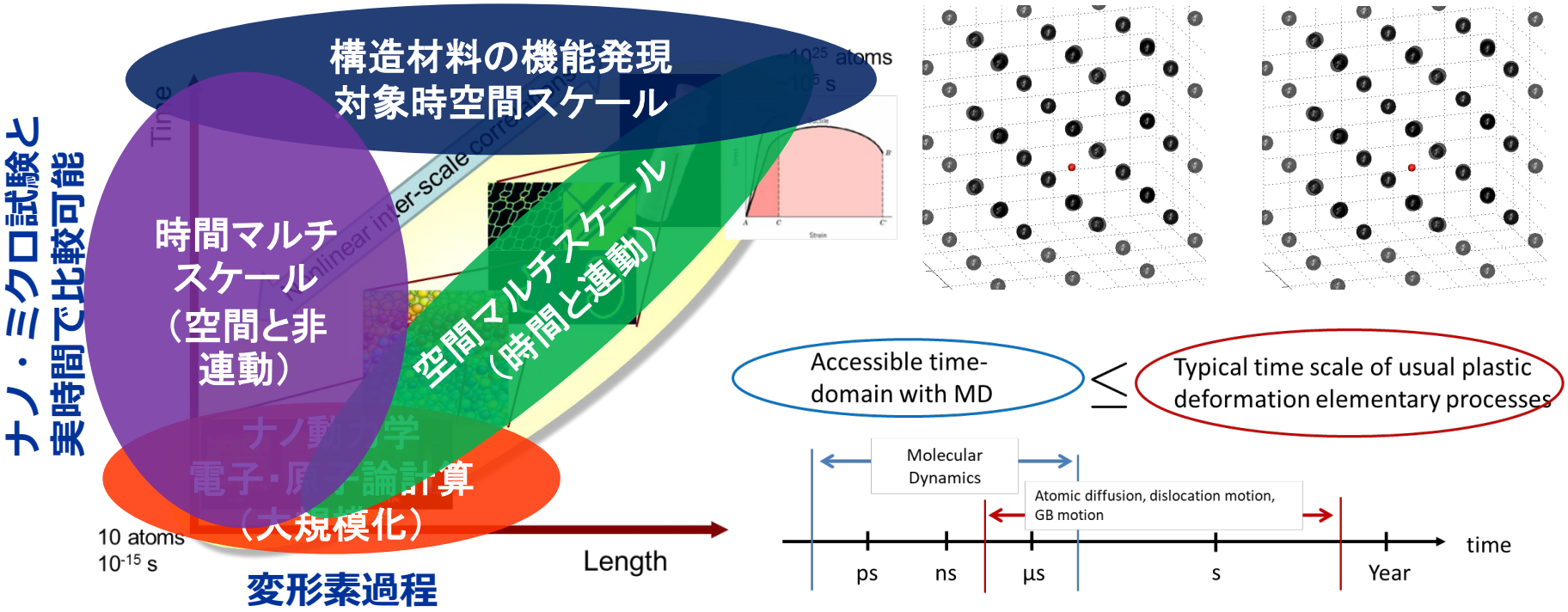

◆ 原子論の空間解像度を保ちつつ長時間スケールの予測解析手法が必要
→ 真の時空間マルチスケール解析へ、原子レベル電顕観察との直接比較へ

原子論の時間スケール拡張のための理論
― 変形素過程の動力学、自由エネルギー地形、反応速度論 ―

力学的・化学的側面から見た変形素過程*

力学負荷と熱活性化により発生・運動し、塑性ひずみをもたらす
局所的な原子の集団的協調運動（変形素過程動力学）

*結合切断、化学反応、転位核生成・運動、変形双晶核生成・成長、相変態核生成・成長、
せん断帯核生成・進展、原子・空孔拡散、etc.

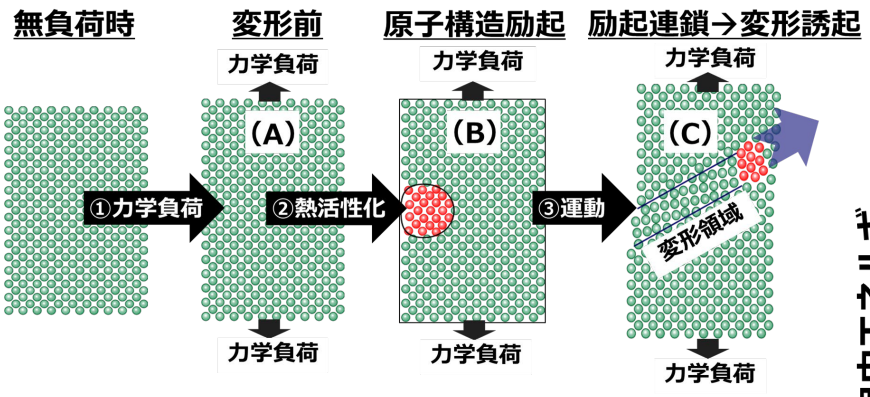

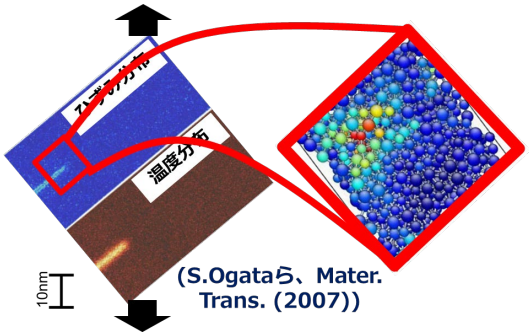

塑性変形プロセス＝メカノケミカル反応
（力学負荷＋熱活性化）

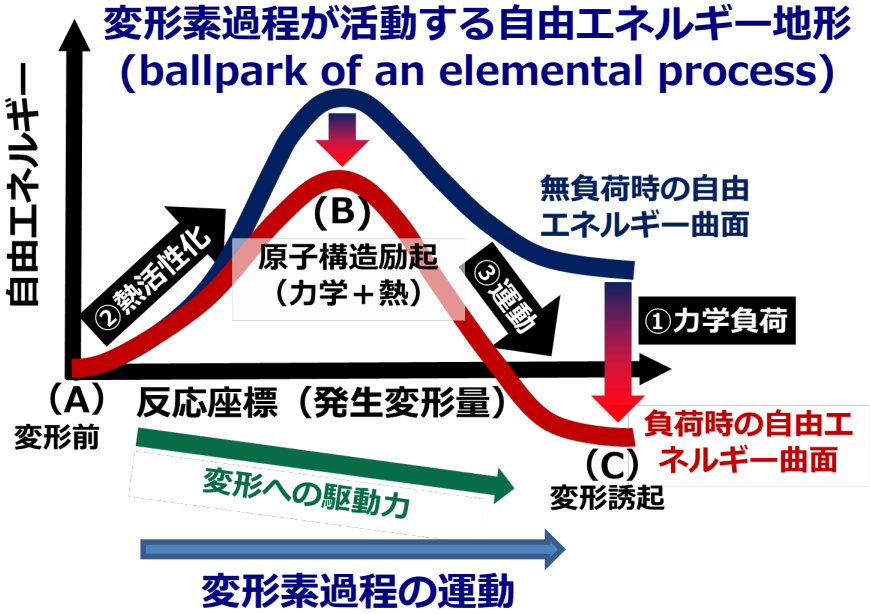

変形素過程の活動から長時間マクロ力学応答の予測

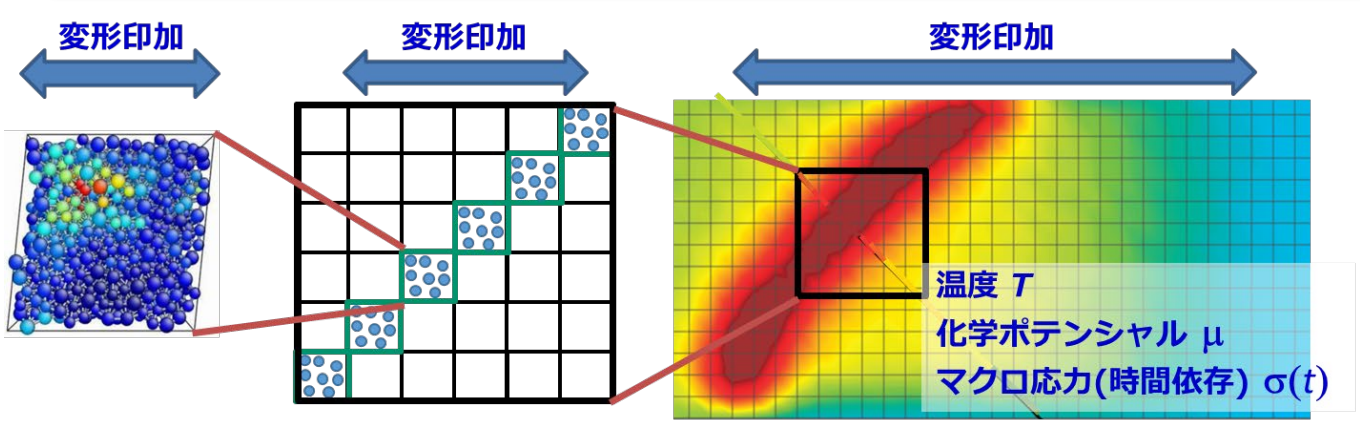

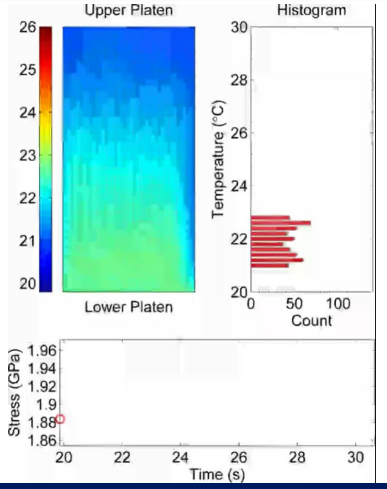

X.Xie, Y.-C.Lo, Y.Tong, J.Qiao, G.Wang, S.Ogata, et al., JMPS (2019)

①変形素過程の活性化

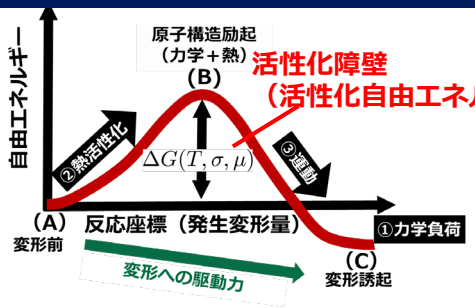

●活性化頻度（アレニウスの式）

$$\nu = \nu_0 \exp\left(-\frac{\Delta G(T,\sigma,\mu)}{k_B T}\right)$$

②局所塑性ひずみ発生

●発生する局所塑性ひずみ速度

$$\dot{\varepsilon}_{\mathrm{nano}}(x) = \varepsilon_{\mathrm{nano}} \times \nu$$

$\varepsilon_{\mathrm{nano}}$：ナノ動力学プロセスが発生する変形（ひずみ）

マイクロメカニクス

●応力場変化解析（弾性場を緩和）

$$\dot{\sigma}(x) = C\left(\dot{\varepsilon}(x) - \dot{\varepsilon}_{\mathrm{nano}}(x)\right)$$

③マクロ応力の変化

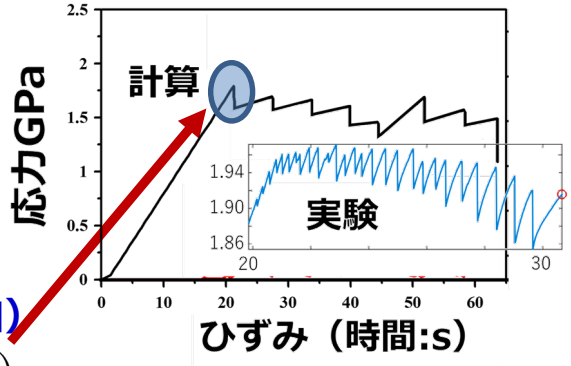

実験と直接比較！

原子論の時間スケール拡張のための具体的手法 I
ー 自由エネルギー地形解析、加速分子動力学法 ー

鉄中炭素拡散

従来分子動力学法

加速分子動力学法
（加速率：最大10^{16}）

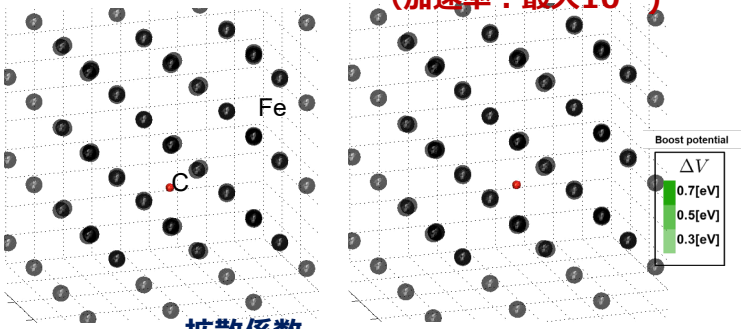

拡散係数
–実験が到達しない時間まで解析可能 -

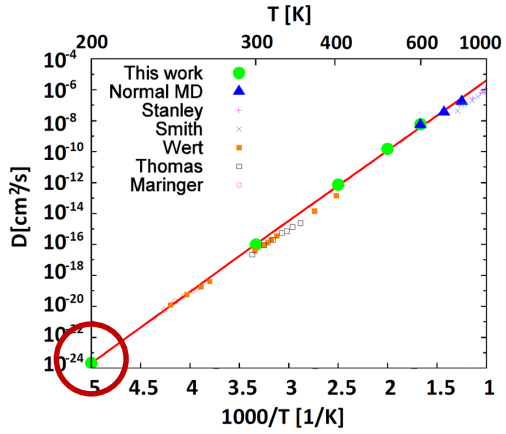

ナノ材料の塑性変形と強度予測

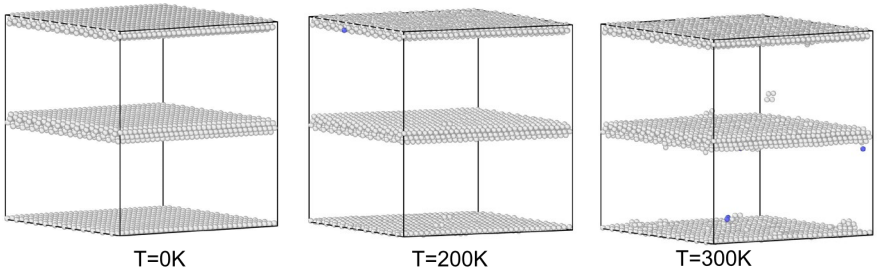

T=0K
Nudged elastic band calculation at 2.5GPa. (24 replicas)

T=200K
AB(accel.)MD simulation at 2.5GPa.

T=300K
AB(accel.)MD simulation at 2.5GPa.

強度の温度と変形速度依存性（加速率: 最大10^{21}）
- 従来法では予測できない日常的な変形速度や温度で予測可能 -

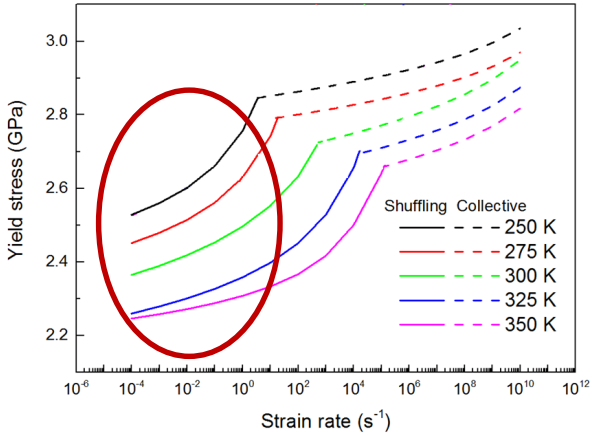

加速分子動力学法

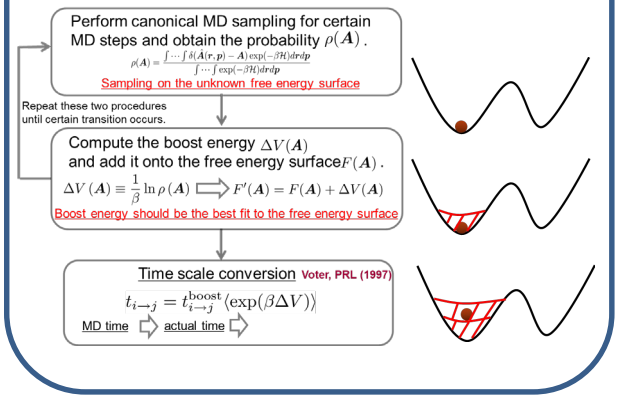

A.Ishii, S.Ogata, H.Kimizuka, J.Li, PRB (2012)
A.Ishii, J.Li, S.Ogata, PLoS ONE (2013)
J.-P.Du, Y.-J.Wang, Y.-C.Lo, L.Wan, S.Ogata, PRB (2016)

DIFFICULTY OF MD SIMULATION OF INFREQUENT PLASTIC DEFORMATION EVENTS

Accessible time-domain with MD

<

Typical time scale of Important elementally process of plastic deformation (dislocation nucleation)

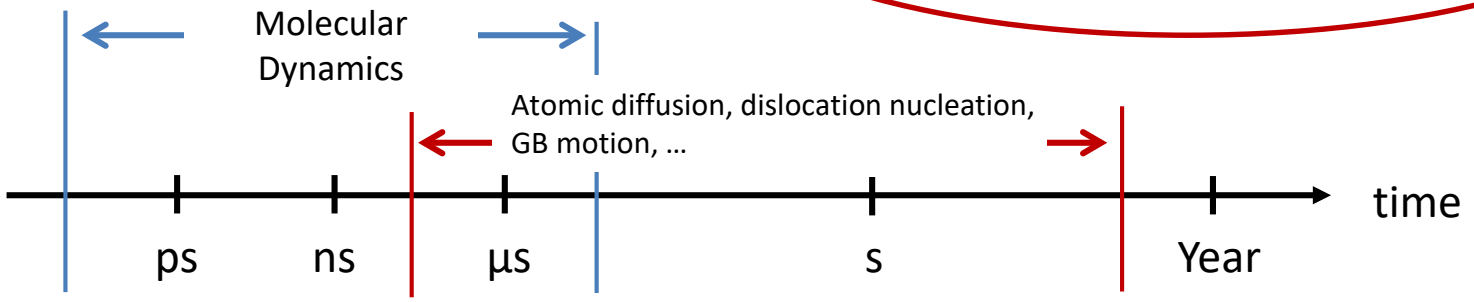

Need to overcome the MD time scale issue
→ Accelerated MD

GENERAL STRATEGY OF ACCELERATED MD METHODS

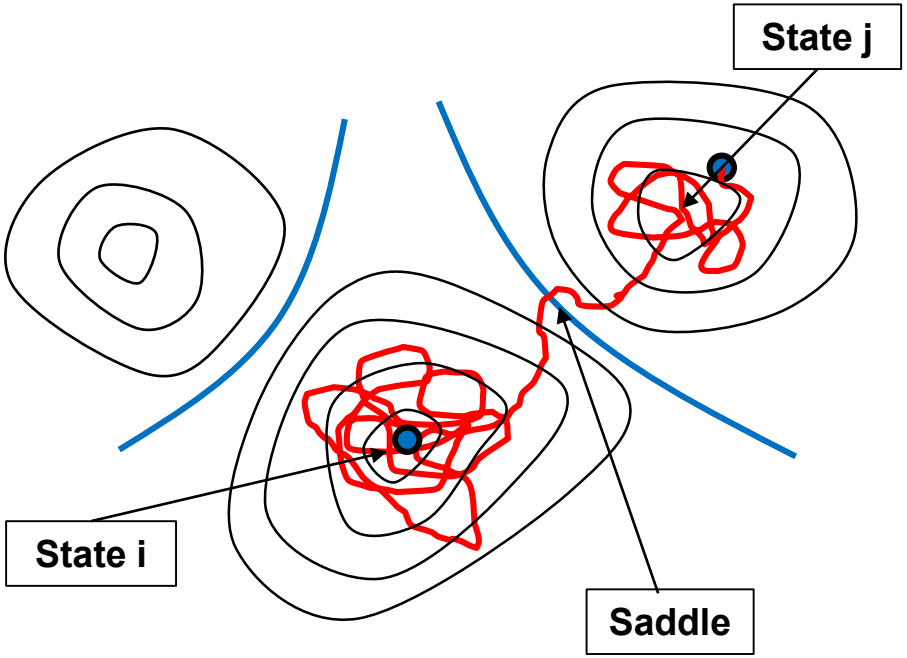

Free energy surface with many local minima

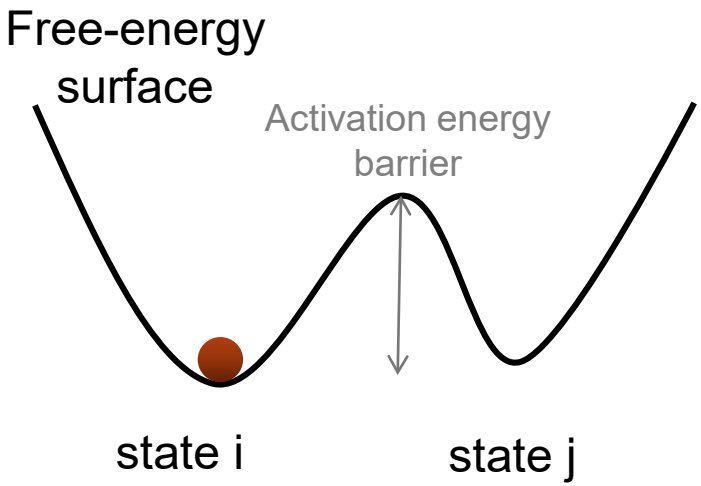

Transition frequency exponentially decreasing with increasing the energy barrier

Making the escape from state i happen sooner without knowing about the escape path and the shape of the free energy surface.

HYPERDYNAMICS ACCELERATED MD METHODS

- **Hyperdynamics and related methods (bond boost, strain boost, …)**

A.F. Voter, PRL 78, 3908 (1997)
R.Miron and K.Fichthorn, JCP 119, 6210 (2003)
S.Hara and J.Li, PRB 82, 184114 (2010)

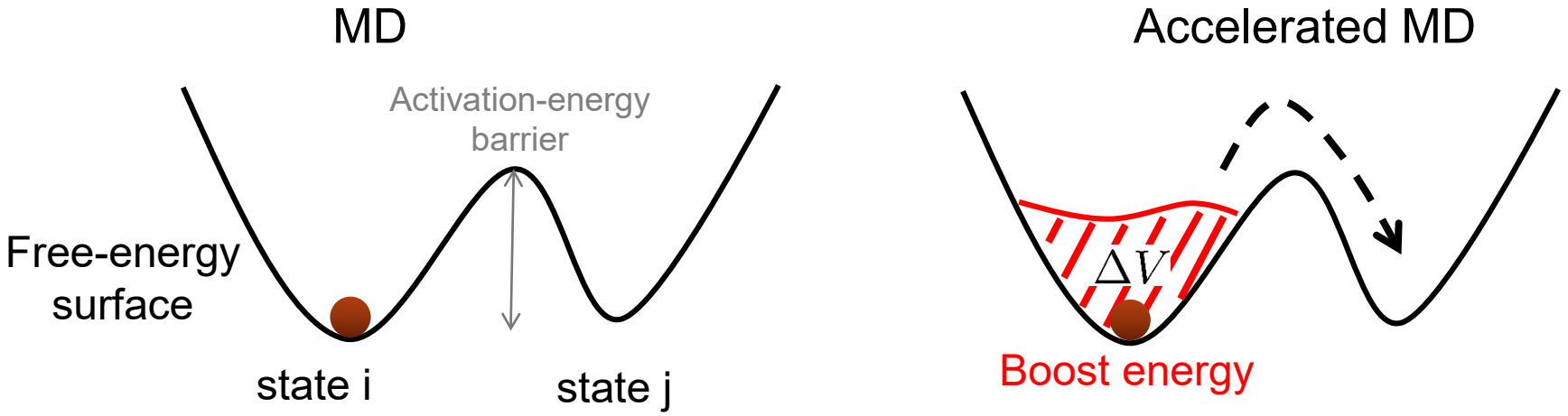

- **Add predetermined boost energy (ΔV) to the original free-energy surface.**
- $t_{i\to j} = t_{i\to j}^{\mathrm{boost}} \langle \exp(\beta \Delta V) \rangle$ **: Hyperdynamics theorem** A.F. Voter, PRL 78, 3908 (1997)

The boost energy should be carefully determined (risk of over-boost). Over-boost violates the assumption of hyperdynamics (saddle point cannot be boosted).

ADAPTIVE BOOST MOLECULAR DYNAMICS METHOD

A.Ishii, S.Ogata, H.Kimizuka, J.Li, PRB (2012).

A.Ishii, J.Li, S.Ogata, PLoS ONE (2013).

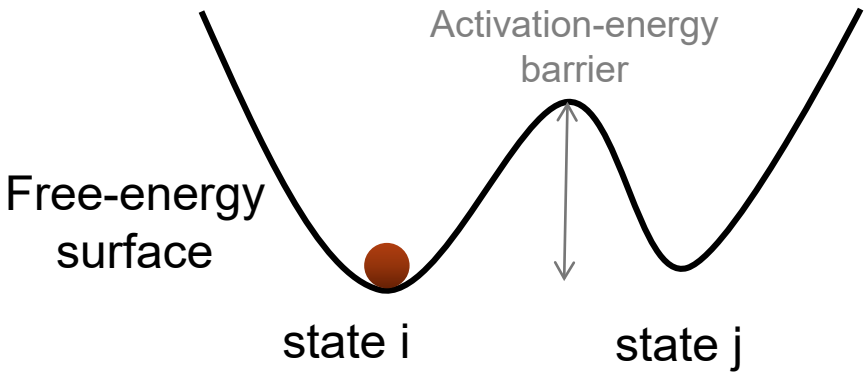

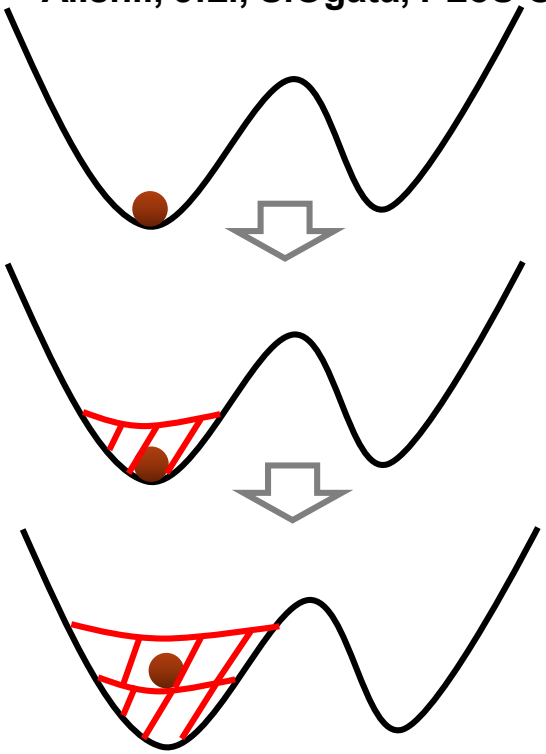

- **Add boost energy (ΔV) to the original free-energy surface.**
- **The boost energy is determined by an adaptive manner (no risk of over-boost)**
- **The boost energy is expressed by a smooth function (not so many Gaussians)**
- $t_{i\to j} = t_{i\to j}^{\mathrm{boost}} \langle \exp(\beta \Delta V) \rangle$ **: Hyperdynamics theorem**

ADAPTIVE BOOST MOLECULAR DYNAMICS METHOD (ACCEL. MD)

Perform canonical MD sampling for certain MD steps and obtain the probability $\rho(\boldsymbol{A})$.

$$\rho(\boldsymbol{A}) = \frac{\int \cdots \int \delta(\hat{\boldsymbol{A}}(\boldsymbol{r},\boldsymbol{p}) - \boldsymbol{A}) \exp(-\beta\mathcal{H}) d\boldsymbol{r}d\boldsymbol{p}}{\int \cdots \int \exp(-\beta\mathcal{H}) d\boldsymbol{r}d\boldsymbol{p}}$$

Sampling and explore the unknown free energy surface

Repeat these two procedures until certain transition occurs.

Compute the boost energy $\Delta V(\boldsymbol{A})$ and add it onto the free energy surface $F(\boldsymbol{A})$.

$$\Delta V(\boldsymbol{A}) \equiv \frac{1}{\beta} \ln \rho(\boldsymbol{A}) \Rightarrow F'(\boldsymbol{A}) = F(\boldsymbol{A}) + \Delta V(\boldsymbol{A})$$

Boost energy is the best fit to the free energy surface

Time scale conversion **Voter, PRL (1997)**

$$t_{i\to j} = t_{i\to j}^{\text{boost}} \langle \exp(\beta \Delta V) \rangle$$

MD time ⇨ actual time ⇨ Frequency (not free energy)

Ishii, Ogata, Kimizuka, Li, PRB, (2012)

Ishii, Li, Ogata, PLoS ONE, (2013)

J.-P.Du, Y.-J.Wang, Y.-C.Lo, L.Wan, S.Ogata, PRB (2016)

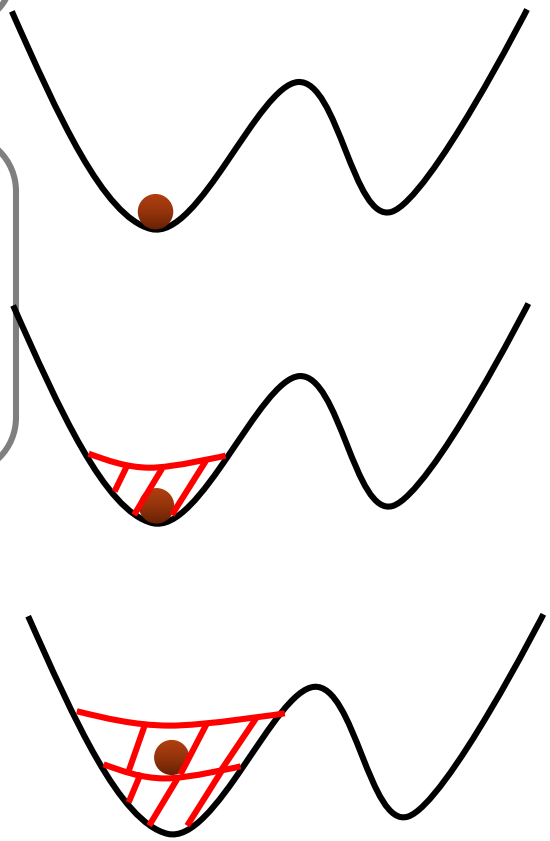

DIFFICULTY OF MD SIMULATION OF CARBON DIFFUSION

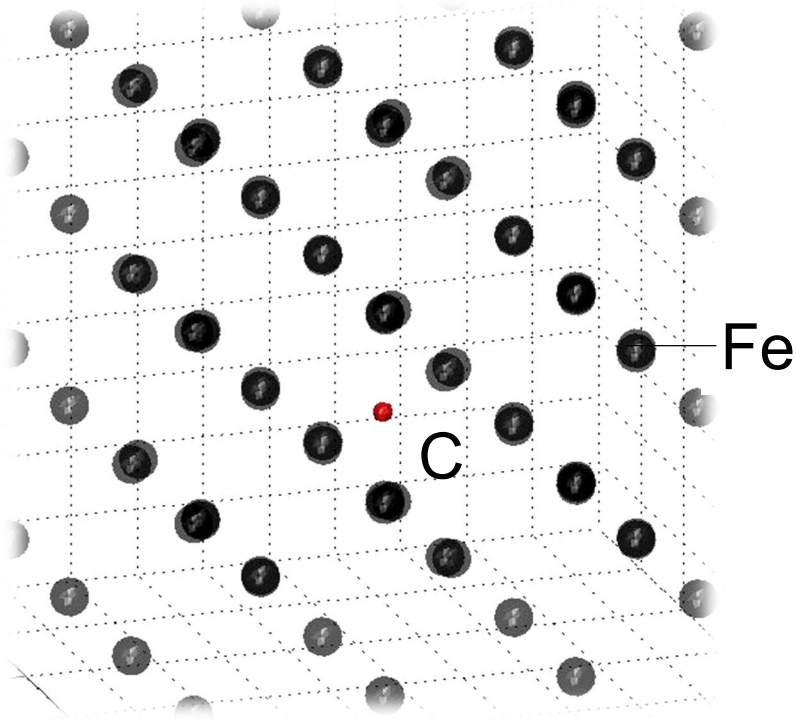

400K

Activation barrier of O-site diffusion:
~ 0.9 eV

⇩

Average time for one jump (400K):
~0.1 ms

⇩

MD steps needed for one jump:
~ 10^{11} steps

⇩

Computational time for one jump:
~ 1~50 days

Carbon diffusion (C atom hopping) is rare event in MD time scale → accelerated MD (adaptive boost method)

CARBON DIFFUSION DYNAMICS IN BCC AT 400K (NORMAL AND AB MD RESULTS)

Normal MD

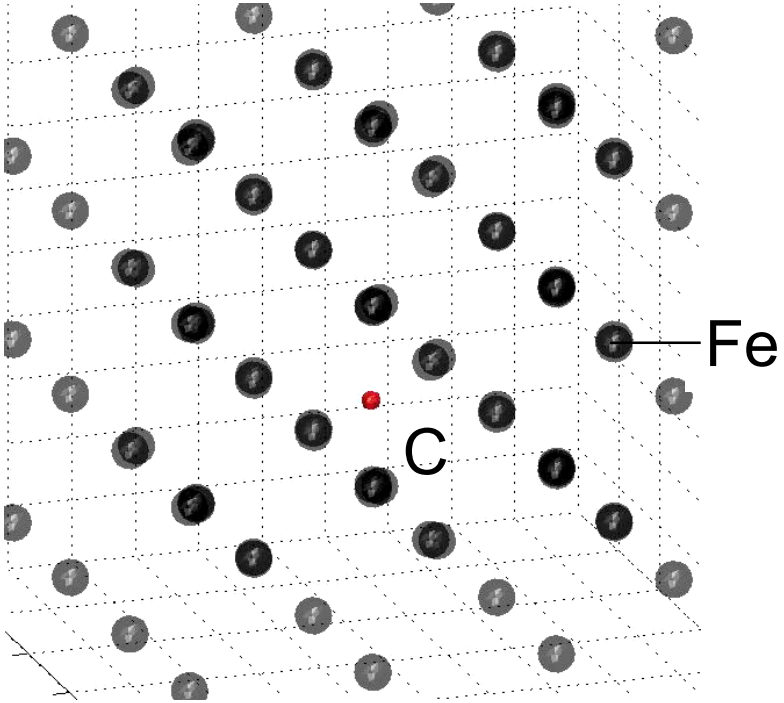

Adaptive boost MD

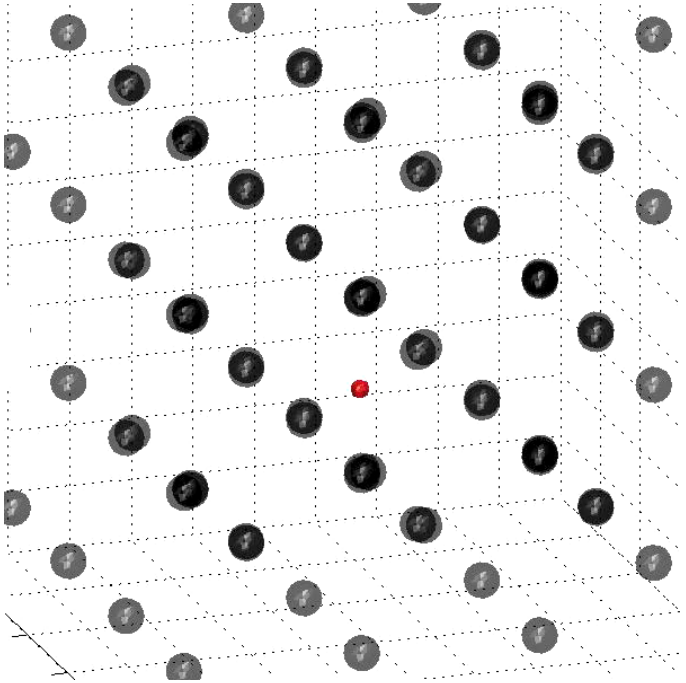

Boost potential

ΔV

0.7[eV]

0.5[eV]

0.3[eV]

- BCC (432 Fe atoms + 1 interstitial C atom) with PBC
- EAM interatomic potentials (Lau. et al. PRL 2007)

Ishii, Ogata, Kimizuka, Li, PRB (2012).

ACCELERATION FACTOR

$$t_{O\to O} = t^{\text{boost}}_{O\to O}\langle \exp((\beta \Delta V(\boldsymbol{A}))\rangle$$

Acceleration factor

Temperature [K]	$\bar{t}_{O\to O}$ [ns]	$\bar{t}^{\text{boost}}_{O\to O}$ [ns]	$\bar{t}_{O\to O}/\bar{t}^{\text{boost}}_{O\to O}$
200	1.48×10^{16}	1.02×10^{-1}	1.45×10^{17}
300	3.24×10^{8}	5.64×10^{-2}	5.72×10^{9}
400	7.08×10^{4}	8.22×10^{-2}	8.78×10^{5}
500	2.48×10^{2}	8.12×10^{-3}	3.07×10^{4}
600	4.64	4.72×10^{-3}	9.78×10^{2}

C DIFFUSIVITY IN BCC IRON

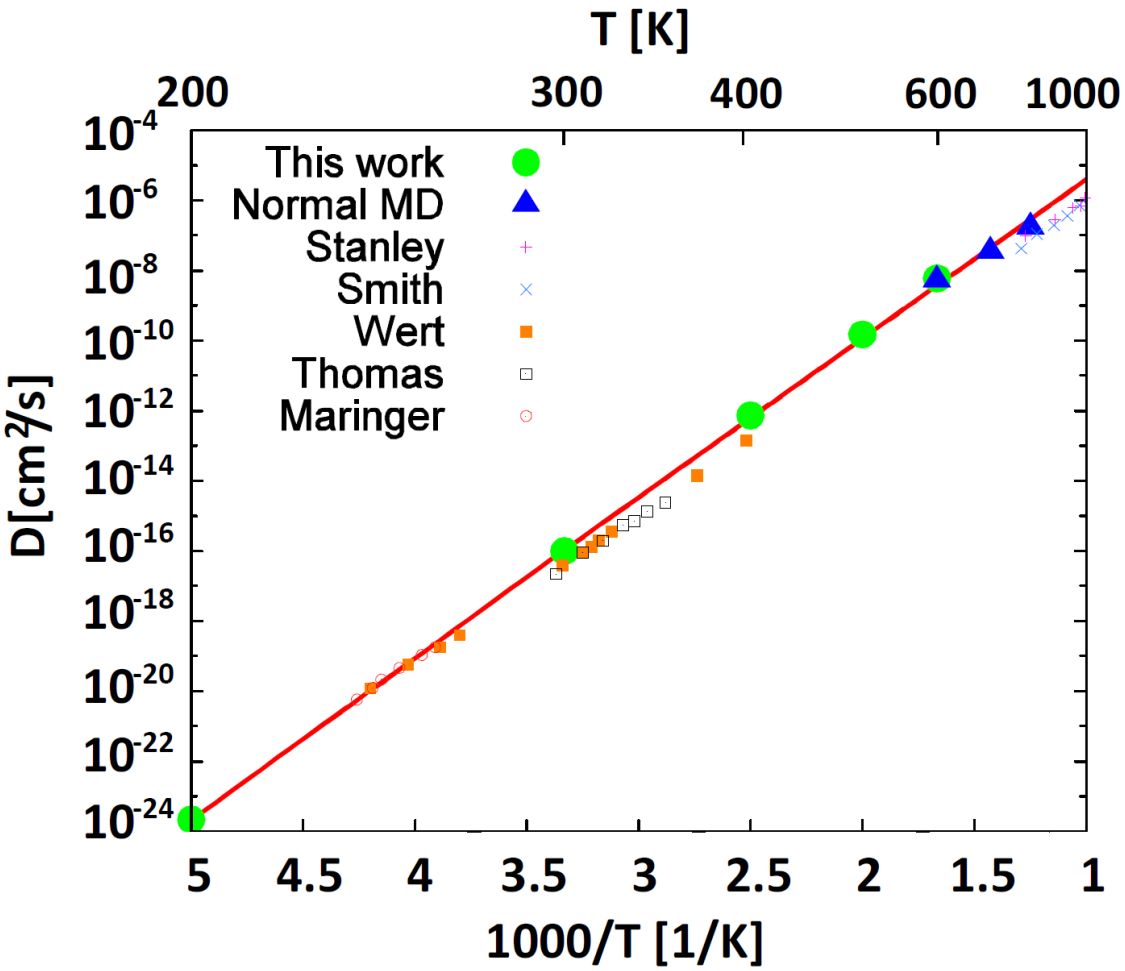

Activation enthalpy

- Adaptive Boost MD estimation
  ~ 0.89 eV
- Experiments:
  0.77 ~ 0.90 eV

Ishii, Ogata, Kimizuka, Li, PRB (2012).

➢ **With the aid of Adaptive Boost MD, diffusivity can be quantitatively analyzed even at low temperature for which no experimental data are available.**

微細結晶の降伏応力予測例

- ナノ結晶塑性変形：粒界からの転位核生成支配 -

Dislocation nucleation at GB

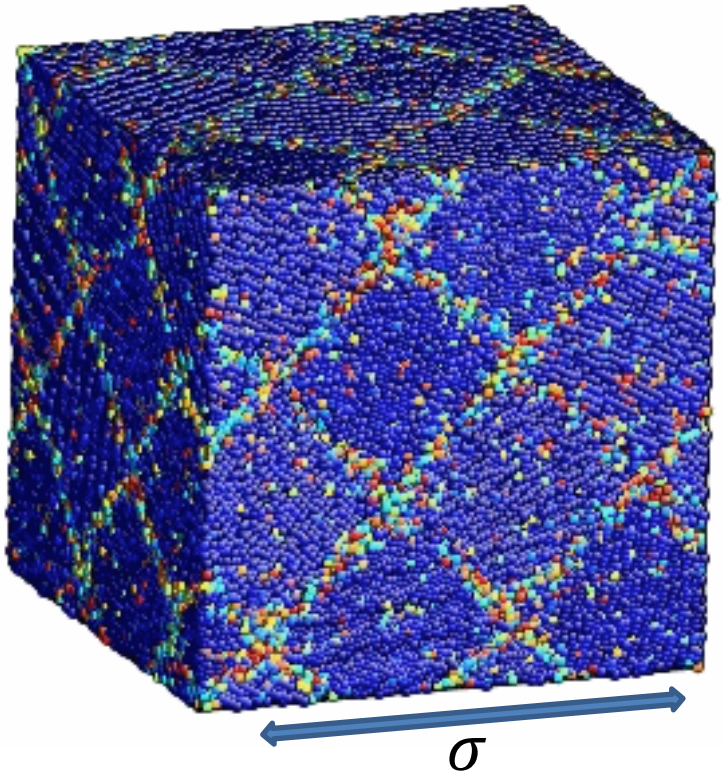

Centro-symmetry Parameter

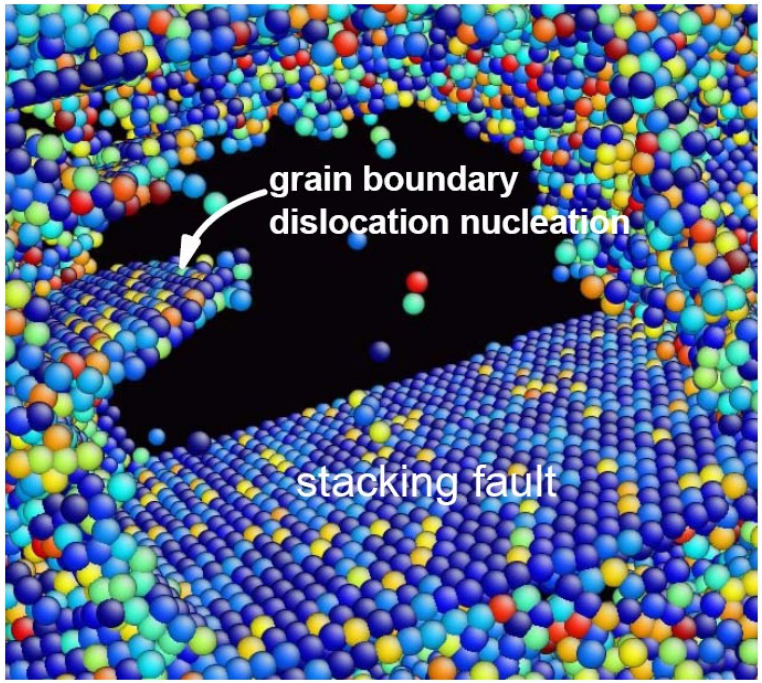

Y. Wang, S.Ogata, PRB (2011)

微細結晶の降伏応力予測例
- 従来分子動力学（原子論的動力学）解析 -

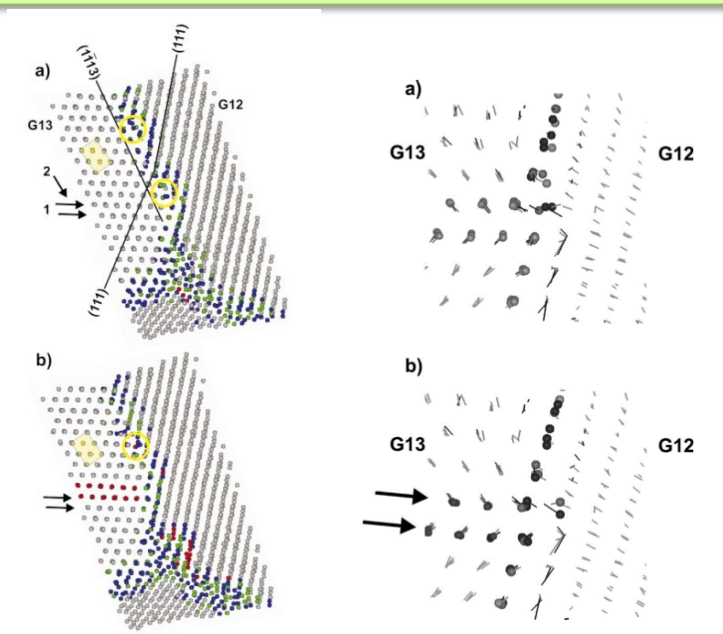

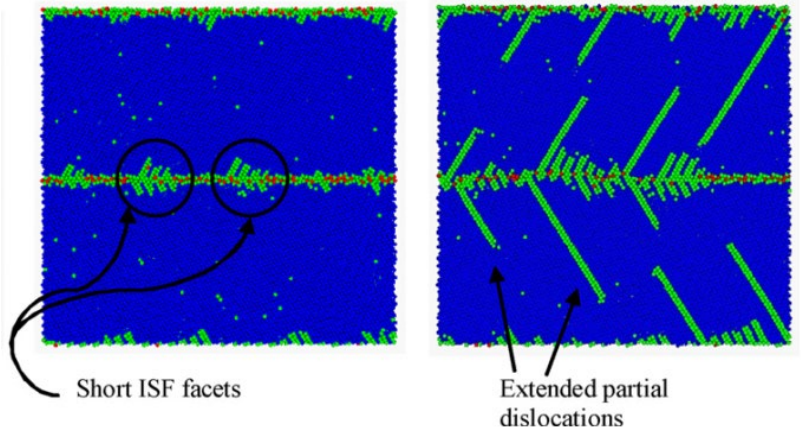

Shuffling-assisted single dislocation nucleation:
Local shuffling of atoms and the stress-assisted free volume migration allow the creation of the necessary Burgers vector of the Shockey partials[1]

Collective multiple dislocation nucleation:
Uniaxial tension of a Σ9 <110>{221} symmetric tilt grain boundary in Cu with strain rate of 10^9 s^{-1} [2]

ひずみ速度が通常の実験よりも10^{10}倍も速い超高速変形解析

1. H. Van Swygenhoven, P.M. Derlet, and A. Hasnaoui, Phys. Rev. B 66, 024101 (2002).
2. D.E. Spearot, M.A. Tschopp, K.I. Jacob, and D.L. Mcdowell, Acta Mater. 55, 705 (2007).

ACCELERATED MD ANALYSIS FOR DISLOCATION NUCLEATION FROM GRAIN BOUNDARY (FCC)

$\Sigma 9 < 110 > \{221\}$ Grain boundary

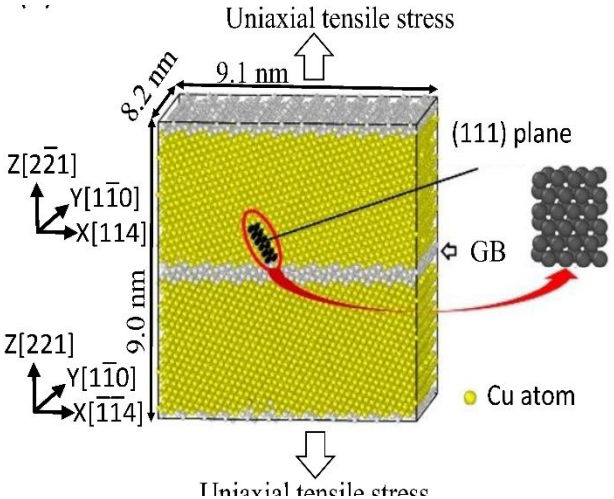

CV Boosting DOF

Relative displacement between centroids of group of atoms in adjacent (111) planes along [11-2]

$$\text{CV: } x = \boldsymbol{k} \cdot \left(\frac{\sum_i^{N_1} \boldsymbol{r}_i}{N_1} - \frac{\sum_j^{N_2} r_j}{N_2}\right),$$

Uniaxial tensile stress is applied by a fixed strain.

EAM potential: Mishin Y, Mehl M J, Papaconstantopoulos D A, et al. Physical Review B, 2001, 63(22): 224106.

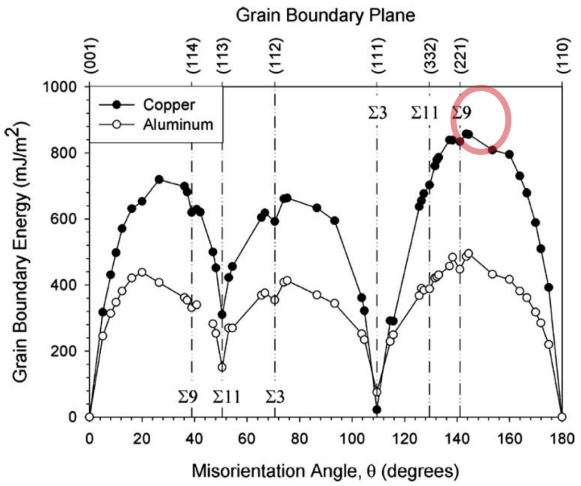

M.A. Tschopp, et al., Dislocation In Solids (2008)

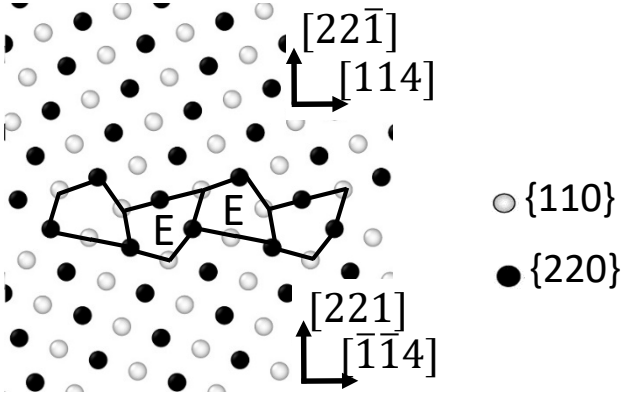

BOOST ENERGY AND ACCELERATION FACTOR

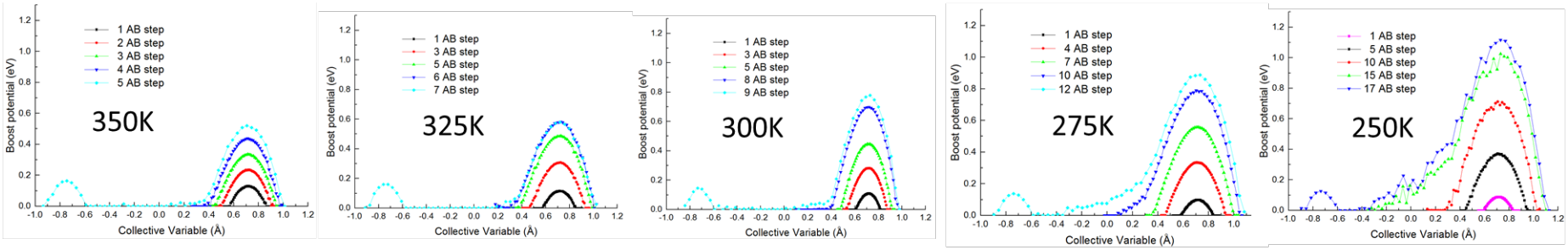

Boost energy at 2.4GPa and different temperature.

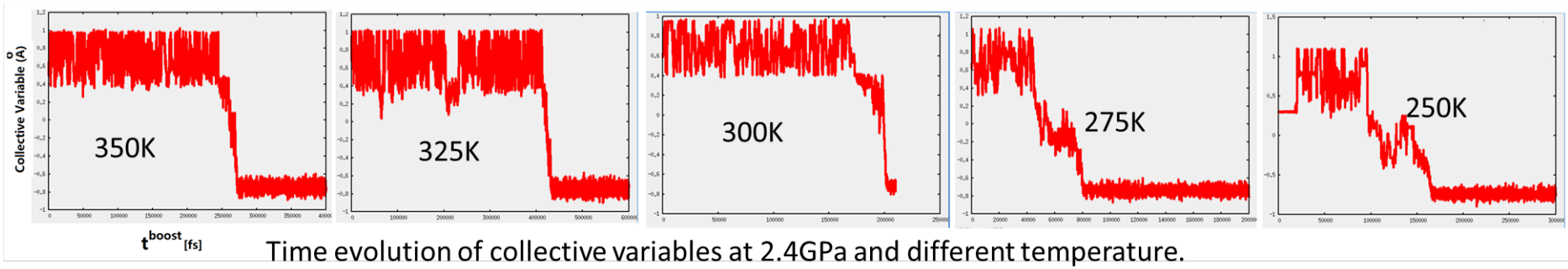

Time evolution of collective variables at 2.4GPa and different temperature.

Acceleration factor and typical time scale.

Temperature	350K	325K	300K	275K	250K
Acceleration factor	~10^{6}	~10^{8}	~10^{11}	~10^{14}	~10^{21}
Typical time scale	~10^{-4}[s]	~10^{-2}[s]	~10^{1}[s]	~10^{4}[s]	~10^{11}[s]

- **Acceleration factor (typical time scale) strongly depends on temperature**

DISLOCATION NUCLEATION PROCESS

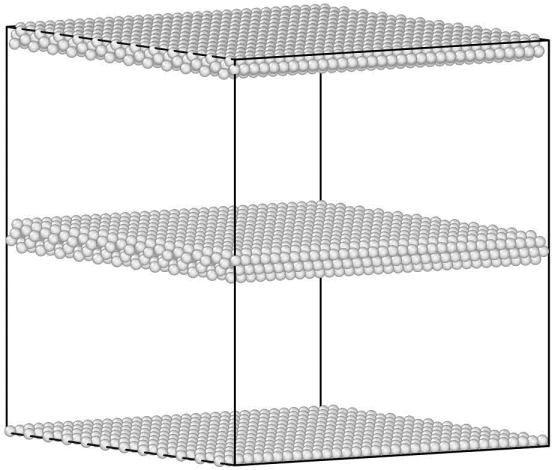

T=0K

Nudged elastic band calculation at 2.5GPa.
(24 replicas)

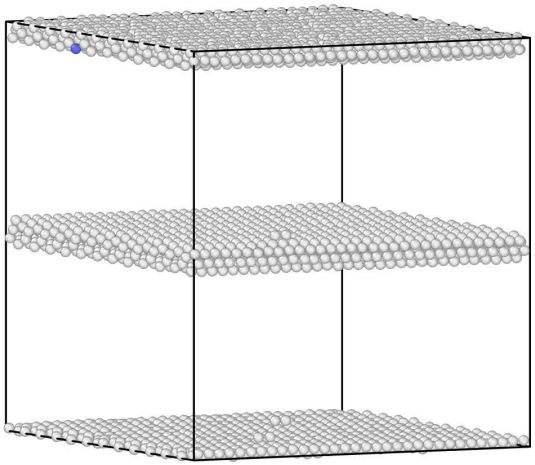

T=200K

AB(accel.)MD simulation at 2.5GPa.

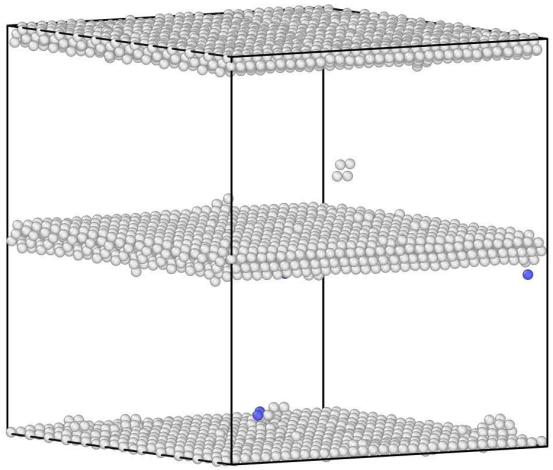

T=300K

AB(accel.)MD simulation at 2.5GPa.

- **Nucleated dislocation shape at saddle point becomes smaller with increasing temperature**

J.-P. Du, S. Ogata, PRB (2016).

TRANSITION OF DISLOCATION NUCLEATION PROCESS

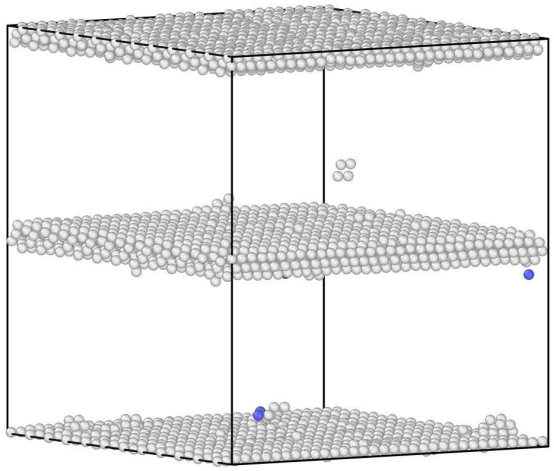

T=300K

ABMD simulation at 2.5GPa

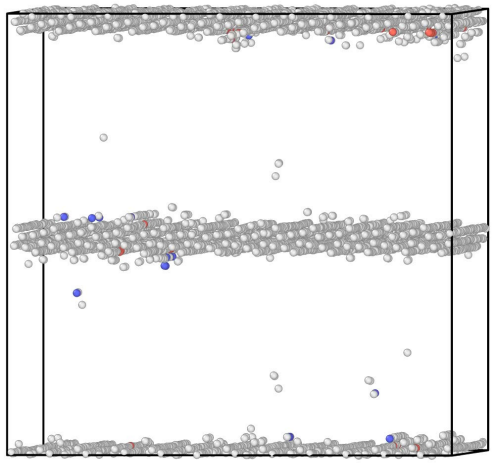

T=300K

Normal MD simulation at 2.81GPa

- **Transition from single to multiple nucleation with increasing applying stress seems to be happened**

J.-P. Du, S. Ogata, PRB (2016).

ACTIVATION FREE ENERGY OF GB DISLOCATION NUCLEATION

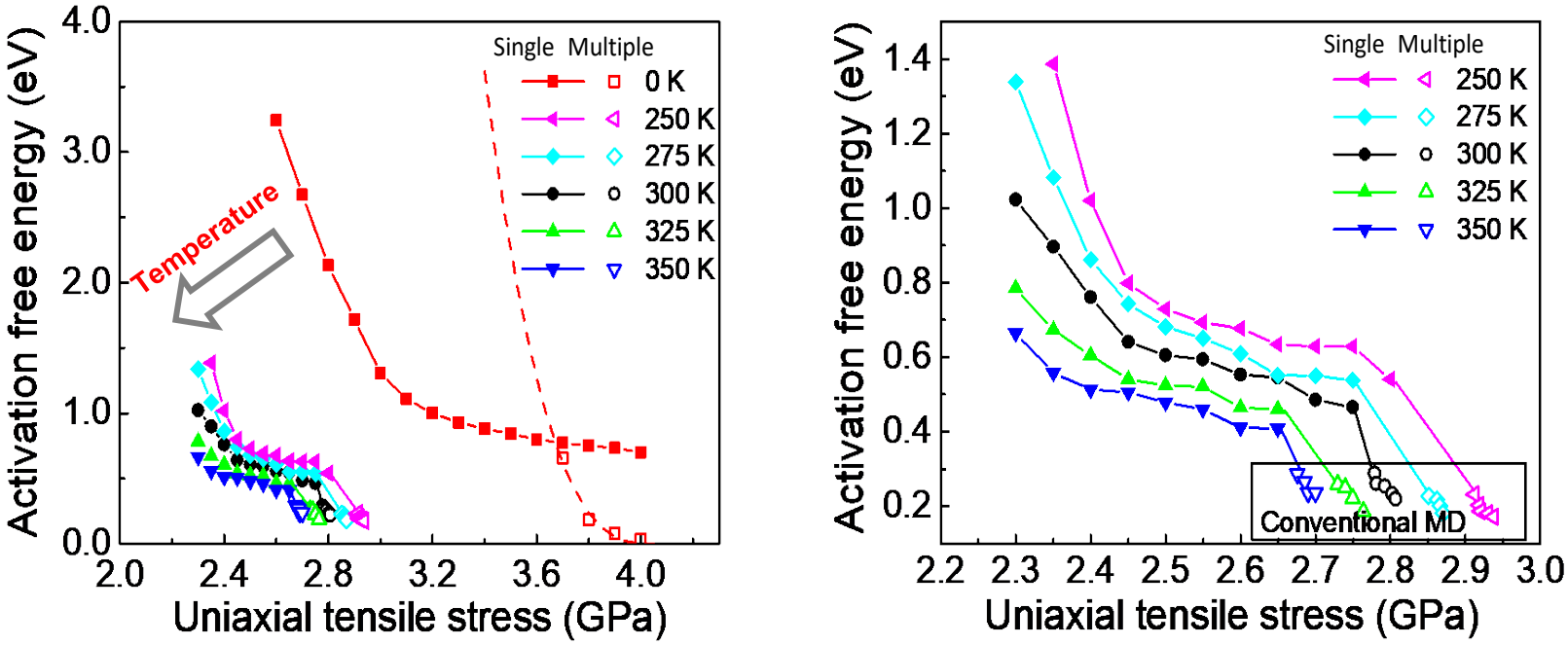

※ T = 0K: NEB, T > 0K: ABMD

Fig. Activation free energy – stress relationship.

- **Activation free energy exhibits very strong temperature dependency → Higher activation entropy**

J.-P. Du, S. Ogata, PRB (2016).

ACTIVATION VOLUME (STRESS SENSITIVITY OF FREE ENERGY BARRIER) CHANGE

This work

J.-P. Du, S. Ogata, PRB (2016).

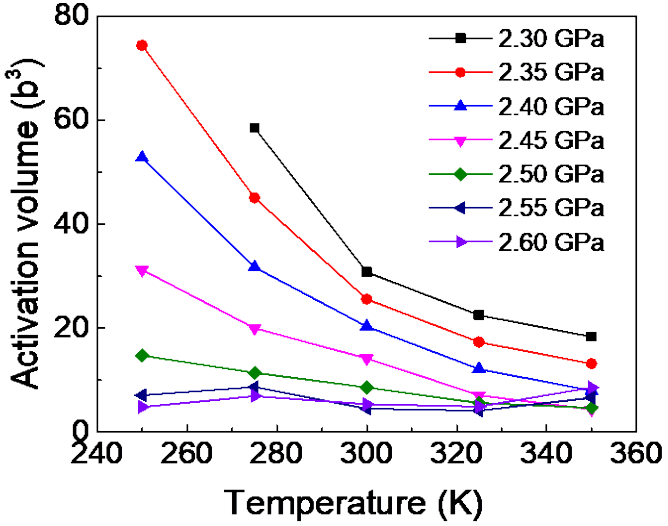

Exp.

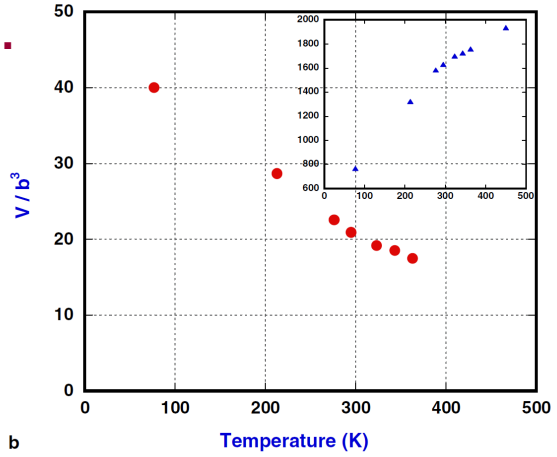

Fig. 5. (a) Strain rate sensitivity m vs. T for conventional coarse-grained Ni (circles) and 373 K, 1 h annealed nc Ni (squares). The data shown were obtained from the first cycle of the stress relaxation curve for each temperature. (b) Normalized apparent activation volume ($\Delta V/b^3$) vs. T for nc Ni (circles). The inset is the same plot for conventional coarse-grained Ni (triangles). Note the different temperature-dependent behavior of these two materials.

Theory

Wang Y.M. *et al.*, Acta Materialia, 2006, 54: 2715.

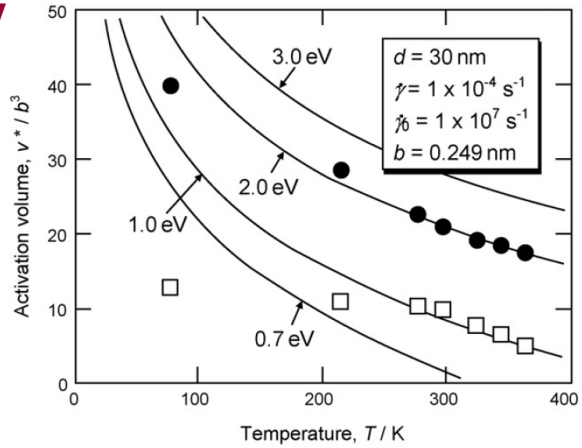

Fig. 4. Temperature dependence of the activation volume of NC Ni with $d = 30$ nm. The solid lines are the present theoretical predictions and closed circles and squares represent measured values for apparent activation volume and effective activation volume, respectively, obtained by Wang et al. [12].

Kato M., Materials Science and Engineering A, 2009, 516: 276.

微細結晶の降伏応力予測例

- 加速分子動力学解析 -

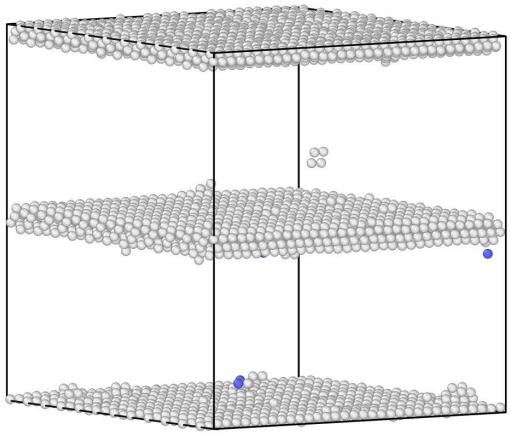

T=300K

ABMD simulation at 2.5GPa

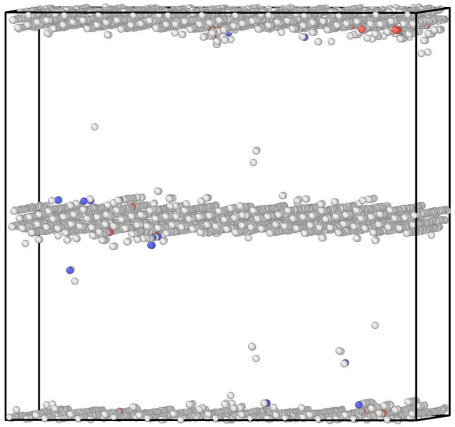

T=300K

Normal MD simulation at 2.81GPa

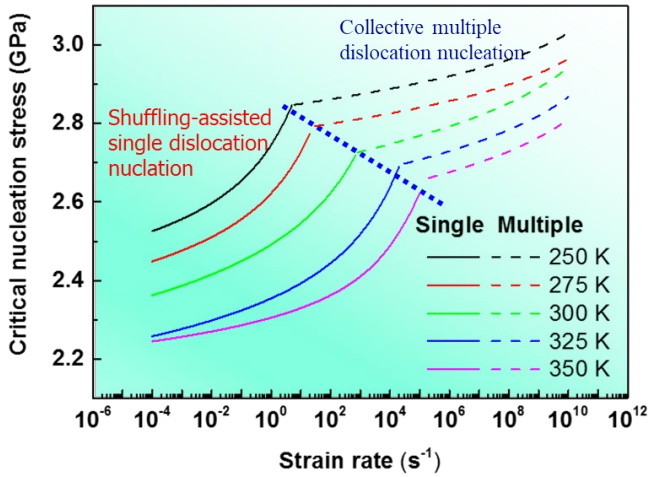

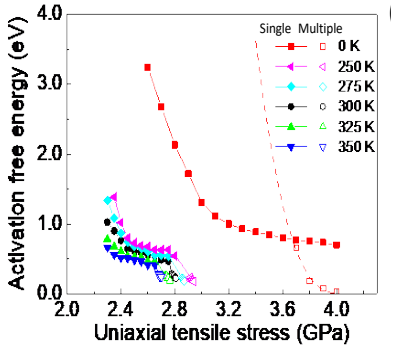

通常のひずみ速度では従来MD予測とは全く異なる転位発生機構となることを発見

J.-P. Du, S. Ogata, PRB (2016)

微細結晶の降伏応力予測例
- 実験との比較 -

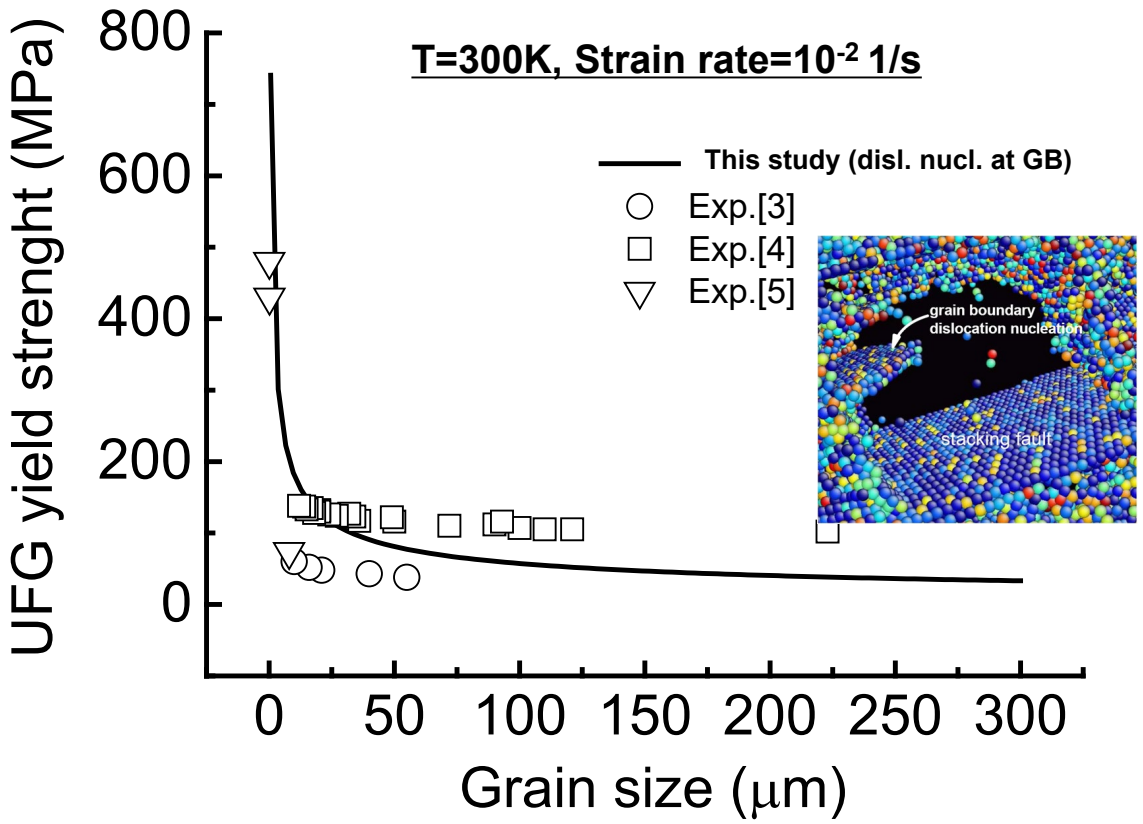

[1] Ogata S, Li J, Hirosaki N, et al. Physical Review B, 2004, 70(10): 104104.
[2] Eshelby J D. physica status solidi (b), 1963, 3(11): 2057-2060.
[3] Ono N, Karashima S. Scripta Metallurgica, 1982, 16(4): 381-384.
[4] Hansen N, Ralph B. Acta Metallurgica, 1982, 30(2): 411-417.
[5] Merz M D, Dahlgren S D. Journal of Applied Physics, 1975, 46(8): 3235-3237.

Stress induced by dislocations piled up at a grain boundary is [1]

$$\tau=\beta n(\tau^{\mathrm{ex}}-\tau_0),$$

where, $\tau^{\mathrm{ex}}$is external stress, *n is the number of dislocations piled up* [2]

$$n=\frac{d}{C\mu b}(\tau^{\mathrm{ex}}-\tau_0),$$

C and β are constants.

When $\tau=\tau_c^{GB}$, dislocation nucleates, which leads to the Hall-Petch relation[3] (τ_c^{GB} : the critical stress for dislocation nucleation from grain boundary)

$$\tau_c^{\mathrm{ex}}=\tau_0+\sqrt{\frac{\tau_c^{GB}C\mu b}{\beta d}}$$

$$\text{Yield Stress}(d)=2\tau_c^{\mathrm{ex}}$$

$b=0.26$ nm

$\mu=33.3$ GPa [1]

$C=\frac{\pi(2-\nu)}{4(1-\nu)}$, $\beta=0.5$, ν=0.33 [2]

原子論の時間スケール拡張のための手法 II
ー 動的モンテカルロ法 (kinetic Monte Carlo法) ー

Al-Cu合金GP-zone核生成

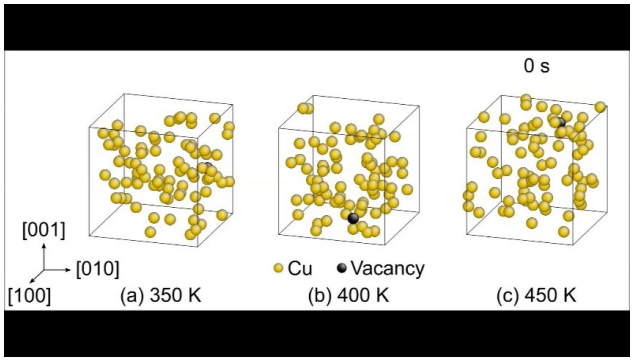

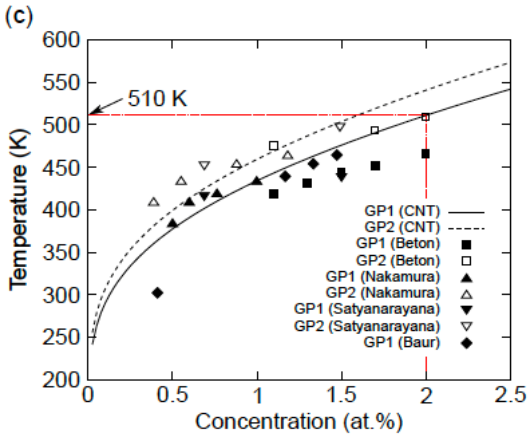

動的モンテカルロ法

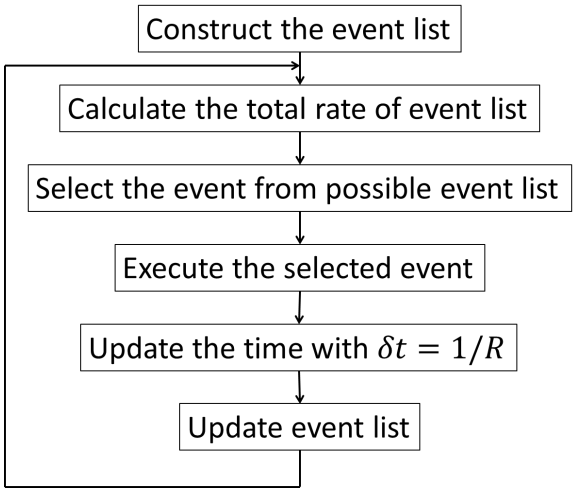

鉄合金中らせん転位運動

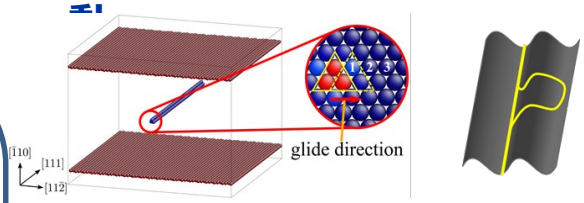

Possible kMC events :
Thermal activated **double kink nucleation** and **kink migration**

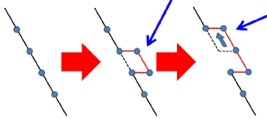

Thermal activated kink migration is possible when solutes affect kink migration process

Event rate for forward(+) / backward(-) dislocation motion

$$R_{\mathrm{kn}}^{+/-} = \nu_{\mathrm{kn}}^{0} \exp\left(-\frac{\Delta G_{\mathrm{kn}}^{+/-}(\tau)}{k_{\mathrm{B}}T}\right) \qquad R_{\mathrm{km}}^{+/-} = \nu_{\mathrm{km}}^{0} \exp\left(-\frac{\Delta G_{\mathrm{km}}^{+/-}(\tau)}{k_{\mathrm{B}}T}\right)$$

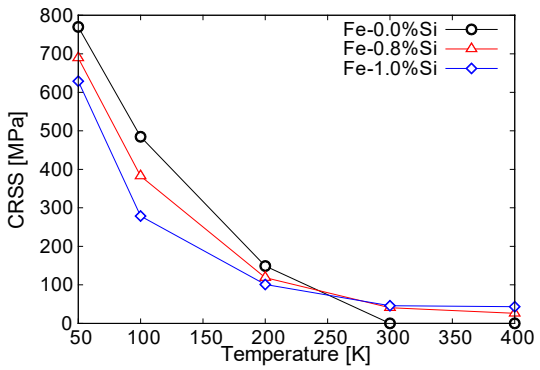

H.Miyoshi, H.Kimizuka, A.Ishii, S.Ogata, Acta Materialia (2019)
M.Wakeda, S.Ogata, et al., Acta Materialia (2017)
S.Shinzato, M.Wakeda, S.Ogata, Int. J. Plasticity, (2019).
T.Mohri, Y.Chen, M. Kohyama, S.Ogata, et al., npj Computational Materials (2017)

鉄合金の降伏強度の非経験的予測例

- 鉄合金降伏強度を支配するらせん転位運動のモデリング -

動的モンテカルロ法を用いた鉄合金中らせん転位運動のマルチスケールモデリング

Atomistic model to coarse grained kMC model

Screw dislocation described as line segments

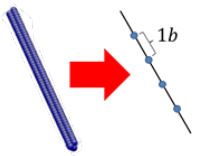

Each segments have length of unit Burgers vector

Dislocation segment moves on $(\bar{1}10)$ slip plane along $[11\bar{2}]$ direction

Dislocation moves in solute distributed field

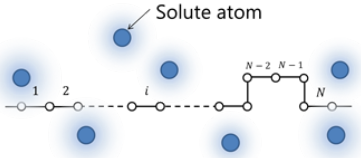

Algorithm of kMC simulation

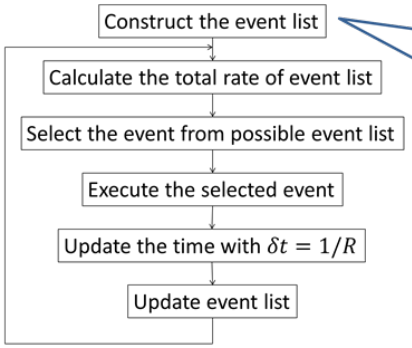

Possible kMC events :

Thermal activated **kink nucleation** and **migration**

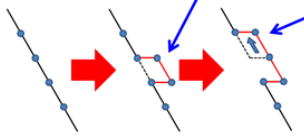

Thermal activated kink migration is possible when solute affects kink migration process

Event rate for forward(+) / backward(-) dislocation motion

$$R_{\mathrm{kn}}^{+/-} = \nu_{\mathrm{kn}}^{0} \exp\left(-\frac{\Delta G_{\mathrm{kn}}^{+/-}(\tau)}{k_{\mathrm{B}}T}\right) \qquad R_{\mathrm{km}}^{+/-} = \nu_{\mathrm{km}}^{0} \exp\left(-\frac{\Delta G_{\mathrm{km}}^{+/-}(\tau)}{k_{\mathrm{B}}T}\right)$$

Time evolution of dislocation with timestep δt

$$\delta t = \frac{1}{R} = \left[\sum_{i}^{N_{\mathrm{seg}}} \left(R_{\mathrm{kn},i}^{+/-} + R_{\mathrm{km},i}^{+/-}\right)\right]^{-1}$$

Screw dislocation

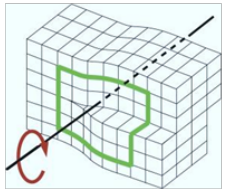

Dislocation motion with kink nucleation

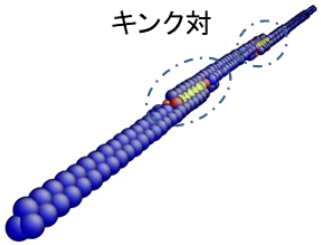

Dislocation motion and activities

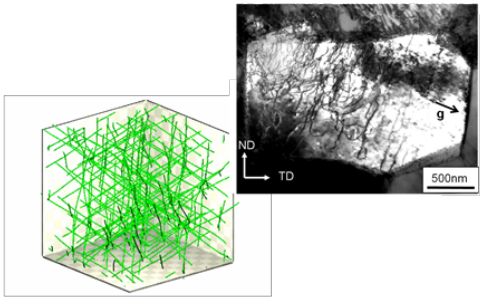

S.Shinzato, M.Wakeda, S.Ogata, Int. J. Plasticity, (2019).

欠陥間相互作用が示す非線形強度上昇

- 固溶元素と転位間の相互作用 -

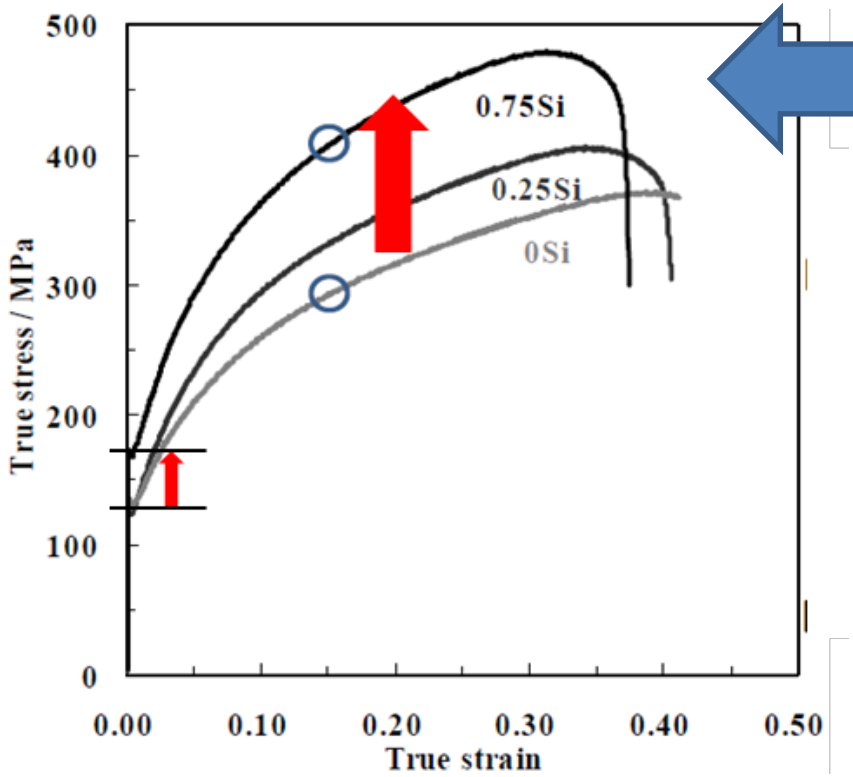

Dislocation-solute interaction (very strong nonlinearity)

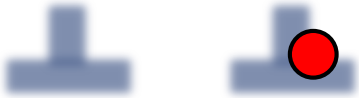

Theoretical prediction is still big challenge

鉄合金の降伏強度の非経験的予測例
- らせん転位運動の素過程の活性化障壁解析 -

Solute effect on elementary process of dislocation motion

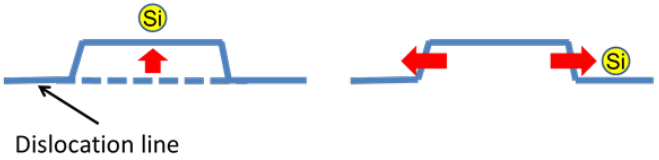

☐Solute effect on kink nucleation process

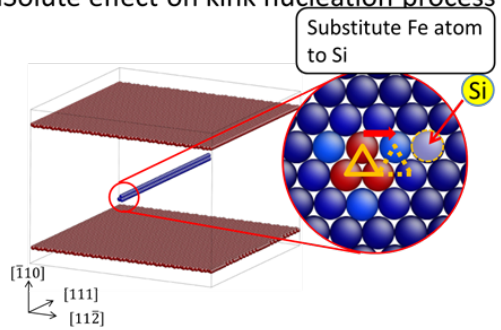

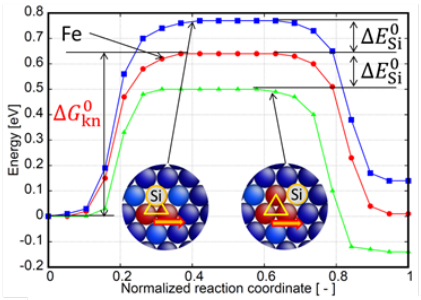

Activation energy varies due to Si doping

☐ Solute effect on kink migration process

Estimate an activation energy required to overcome Si atom

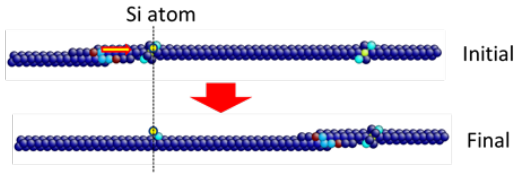

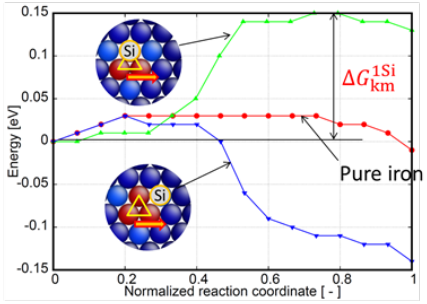

S.Shinzato, M.Wakeda, S.Ogata, Int. J. Plasticity, (2019).

鉄合金の降伏強度の非経験的予測例
- 合金中らせん転位運動の動的モンテカルロ解析 -

Change in interaction energy between moving dislocation and solutes

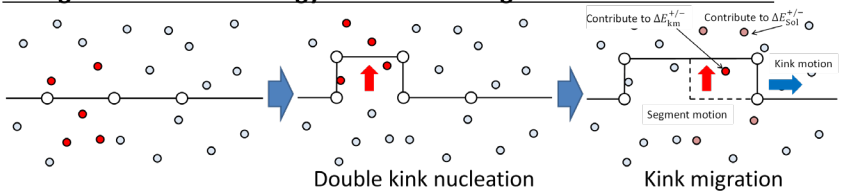

計算条件：Fe-1%Si, 300 K, 50 MPa

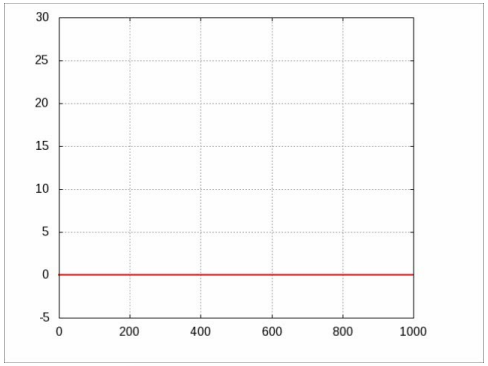

計算条件：Fe-3%Si, 300 K, 50 MPa

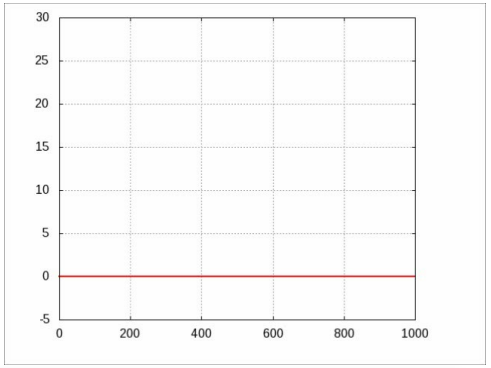

Solute effect on dislocation velocity

50 K

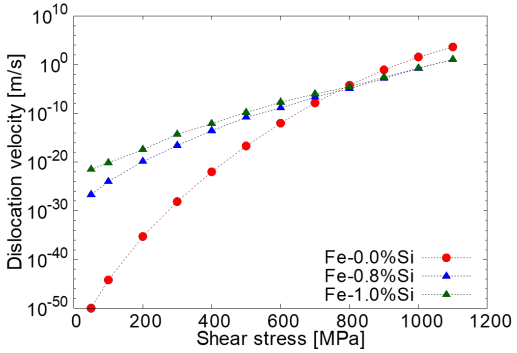

300 K

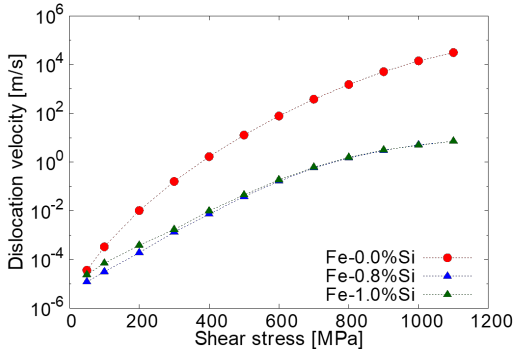

Solute effect on yield strength

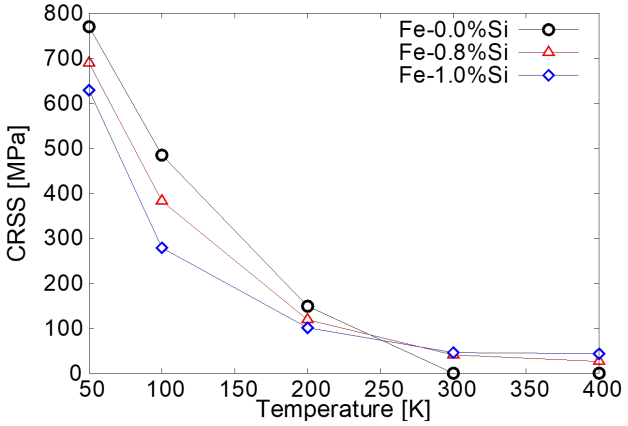

S.Shinzato, M.Wakeda, S.Ogata, Int. J. Plasticity, (2019).

鉄合金の降伏強度の非経験的予測例

- 様々な合金元素における降伏強度予測（実験との比較） -

実験値との比較

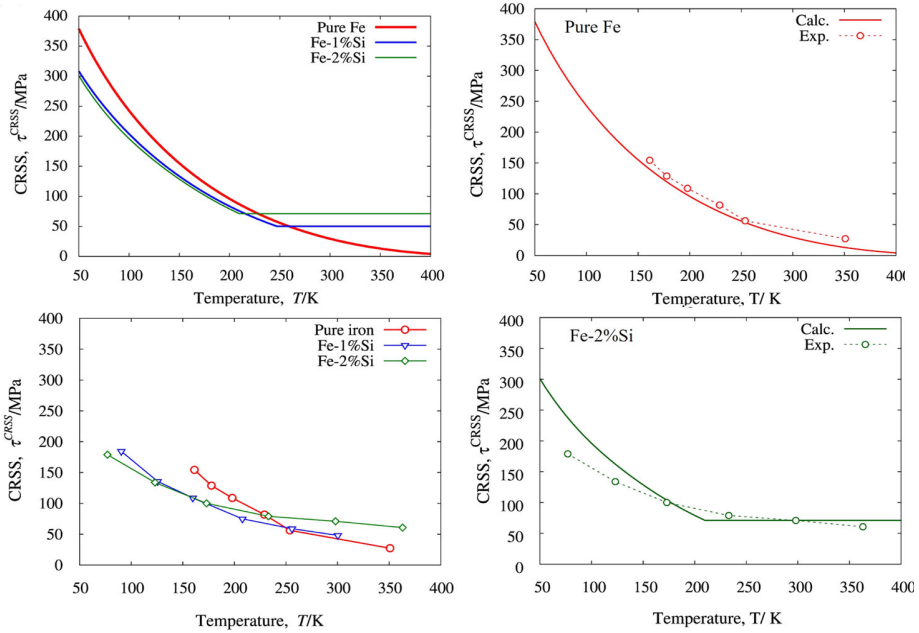

Mohri, Chen, Kohyama, Ogata, et al., npj Computational Materials (2017)

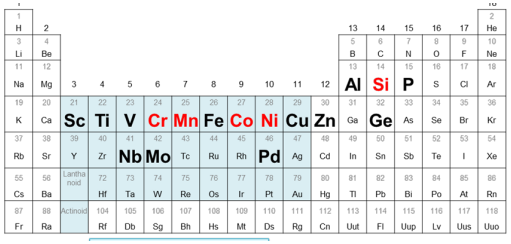

様々な鉄合金の降伏強度予測

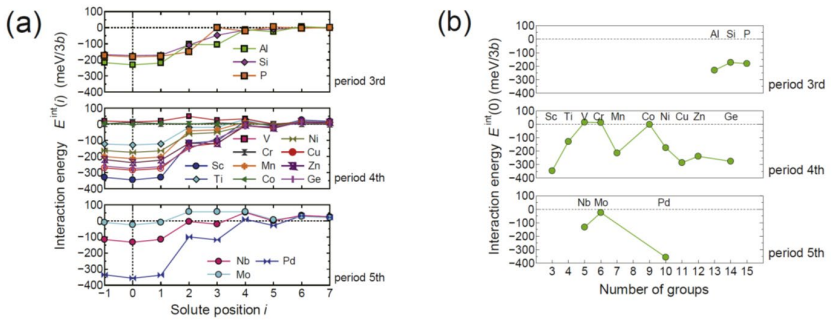

Fig. 5. The interaction energy between a screw dislocation with Easy-core and solute atoms. (a) Dislocation-solute interaction energies as a function of the solute position i (from −1 to 7), which is depicted in Fig. 3. (b) The interaction energies with solute atoms at $i = 0$. The solute elements are classified and represented by the period of the periodic table in (a) and (b), and the elements are ordered by the group in (b).

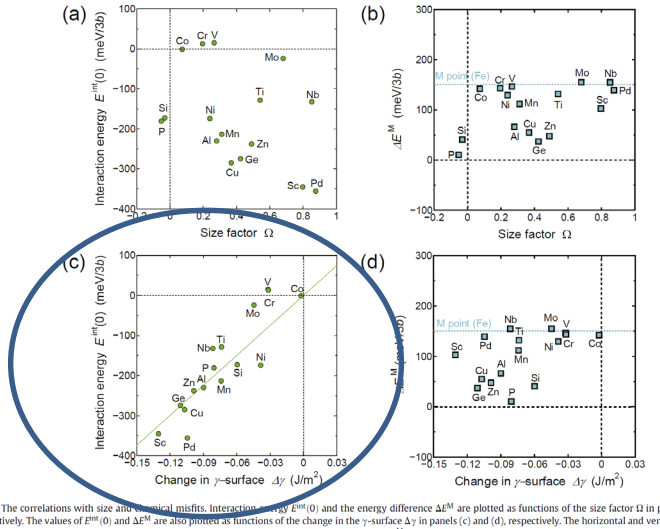

Fig. 7. The correlations with size and chemical misfits. Interaction energy $E^{int}(0)$ and the energy difference ΔE^M are plotted as functions of the size factor Ω in panels (a) and (b), respectively. The values of $E^{int}(0)$ and ΔE^M are also plotted as functions of the change in the γ-surface $\Delta\gamma$ in panels (c) and (d), respectively. The horizontal and vertical black dashed lines represent the zero level in all the panels, while blue horizontal lines in (b) and (d) represent ΔE^M of pure Fe. The solid green line in (c) represents the least squares fitting of the data. (For interpretation of the references to colour in this figure legend, the reader is referred to the web version of this article.)

Wakeda, Ogata, et al., Acta Materialia (2017)

鉄合金の降伏強度の非経験的予測例

- 固溶元素が与える転位運動への影響 -

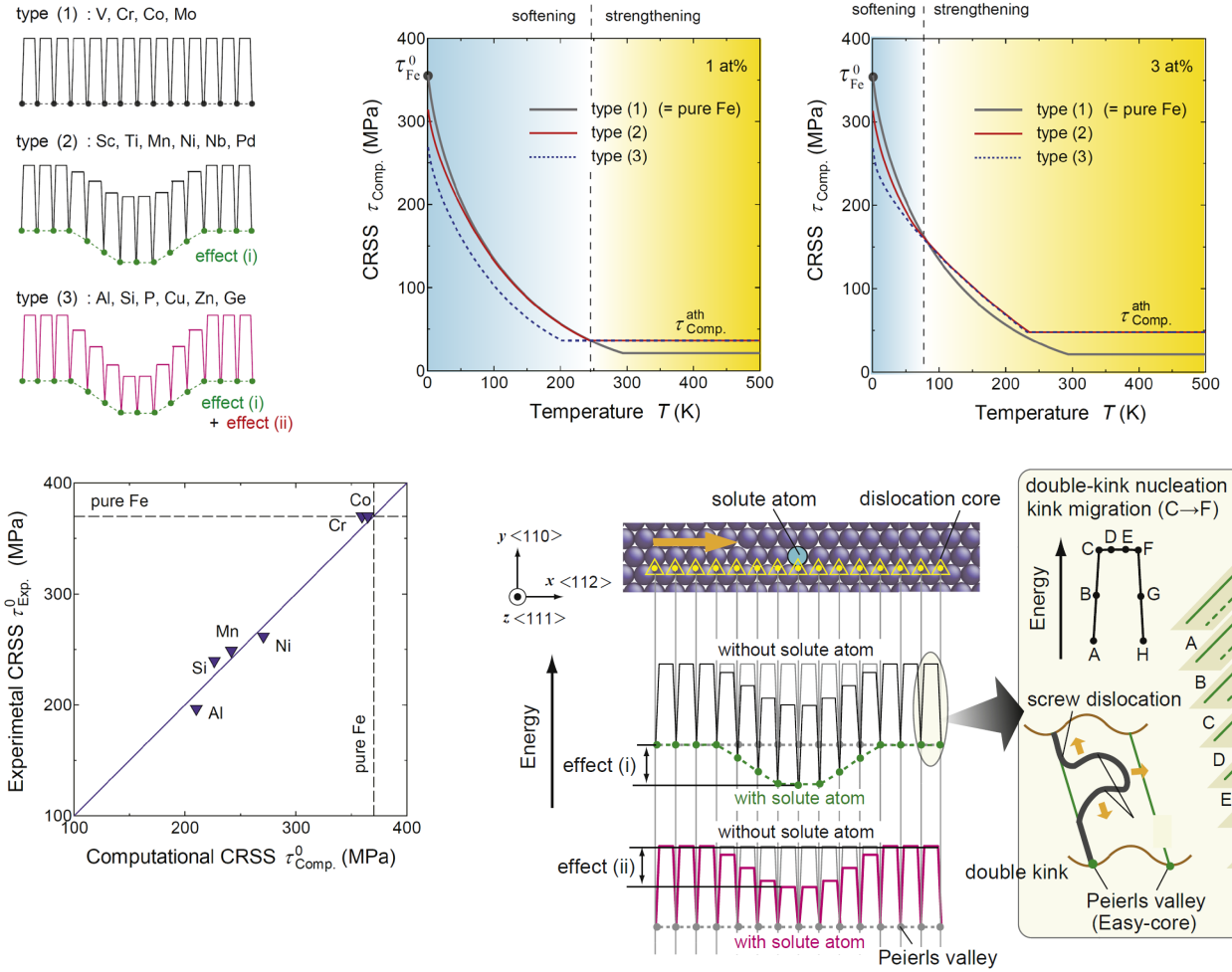

Wakeda, Ogata, et al., Acta Materialia (2017)

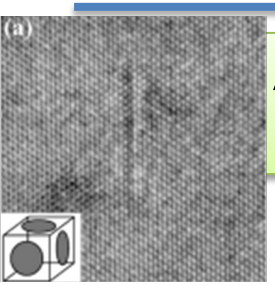

1] T. Sato, J. JILM, **56**, 592 (2006)

Al-Cu合金中のGP zone（Cu析出）核生成解析
- kinetic Monte Carlo + Classical Nucleation Theory -

空孔拡散による核生成過程kMC解析

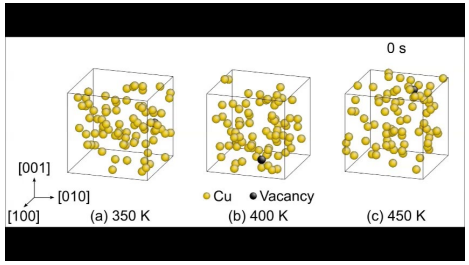

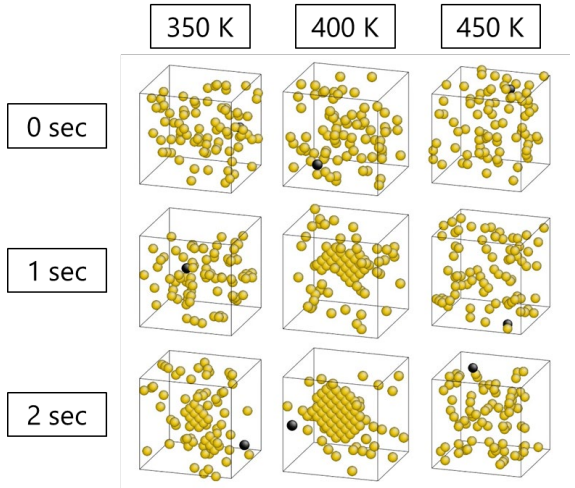

核生成臨界核サイズ予測

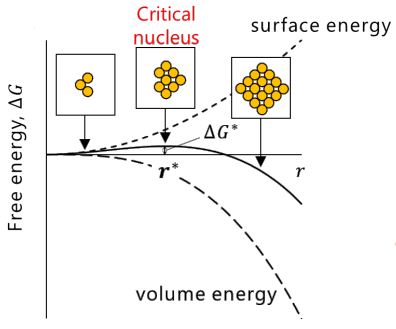

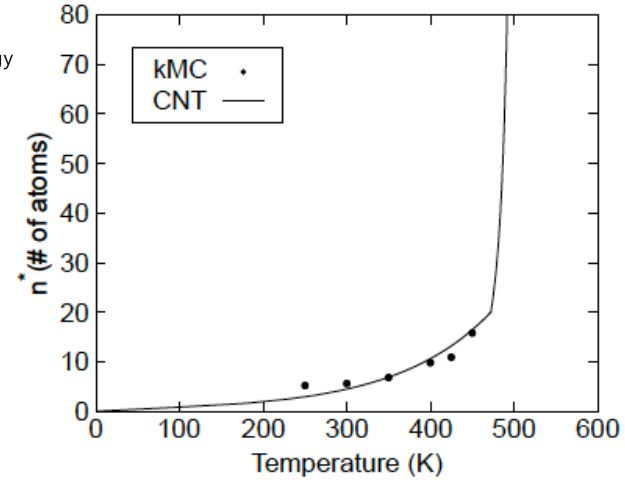

核生成臨界温度予測

$$T = \frac{\Delta H(n^* + 1) - \Delta H(n^* - 1)}{2k_B \ln x}$$

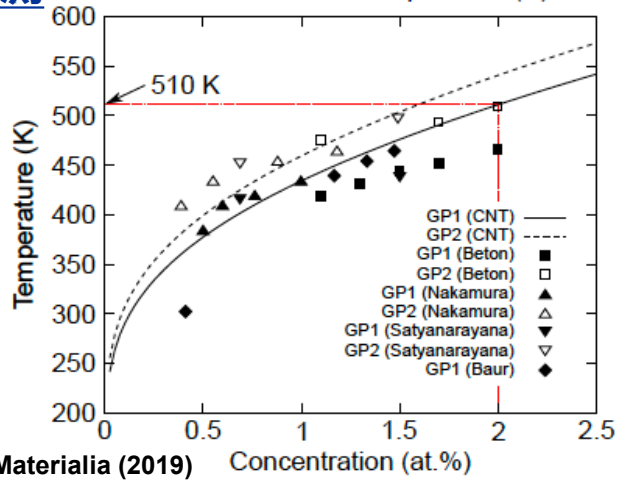

H. Miyoshi, H.kimizuka, A.Ishii, S.Ogata, Acta Materialia (2019)

内容

- **イントロダクション**　原子論からの材料力学特性のモデリングと材料設計　～マルチスケールの観点から
- **ナノ力学**　原子論からのナノ材料力学の特異性の検討
- **原子論における時間スケール拡張への挑戦**　原子解像度で長時間現象を予測する
- **原子論によるマルチフィジクスへの挑戦**
  水素や酸素などの力学特性への影響　～力学・化学・物理
- **材料設計への展開**　強度と延性、靭性を両立した材料設計

耐環境性の解析
- 水素による破壊（粒界破壊）メカニズム① -

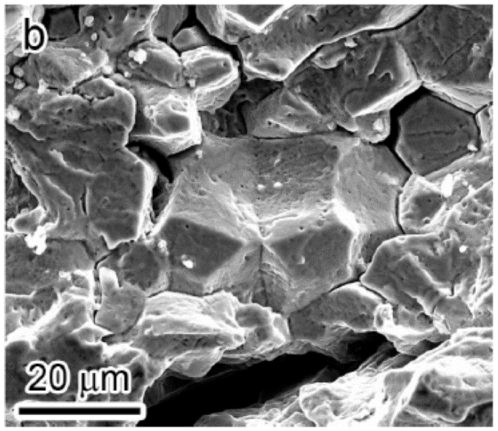

Hydrogen-induced **intergranular** fracture surface of a commercial grade pure Fe

S. Wang et al., Acta Mater., 2014

■ Σ9-GB → 水素濃度高

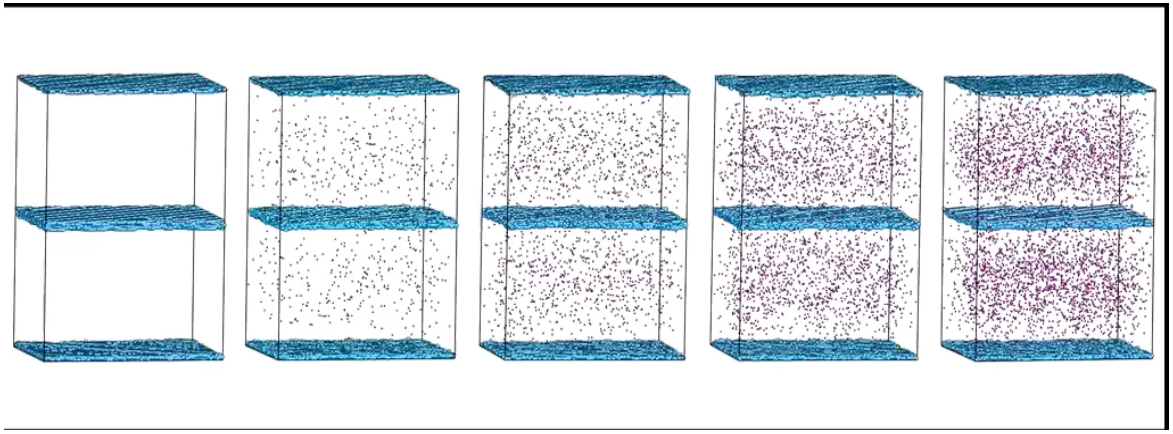

転位と粒界との衝突による粒界構造のみだれに水素が反応し破壊起点に

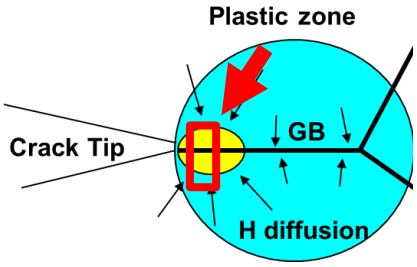

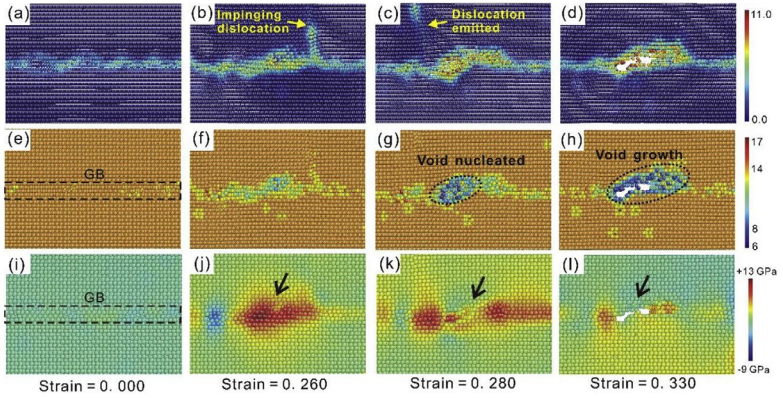

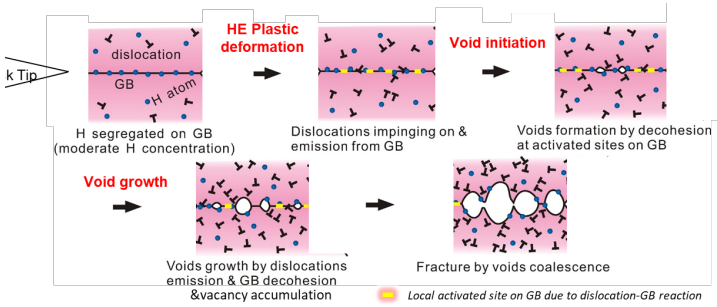

L.Wan, S.Ogata et al., Int. J. Plasticity（2019）

Fe-H系高信頼性ニューラルネットワーク原子間相互作用(NNP)の構築

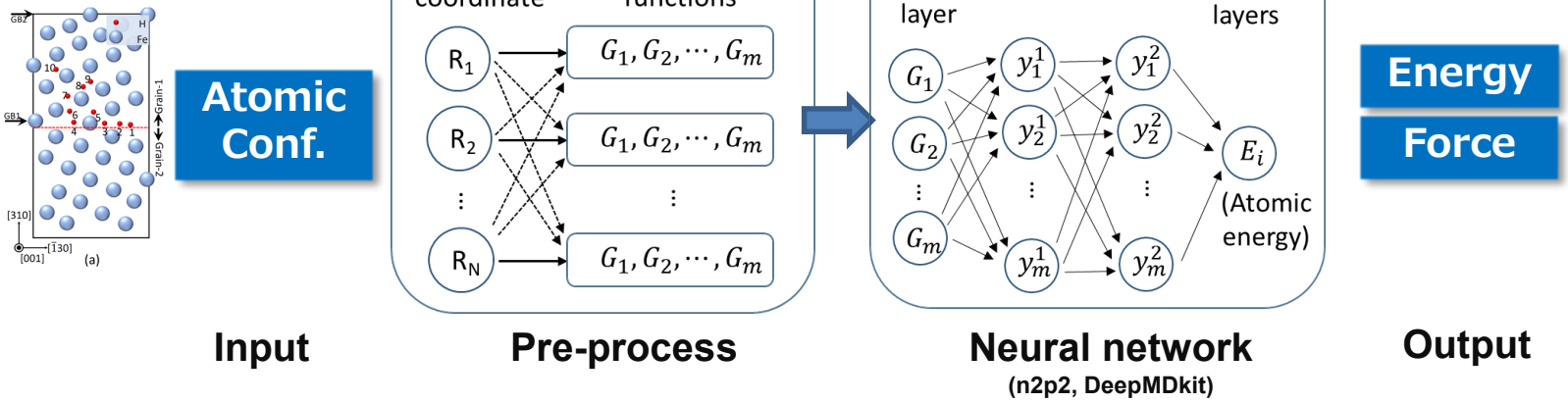

Training database (DFT based) and potential files (n2p2 version) are available at

https://github.com/mengfsou/NNIP-FeH

Fan-Shun Meng, et al., Phys. Rev. Materials, 5, 113606 (2021)

DeepMDkit version (100x faster)

学習用データセット（第一原理計算）

Subset (i)
(1) Tensile and shear deformation, and volume expansion of ±2.5% and 0% in the α-iron supercell, respectively.
(2) Monovacancy to quadravacancy-complexes with various configurations.
(3) Self-interstitial atoms (SIA) with various configurations.
(4) Low index surfaces including (001), (110), (111), (112), (210), and (310).
(5) γ-surface for (110) and (112) planes.
(6) Atomic clusters with one to four atoms, Bain path.
(7) Transition states in the monovacancy diffusion pathway,
(8) Symmetric tilt GBs with tilt axes of ⟨001⟩ ⟨110⟩ and ⟨111⟩.
(9) Dislocation structures.
(10) Inherent structures in the liquid state.

Subset (ii)
(11) Isolated H atom, H_2 molecule, H_2+H cluster and H_2 + H_2 cluster, H_2 molecular clusters.

Subset (iii)
(12) H atoms in the structures of the above (1), (2), (4), (8), H_2 molecule above the surfaces in the structures of (4), and H atoms in a nano-void with 9-vacancy.
(13) H atoms in the structures of (7) and (9).

Fan-Shun Meng, et al., Phys. Rev. Materials, 5, 113606 (2021)

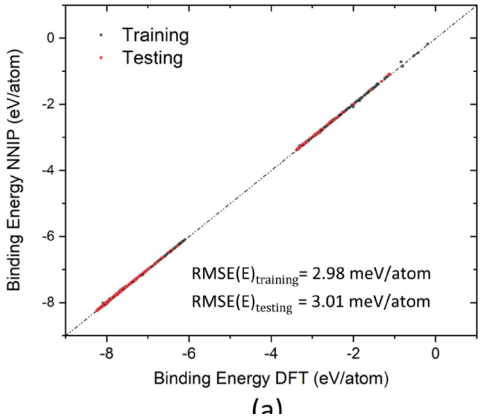

(a)

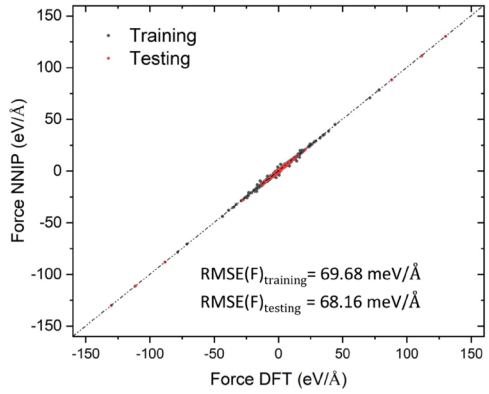

(b)

NNPのパフォーマンス (pure Fe properties)

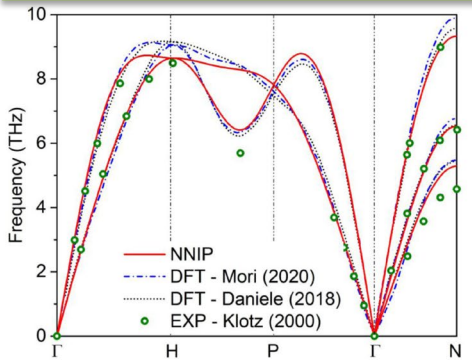

Phonon

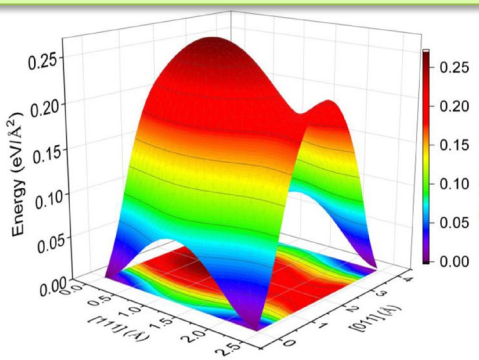

γ-surface (112)

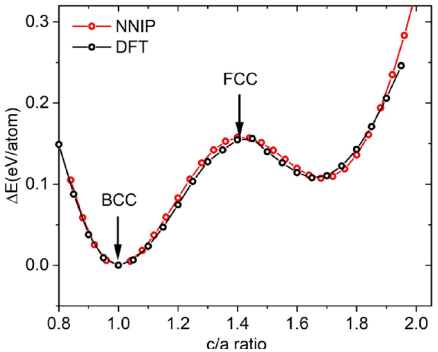

Bain path

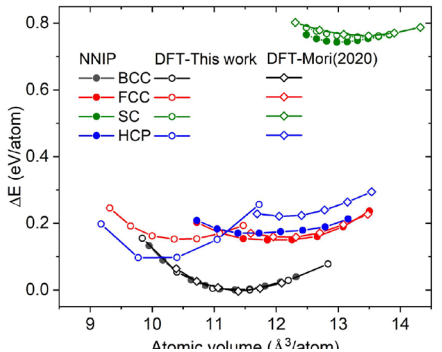

Energy-volume (BCC, FCC, SC, HCP)

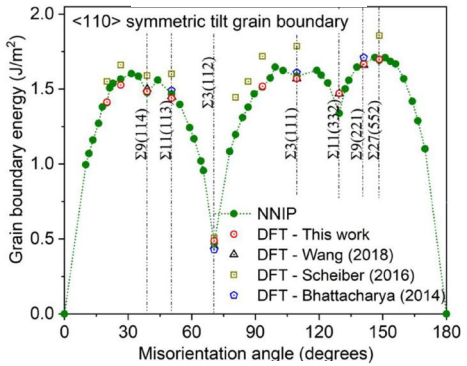

Tilt GB energy

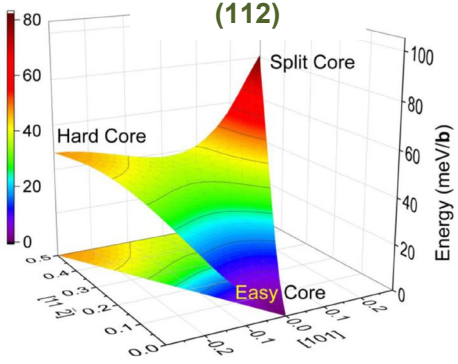

Energy for Screw dislocation core motion

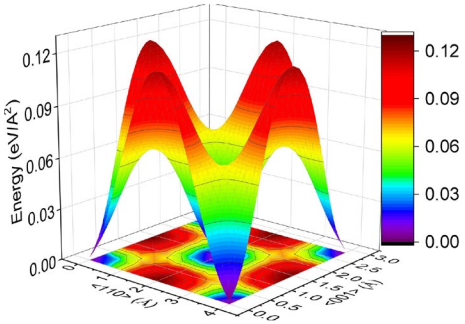

γ-surface (110)

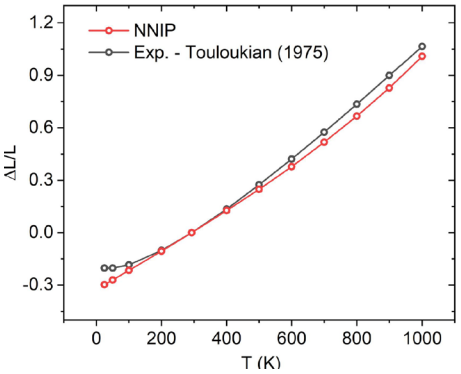

Thermal expansion

Fan-Shun Meng, et al., Phys. Rev. Materials, 5, 113606 (2021)

NNPのパフォーマンス (screw dislocation motion in pure Fe)

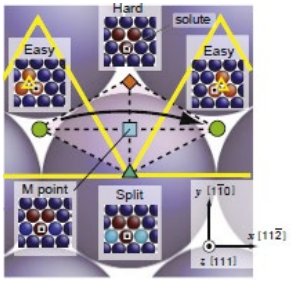

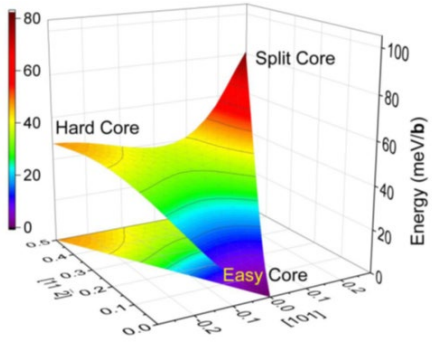

Energy surface with respect to screw dislocation core position

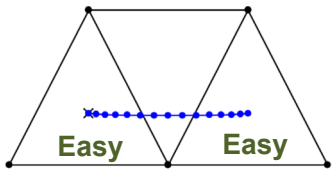

MEP of screw dislocation motion (D.Rodney, private communication)

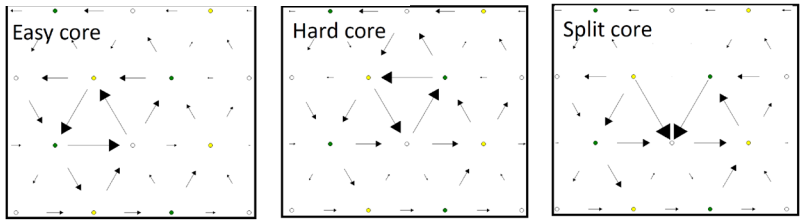

Screw dislocation core structures

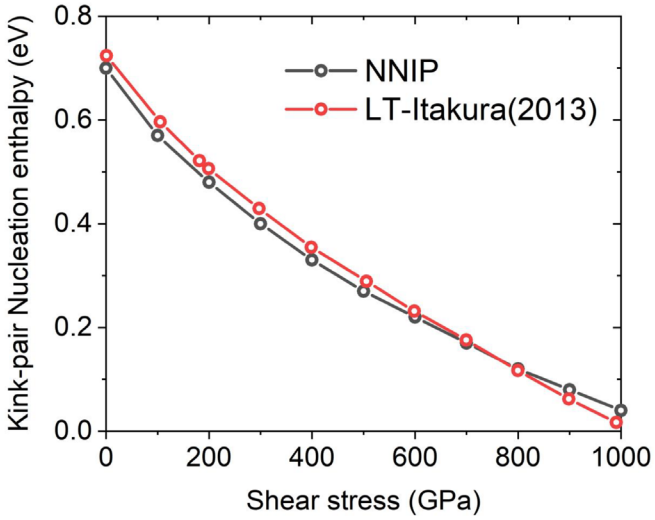

Energy barrier for kink-pair nucleation energetics

Fan-Shun Meng, et al., Phys. Rev. Materials, 5, 113606 (2021)

NNPのパフォーマンス (Vac. – H and GB - H interactions)

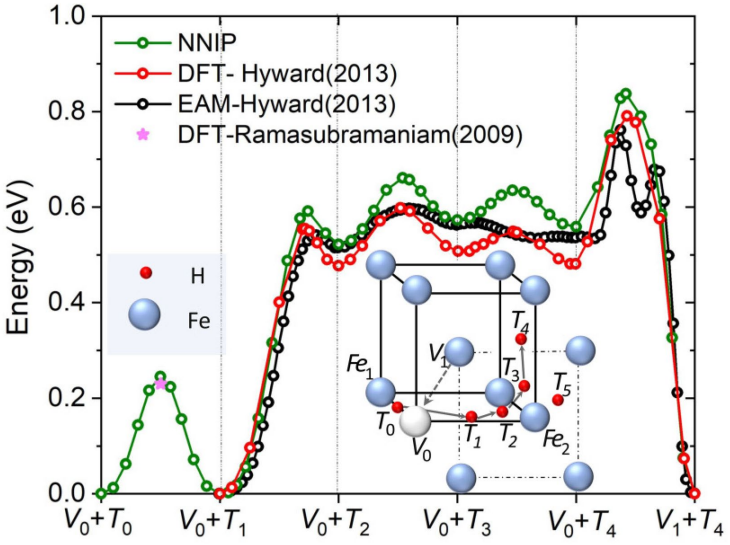

H-V complex formation energy and H migration energy

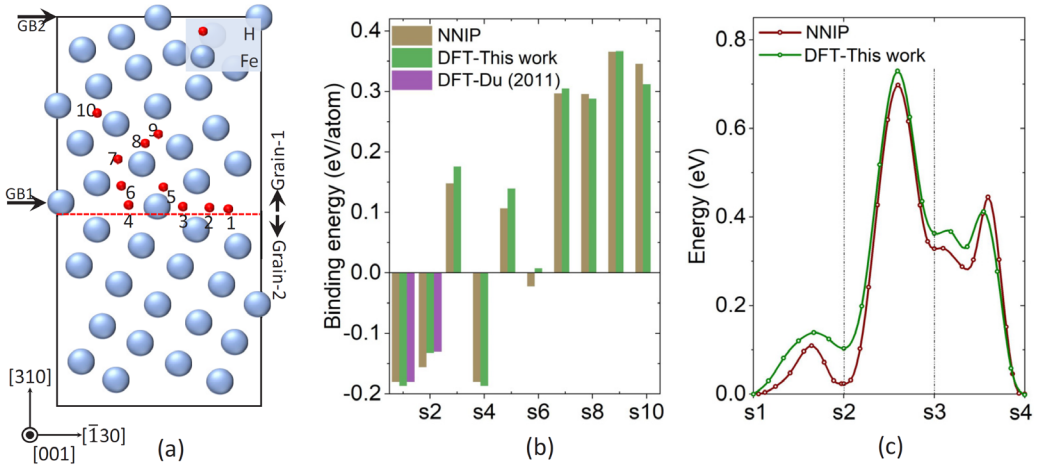

Solution energy and migration energy at GB

Fan-Shun Meng, et al., Phys. Rev. Materials, 5, 113606 (2021)

NNPのパフォーマンス (Screw dis. - H interactions)

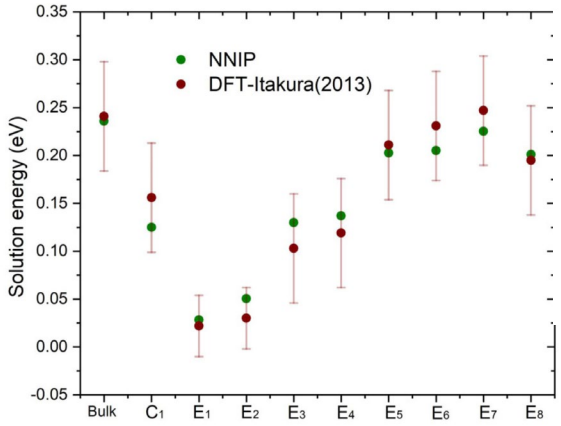

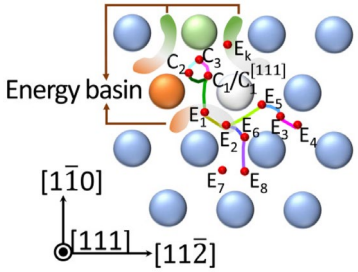

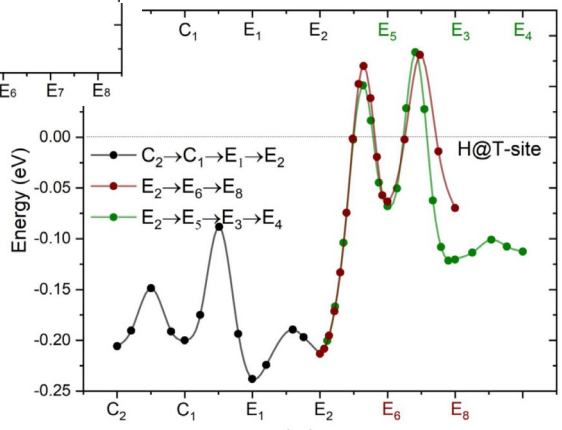

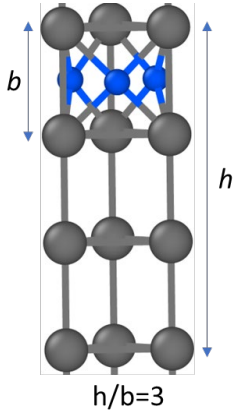

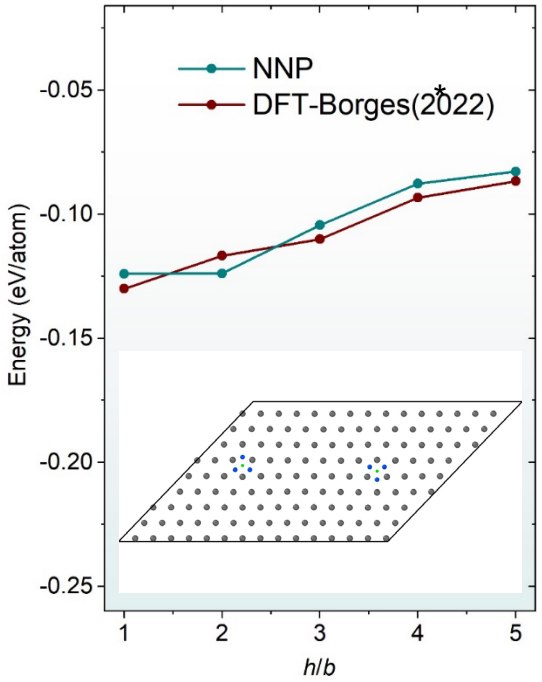

Solution and migration energies around screw core (easy core)

Fan-Shun Meng, et al., Phys. Rev. Materials, 5, 113606 (2021)

Hard core stabilization by Hs

*Pedro P.P.O.Borges, et al., Acta Materialia, 234, 118048 (2022)

NNPのパフォーマンス (H - Fe-surface reaction)

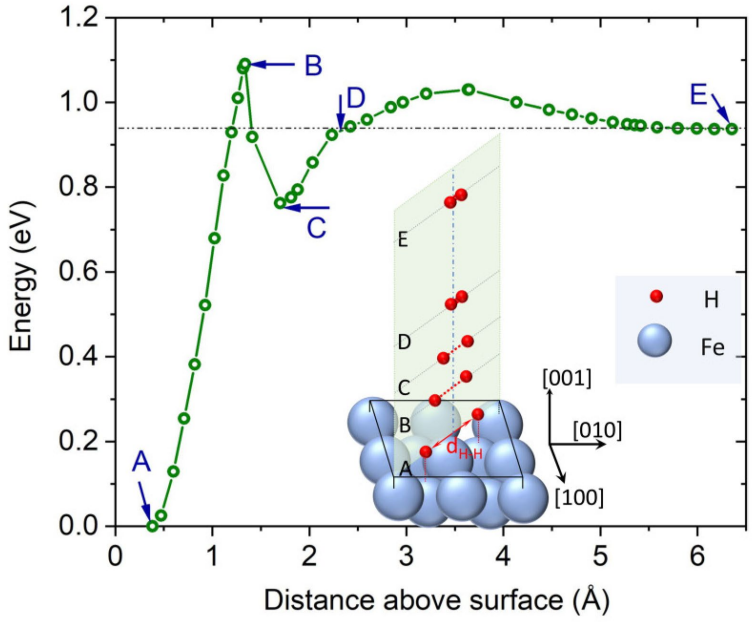

H – Fe-surface reaction
(dissociation and formation of H_2 molecule)

Fan-Shun Meng, et al., Phys. Rev. Materials, 5, 113606 (2021)

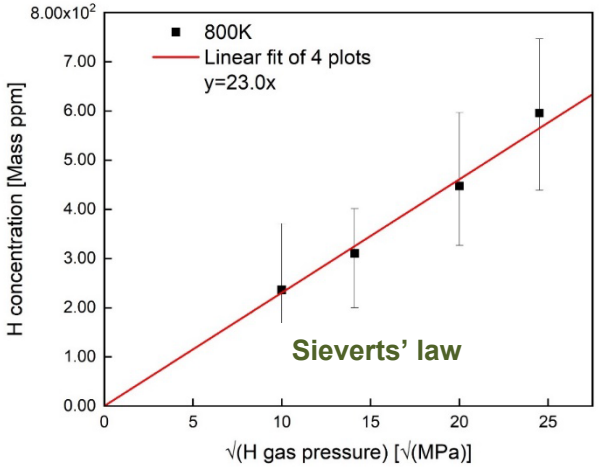

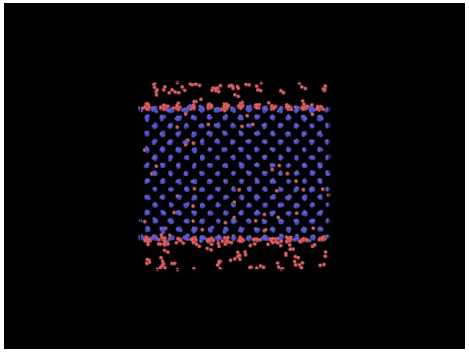

Thermodynamics - H-defect thermodynamic interaction
欠陥にトラップされた水素の昇温脱離 (GCMC解析)

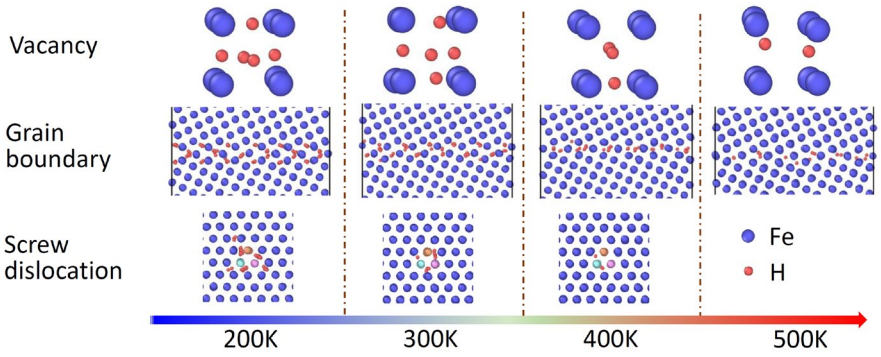

Grand Canonical Monte Carlo simulation (GCMC)
(bulk H concentration: 40appm)

Fan-Shun Meng, et al., Phys. Rev. Materials, 5, 113606 (2021)

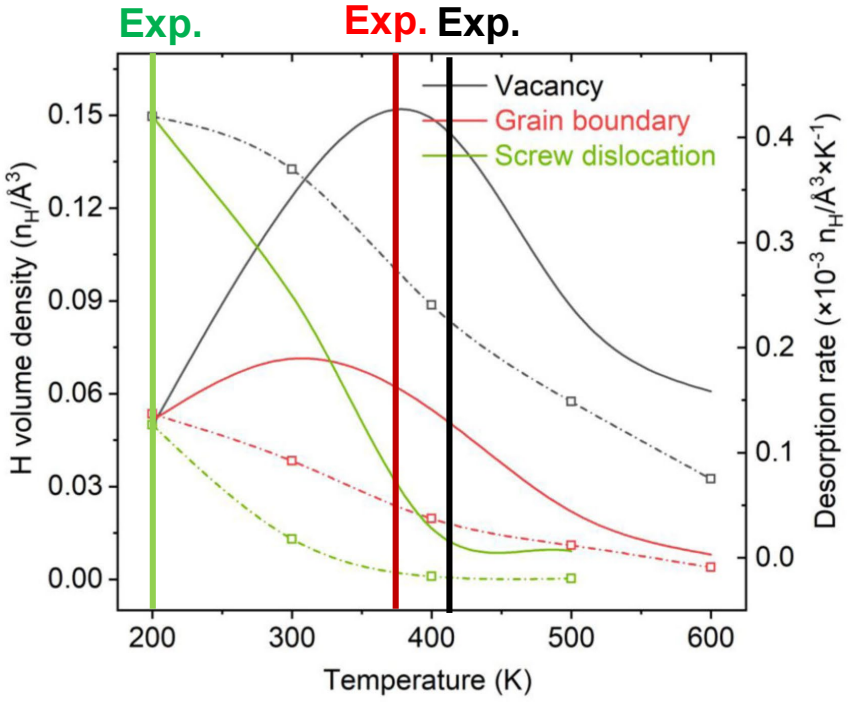

Thermal Desorption Spectroscopy (TDS) Exp.:
M. Iwamoto and Y. Fukai, Mater. Trans. JIM 40 (1999) 606.
K. Ono and M. Meshii, Acta Metall. Mater. 40 (1992) 1357.

Kinetics –Hydrogen diffusion
らせん転位に沿った水素拡散 (MD解析)

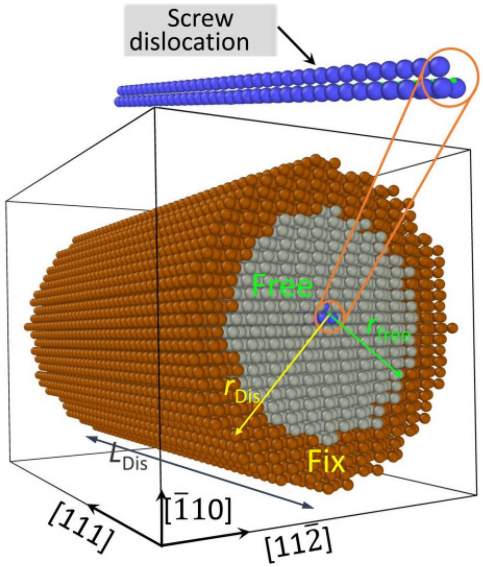

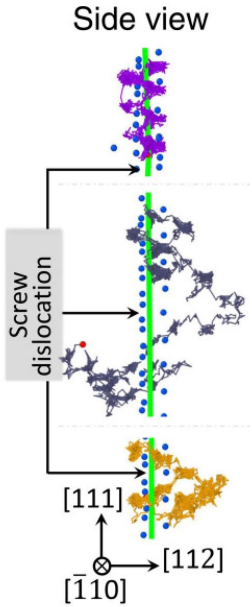

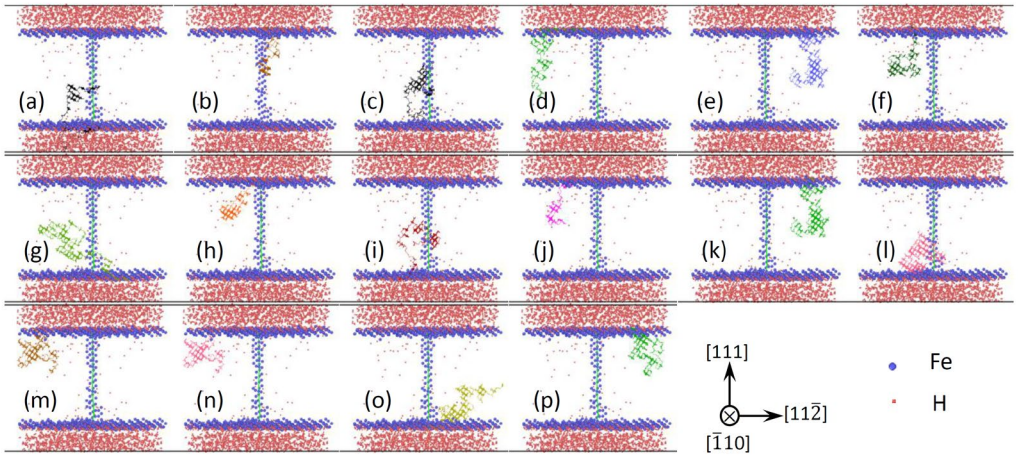

- Diffusivity along screw core is lower than diffusivity in bulk
- But, H mostly flows around screw core because of H-Dis attractive interaction

Fan-Shun Meng, et al., Phys. Rev. Materials, 5, 113606 (2021)

Kinetics –Hydrogen diffusion
なぜらせん転位が高速拡散経路にならないのか?

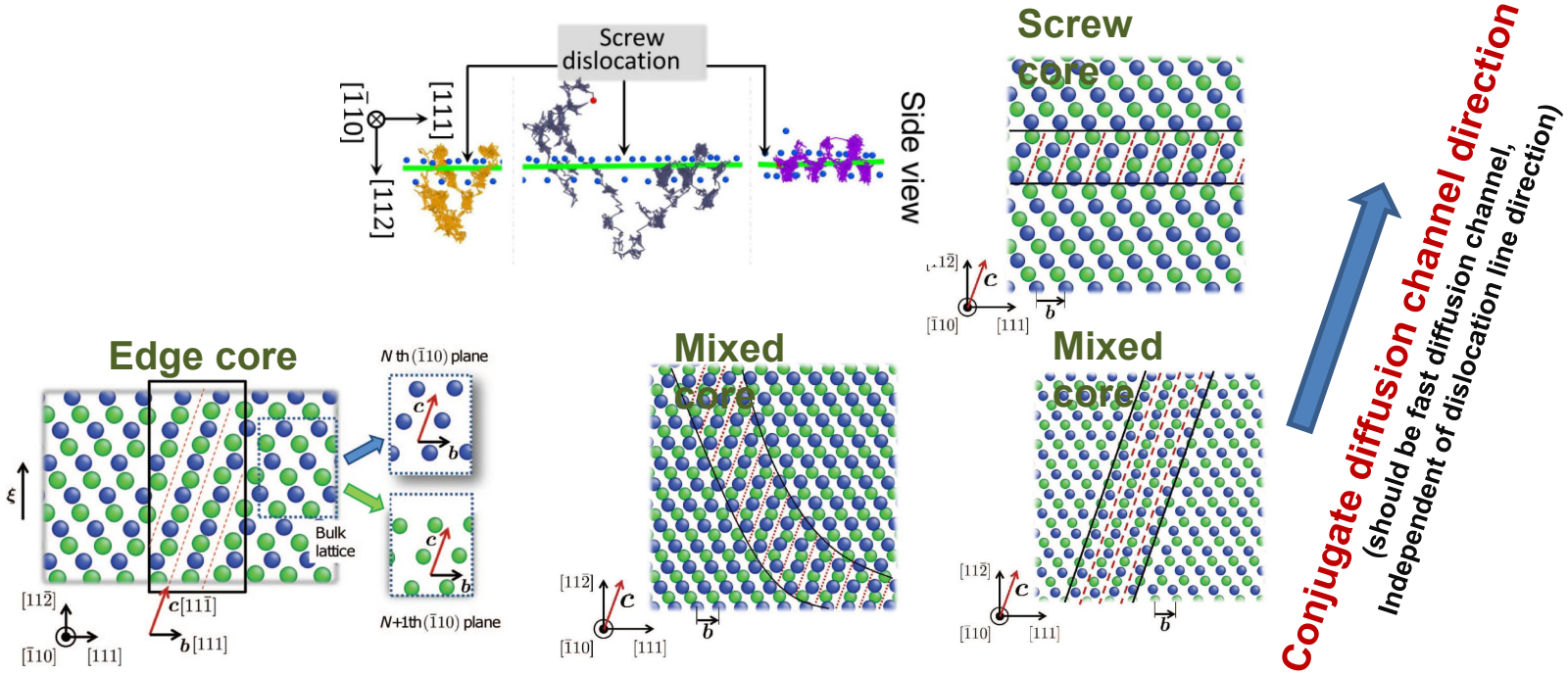

A.Ishii, J.Li, S.Ogata, PLOS One, 8 (2013) e60586.

- Screw core is not the fast diffusion path because Hydrogen should cross the density-packed atomic plane.

Kinetics –Hydrogen diffusion

Σ5傾角粒界に沿った水素拡散 (MD解析)

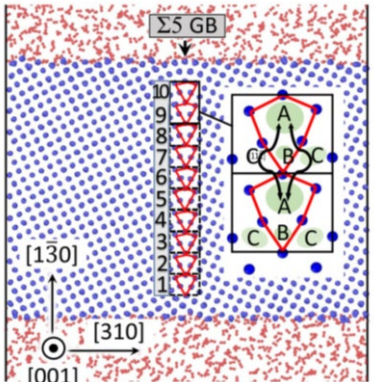

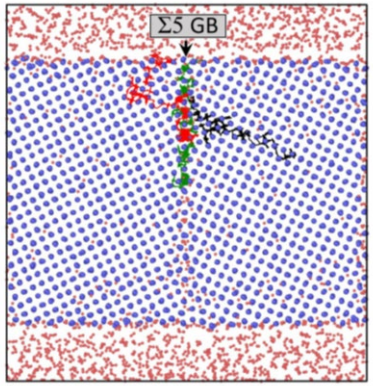

Fan-Shun Meng, et al., Phys. Rev. Materials, 5, 113606 (2021)

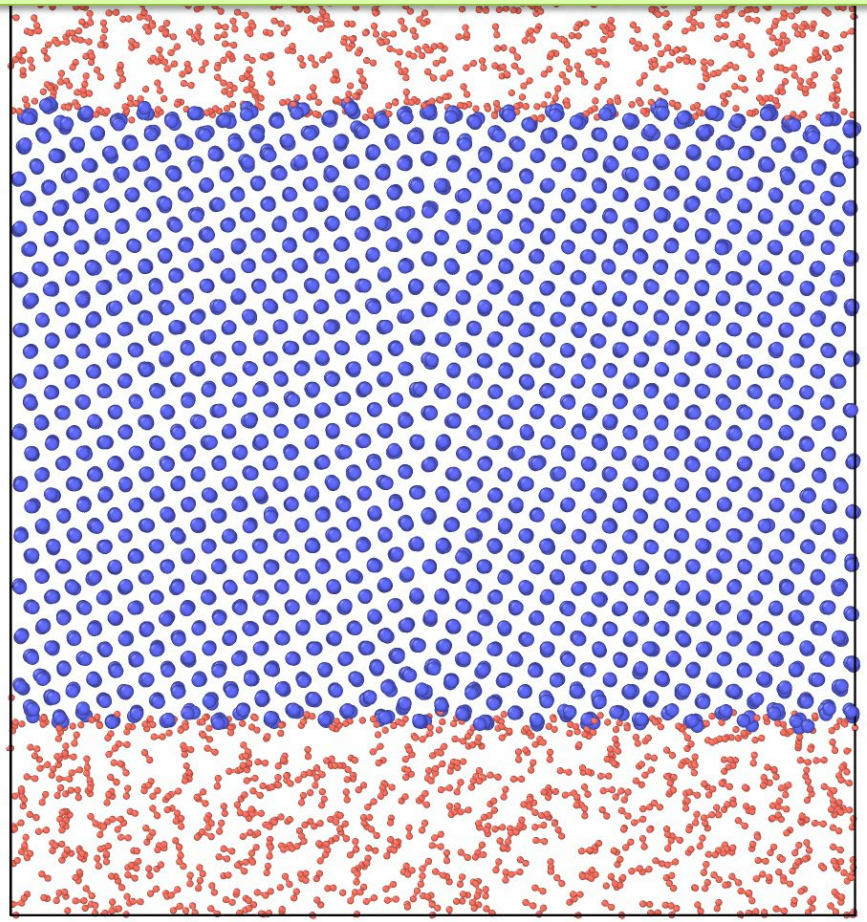

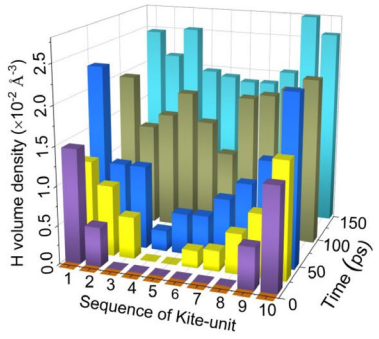

Fan-Shun Meng, et al., Phys. Rev. Materials, 5, 113606 (2021)

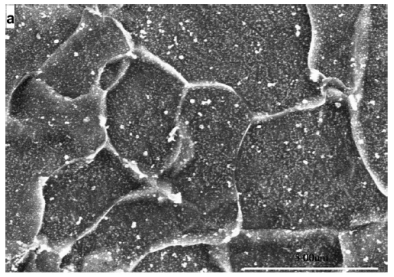

Hydrogen microprint technique micrograph of X60 grade steel.

M. A. Mohtadi-Bonab et al., Eng. Fail. Ana., 13 (2013) 163.

Kinetics –Hydrogen impacts on defect kinetics

水素は金属中の欠陥の運動を加速させるのか減速させるのか？

Vacancy traps hydrogen → H slows down the vacancy diffusion?

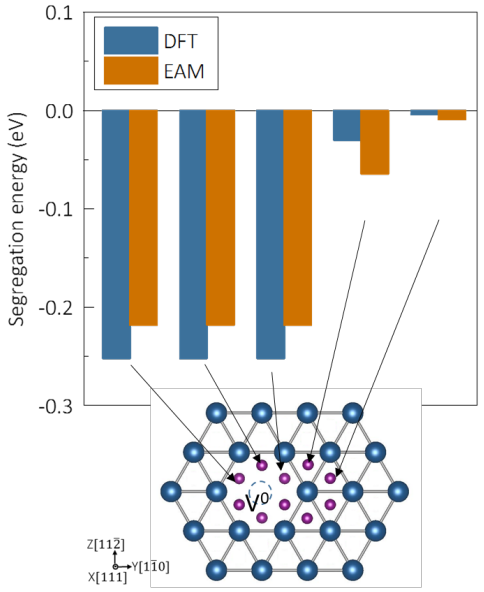

H stabilizes the vacancy by forming H-Vac. complex

vacancy diffusivity as a function of average H-concentration (c_H), at 600 K, in Ni

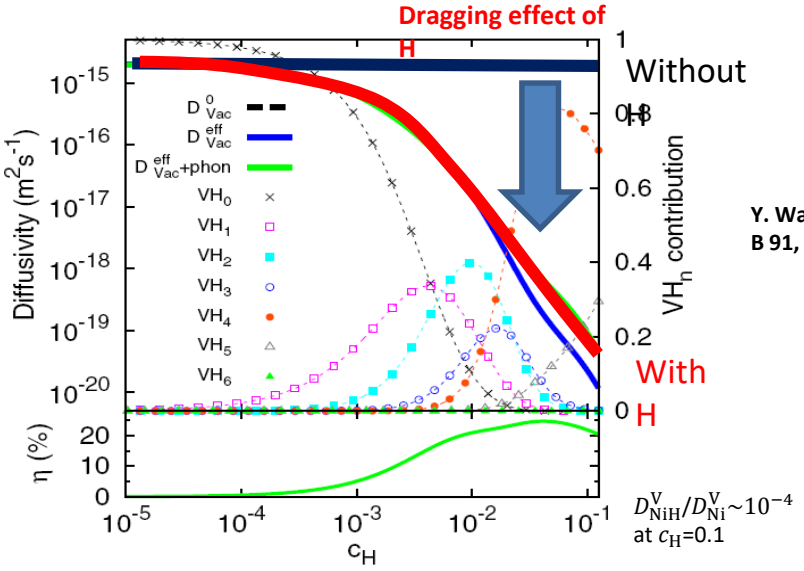

Y. Wang, et al., Phys. Rev. B 91, 1 (2015).

Activation energy barrier was computed only taking into account trapped H at initial (on-lattice) stable position of H-Vac. Complex.

Kinetics –Hydrogen impacts on defect kinetics
直接分子動力学計算が全く逆の結果を示す

Vacancy diffusion acceleration by Hydrogen
(MD at 870 K, 4000 atoms Cu-H system with one vac., EAM potential, NPT (p=0), MSD of vac.)

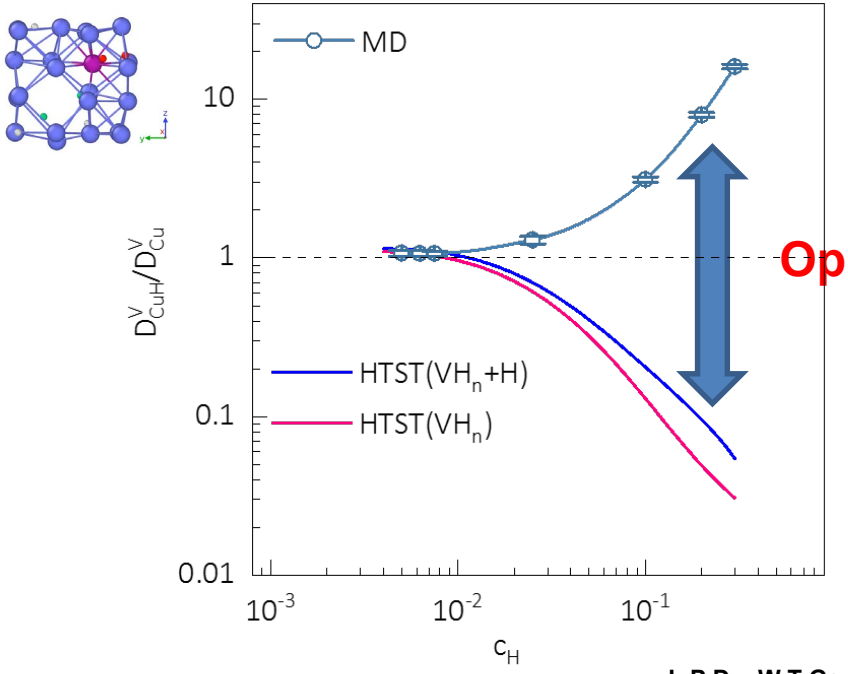

Opposite!!

Direct MD simulation shows totally opposite H effect on vacancy diffusion to previous prediction based on minimum energy path + TST

(※Same EAM potential is used)

J.-P.Du, W.T.Geng, K.Arakawa, J.Li and S.Ogata, J. Phys. Chem. Letters, 11 (2020) 7015.

Kinetics –Hydrogen impacts on defect kinetics
直接分子動力学計算が全く逆の結果を示す

Vacancy diffusion acceleration by Hydrogen
(MD at 870 K, 4000 atoms Cu-H system with one vac., EAM potential, NPT (p=0), MSD of vac.)

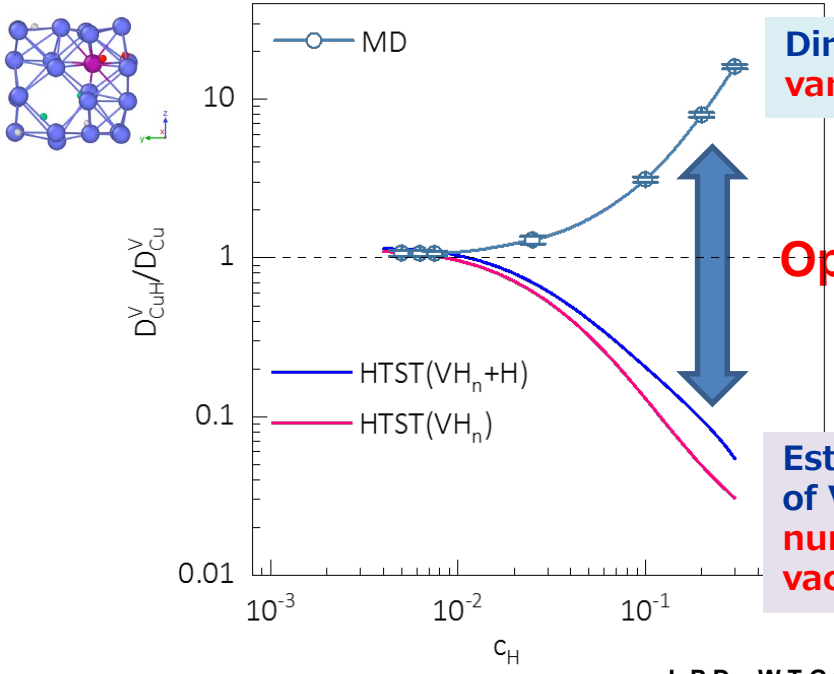

Direct MD estimation (Ensemble of various H configurations)

Opposite!!

Direct MD simulation shows totally opposite H effect on vacancy diffusion to previous prediction based on minimum energy path + TST

(※The same EAM potential is used)

Estimation by minimum energy path of V-H complex jump for fixed number of H atoms at the stable vacancy position (on-lattice)

J.-P.Du, W.T.Geng, K.Arakawa, J.Li and S.Ogata, J. Phys. Chem. Letters, 11 (2020) 7015.

Kinetics –Hydrogen impacts on defect kinetics

分子動力学解析結果の検証（他の手法による解析との比較）

Vacancy diffusion coefficient ratio btw w/wo Hydrogen at 870 K for Cu-H system

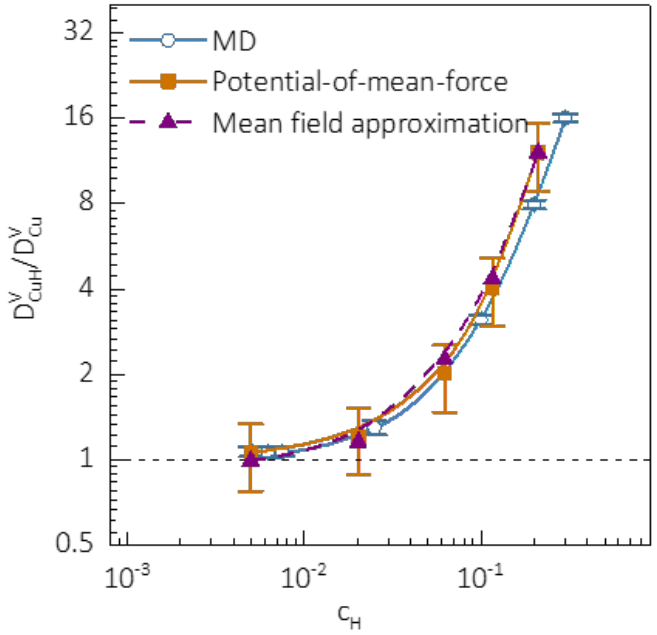

J.-P.Du, W.T.Geng, K.Arakawa, J.Li and S.Ogata, J. Phys. Chem. Letters, 11 (2020) 7015.

The acceleration trend is confirmed also by the other methods, which take ensemble average of various H configuration

Potential-of-mean-force method

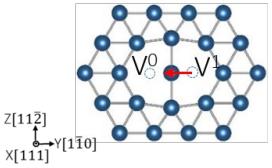

$$G^m = -\int_{initial}^{saddle} \vec{F}_M d\vec{r}_M$$

$$R = \upsilon_0 \exp\left(-\frac{G^m}{k_B T}\right) \qquad \frac{D^V_{MH}}{D^V_M} = \exp\left(-\frac{\Delta G^m}{k_B T}\right)$$

$$D^V = a_0^2 R \qquad \Delta G^m = G^m - G^m_0$$

with H - without H

GCMC+MD hybrid for sampling of H configurations

Mean-field-approximation:

Lattice gas model

$$\frac{D^V_{MH}}{D^V_M} = \exp\left(-\frac{\Delta G^m}{k_B T}\right) = \left(\frac{\Gamma^*_{sat}}{\Gamma^*_{sat} - \Gamma^*_H}\right)^{\Gamma^*_{sat}} \left(\frac{\Gamma^0_{sat} - \Gamma^0_H}{\Gamma^0_{sat}}\right)^{\Gamma^0_{sat}} \times \exp\left\{\frac{W}{k_B T}\left[\Gamma^*_{sat}\left(\frac{\Gamma^*_H}{\Gamma^*_{sat}}\right)^2 - \Gamma^0_{sat}\left(\frac{\Gamma^0_H}{\Gamma^0_{sat}}\right)^2\right]\right\}$$

Partial occupation of H at possible interstitial sites

Kinetics –Hydrogen impacts on defect kinetics
空孔拡散の鞍点における過剰水素吸着

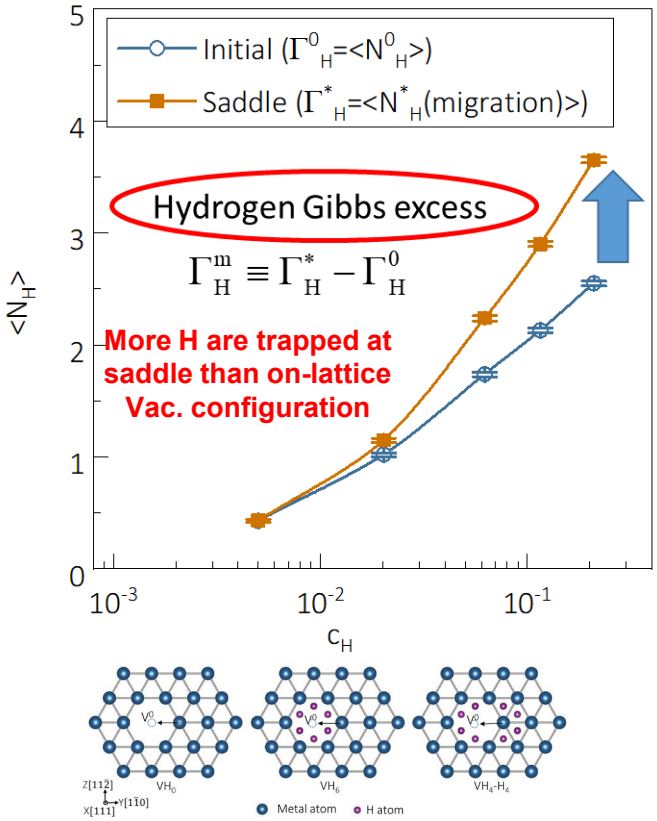

Gibbs adsorption isotherm
(a reduction of activation free energy by excess H)

$$\Delta G^m = -\int_{-\infty}^{\mu_H} \Gamma_H^m d\mu_H = -\int_{-\infty}^{\mu_H} \left(\Gamma_H^* - \Gamma_H^0\right) d\mu_H$$

10× increase in P_{H_2}

$$\mu_H = \frac{1}{2}\mu_{H_2} = \frac{1}{2}\left(\varepsilon_b + k_B T \ln \frac{P_{H_2}}{P_0}\right)$$

Gibbs adsorption isotherm:

$$\Delta G^m = -\int_{P_0}^{10P_0} \Gamma_H^m d\mu_H \qquad \Gamma_H^m \sim 1\mathrm{H}$$

$$= -k_B T \ln\sqrt{10}$$

$$\frac{D_{MH}^V}{D_M^V} = \exp\left(-\frac{\Delta G^m}{k_B T}\right) = 3.162$$

3× increase in vacancy diffusivity, regardless of T

J.-P.Du, W.T.Geng, K.Arakawa, J.Li and S.Ogata,
J. Phys. Chem. Letters, 11 (2020) 7015.

Kinetics –Hydrogen impacts on defect kinetics

Gibbs excess theory (まとめ)

Gibbs adsorption isotherm

(predicting reduction of activation free energy)

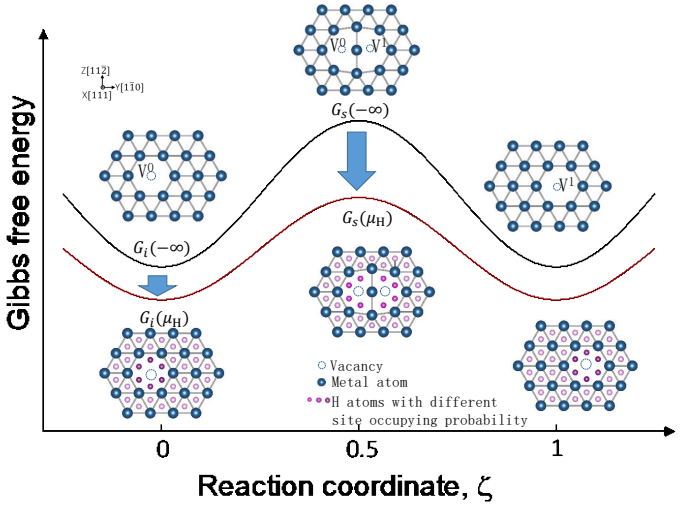

DFT Gibbs free energy analysis at 0K for Cu-Vac-H

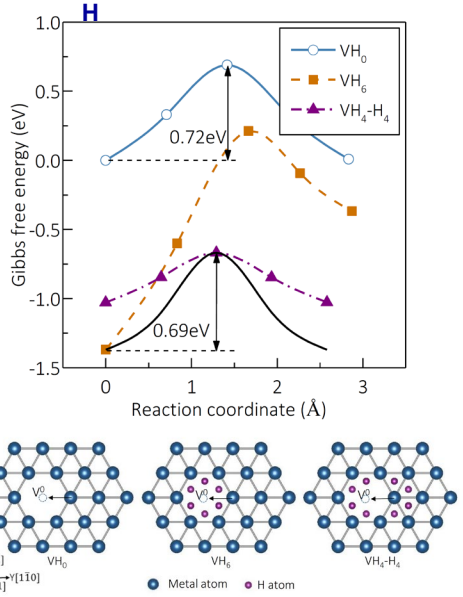

"Hydrogen lubrication effect" (if $\Delta G_s > \Delta G_i$)

J.-P.Du, W.T.Geng, K.Arakawa, J.Li and S.Ogata, J. Phys. Chem. Letters, 11 (2020) 7015.

Kinetics –Hydrogen impacts on defect kinetics
高圧水素ガス下での表面拡散 - Fe(001) 表面 (MD解析)

Acceleration of surface diffusion (Direct MD simulation using NNP)

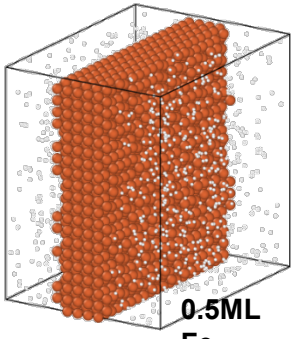

0.5ML Fe surface

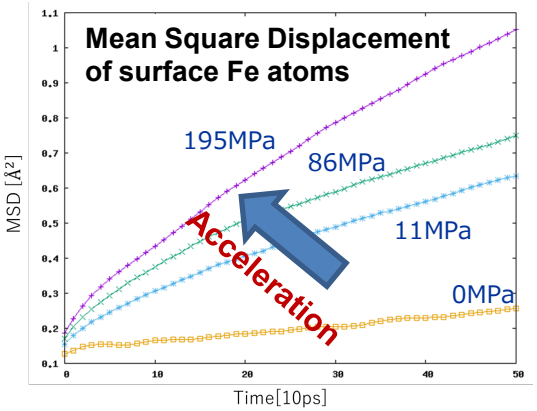

H_2 gas pressure: 11MPa

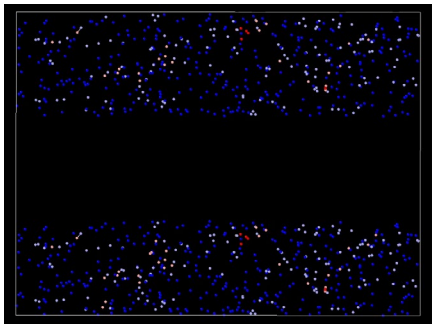

H_2 gas pressure: 195MPa

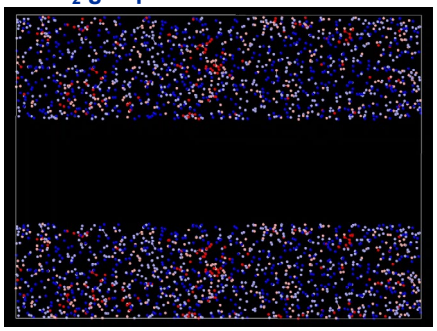

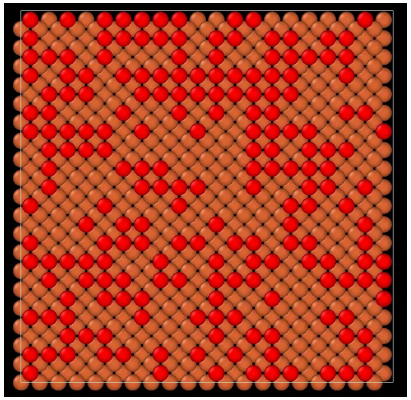

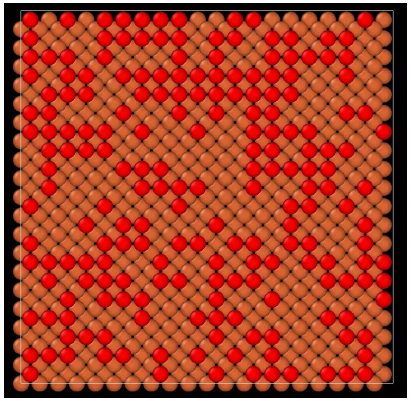

Experiment - acceleration of void migration by H (void surface diffusion)

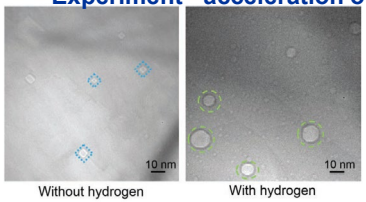

Fig. 1. Microstructure for cavities without hydrogen and those with hydrogen, after specimen heating to 773 K. Some of cavities without hydrogen are guided by polygon, and some of cavities with hydrogen are guided by circle, to emphasize the feature of their image shapes. (Online version in color.)

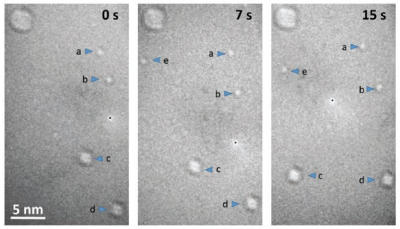

Fig. 2. Migration behavior of the cavities with hydrogen at 973 K. These sequential pictures were taken from an originally recorded movie after the sample-drift correction. The black dot around cavity b is a stain on the CMOS camera, which looks to move because of the drift correction. (Online version in color.)

K.Arakawa, SO, et al., ISIJ International 61 (2021) 2305.

Kinetics –Hydrogen impacts on defect kinetics
表面原子拡散の活性化自由エネルギーの計算

Activation free energy analysis

Potential of mean force method

$$G^m = -\int \vec{F}_M d\vec{r}_M$$

(010)

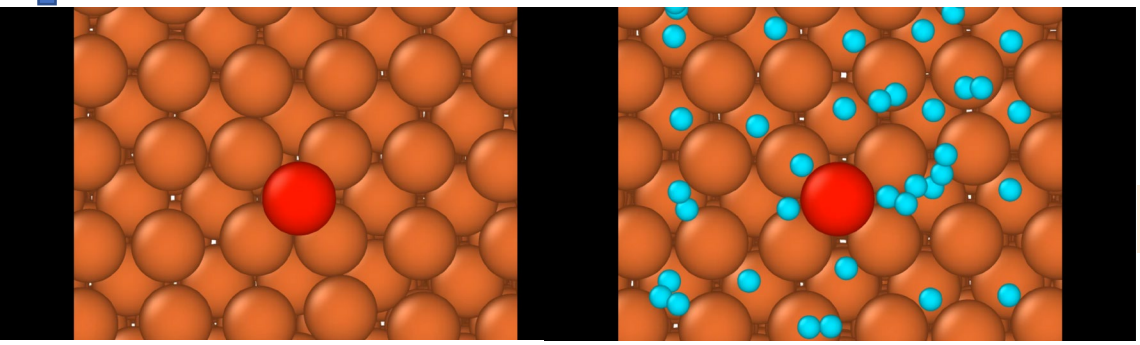

600K

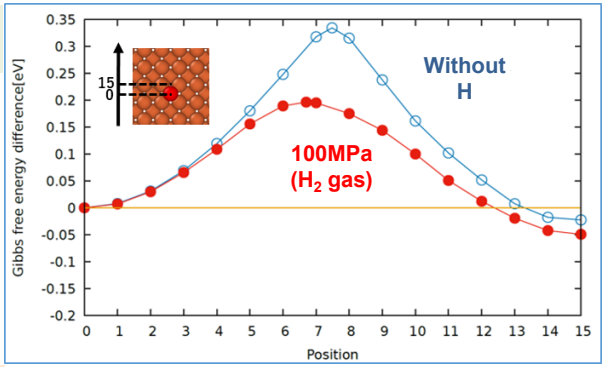

800K

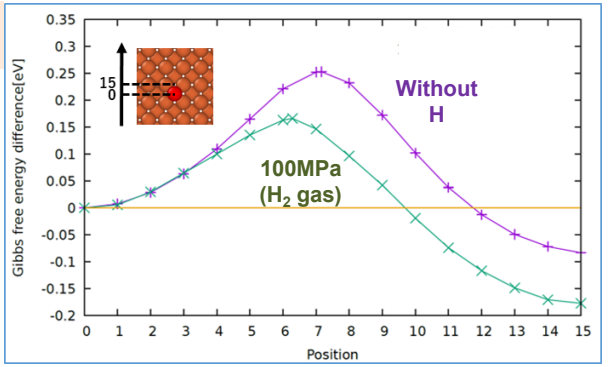

- H Gibbs excess and temperature (entropic) effects reduce the activation free energy

y

Kinetics –Hydrogen impacts on defect kinetics
らせん転位運動に対する水素の影響

γ-surface and activation energy for kink-pair nucleation are both reduced (Fe-H NNP)

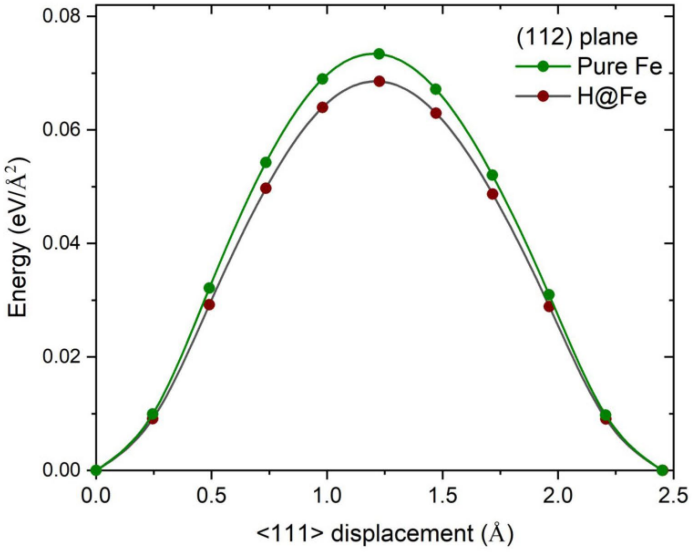

Hydrogen effect on γ-surface (112)
(H at T-site in the sliding layer)

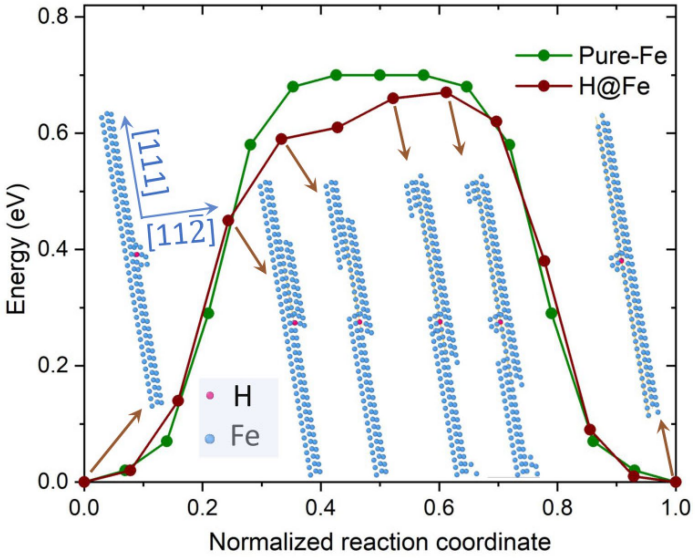

Hydrogen effect on kink-pair nucleation energetics

Fan-Shun Meng, et al., Phys. Rev. Materials, 5, 113606 (2021)

Kinetics –Hydrogen impacts on defect kinetics
らせん転位ー水素場連成運動の1次元モデル

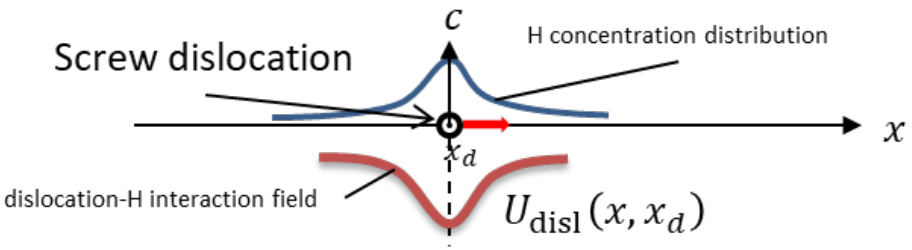

Solving diffusion and dislocation motion equations

Update hydrogen distribution

$$\frac{\partial c(x,t)}{\partial t} = \frac{\partial}{\partial x}\left(\frac{D(x)c(x,t)}{k_B T}\frac{\partial \mu_{\mathrm{H}}\left(x, x_{\mathrm{d}}(t)\right)}{\partial x}\right)$$

Calculate drag force caused by hydrogen

$$\tau_H = \frac{F_H}{b}, F_H = -\int_{-\infty}^{\infty} c(x)\frac{dU_{\mathrm{disl}}\left(x, x_{\mathrm{d}}(t)\right)}{dx}dx$$

Update dislocation position and chemical potential

$$\frac{dx_{\mathrm{d}}}{dt} = v_{\mathrm{d}}(\tau_{\mathrm{ext}} - \tau_{\mathrm{H}})$$

$$\mu_{\mathrm{H}}\left(x, x_{\mathrm{d}}(t)\right) = k_B T \ln\frac{\tilde{c}(x)}{1-\tilde{c}(x)} + 2W\tilde{c}(x) + U_{\mathrm{disl}}\left(x, x_{\mathrm{d}}(t)\right)$$

Kinetics –Hydrogen impacts on defect kinetics
らせん転位ー水素場連成運動の1次元モデル

To be submitted.

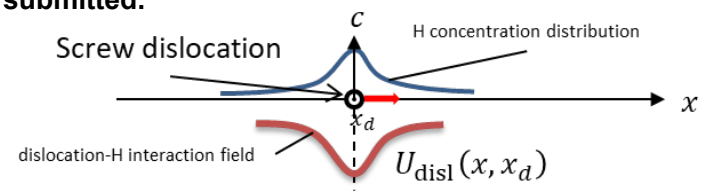

Update hydrogen distribution

$$\frac{\partial c(x,t)}{\partial t} = \frac{\partial}{\partial x}\left(\frac{D(x)c(x,t)}{k_B T}\frac{\partial \mu_{\mathrm{H}}(x, x_{\mathrm{d}}(t))}{\partial x}\right)$$

Calculate drag force caused by hydrogen

$$\tau_H = \frac{F_H}{b}, F_H = -\int_{-\infty}^{\infty} c(x)\frac{dU_{\mathrm{disl}}(x, x_{\mathrm{d}}(t))}{dx}dx$$

Update dislocation position and chemical potential

$$\frac{dx_{\mathrm{d}}}{dt} = v_{\mathrm{d}}(\tau_{\mathrm{ext}} - \tau_{\mathrm{H}})$$

$$\mu_{\mathrm{H}}(x, x_{\mathrm{d}}(t)) = k_B T \ln\frac{\tilde{c}(x)}{1-\tilde{c}(x)} + 2W\tilde{c}(x) + U_{\mathrm{disl}}(x, x_{\mathrm{d}}(t))$$

☐ Diffusion equation of hydrogen under dislocation – hydrogen interaction field

$$\frac{\partial c}{\partial t} = \frac{\partial}{\partial x}\left(\frac{Dc(x,t)}{k_B T}\frac{\partial \mu_{\mathrm{H}}(x, x_{\mathrm{d}}(t))}{\partial x}\right)$$

$$D(x) = D_0 \exp\left(-\frac{\Delta E_H(x)}{k_B T}\right)$$

$$U_{\mathrm{disl}}(x, x_{\mathrm{d}}(t)) = U_0 \exp\left(-\frac{(x - x_{\mathrm{d}}(t))^2}{2\sigma^2}\right)$$

c : Number density of hydrogen (H) atom
$c_0 = 12/a^3$: Number density of possible site (T-site)
$\tilde{c} = c/c_0$: Normalized number density (i.e. Occupation probability of T-site
μ_{H} : Chemical potential of H atom
D_0 : Prefactor
ΔE_{H} : Diffusion barrier of H atom
W : Interaction energy between H atoms
U_{disl} : Interaction potential energy field between H atom and screw dislocation
U_0 : Interaction potential energy at which H atom is in dislocation core
x_{d} : Dislocation position

Kinetics –Hydrogen impacts on defect kinetics
らせん転位ー水素場連成運動の1次元モデル

To be submitted.

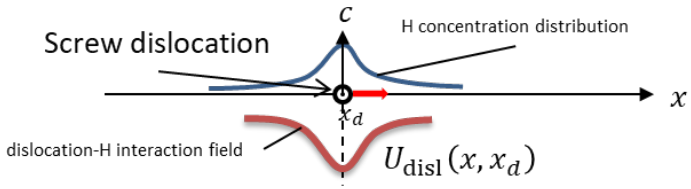

Update hydrogen distribution

$$\frac{\partial c(x,t)}{\partial t} = \frac{\partial}{\partial x}\left(\frac{D(x)c(x,t)}{k_B T}\frac{\partial \mu_{\mathrm{H}}(x, x_{\mathrm{d}}(t))}{\partial x}\right)$$

Calculate drag force caused by hydrogen

$$\tau_H = \frac{F_H}{b}, F_H = -\int_{-\infty}^{\infty} c(x)\frac{dU_{\mathrm{disl}}(x, x_{\mathrm{d}}(t))}{dx}dx$$

Update dislocation position and chemical potential

$$\frac{dx_{\mathrm{d}}}{dt} = v_{\mathrm{d}}(\tau_{\mathrm{ext}} - \tau_{\mathrm{H}})$$

$$\mu_{\mathrm{H}}(x, x_{\mathrm{d}}(t)) = k_B T \ln\frac{\tilde{c}(x)}{1-\tilde{c}(x)} + 2W\tilde{c}(x) + U_{\mathrm{disl}}(x, x_{\mathrm{d}}(t))$$

☐ BCC screw dislocation mobility by kink-pair nucleation mechanism under external stresses

$$\frac{dx_{\mathrm{d}}}{dt} = v_{\mathrm{d}}(\tau_{\mathrm{ext}} - \tau_{\mathrm{H}})$$

Dislocation velocity in BCC metal with H

Activation energy reduction by H

$$v_{\mathrm{d}} = \begin{cases} \dfrac{(\tau_{\mathrm{ext}} - \tau_H)b}{B} v_{\mathrm{kn}}(\tau) & \Delta G_{\mathrm{kn}} + \Delta G_{\mathrm{H}} > 0 \\ \dfrac{(\tau_{\mathrm{ext}} - \tau_{\mathrm{H}})b}{B} & \Delta G_{\mathrm{kn}} + \Delta G_{\mathrm{H}} \le 0 \end{cases}$$

$$B = \begin{cases} \dfrac{a\left[2a v_{\mathrm{kn}}^{-1}(\tau) + L\right]}{2hL} B_k & \Delta G > 0 \\ B_0 + B_1 T & \Delta G \le 0 \end{cases}$$

$$v_{\mathrm{kn}}(\tau) = \left(1 - \frac{c}{2}\right)\exp\left(-\frac{\Delta G_{\mathrm{kn}}}{2k_B T}\right) + \frac{c}{2}\exp\left(-\frac{\Delta G_{\mathrm{kn}} + (1 - c_L w)\Delta G_H}{2k_B T}\right)$$

$$\Delta G_{\mathrm{kn}}(\tau) = \Delta G_{\mathrm{kn}}^0\left[1 - \left|\frac{\tau}{\tau_{\mathrm{kn}}}\right|^p\right]^q \qquad \Delta G_{\mathrm{H}}(\tau) = \Delta G_{\mathrm{H}}^0\left[1 - \left|\frac{\tau}{\tau_{\mathrm{kn}}}\right|^p\right]^q$$

$$\tau_H = \frac{F_H}{b} \qquad F_H = -\int_{-\infty}^{\infty} c(x)\frac{dU_{\mathrm{disl}}}{dx}dx$$

Original formulation for pure metal: G. Po, et al., *Acta Mater*, 119 (2016), 123-135.

v_{d} : Dislocation velocity
τ_{ext} : External shear stress
a : Lattice constant
$b(=\sqrt{3}a/2)$: Burgers vector
$h(=\sqrt{2/3}a)$: Lattice spacing along glide direction
L: Dislocation length
ΔG_{kn}: Activation barrier of dislocation glide in pure Fe
ΔG_{kn}^0 : ΔG_{kn} without external shear stress
ΔG_{H}: Activation barrier change by one H atom

ΔG_{H}^0: ΔG_{H} without external shear stress
τ_{kn} : Critical shear stress at which $\Delta G_{\mathrm{kn}} = 0$ (i.e. Peierls stress)
p, q : Parameters for stress dependency of activation barrier
c_L : Number density of H atom per unit dislocation length at dislocation core
τ_{H} : Drag stress caused by H atom
F_{H} : Drag force cause d by H atom
B_0, B_1, B_k : Parameters for phonon drag of dislocation
w: kink-pair width

Kinetics –Hydrogen impacts on defect kinetics
らせん転位ー水素場連成運動の1次元モデルによる解析結果

Dislocation and Hydrogen coupled and de-coupled motion under external shear stress (300K, 5.3 mppm B.C.)

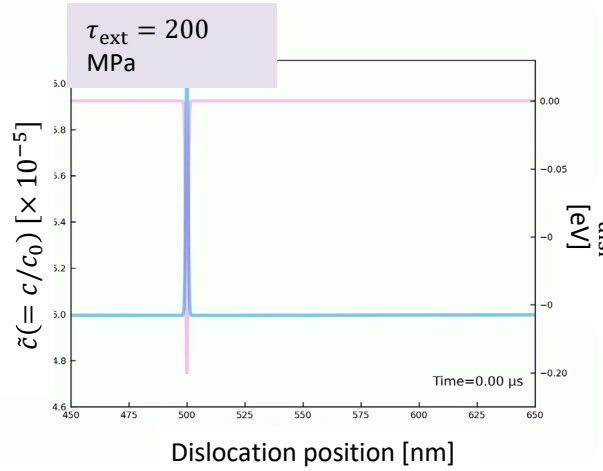

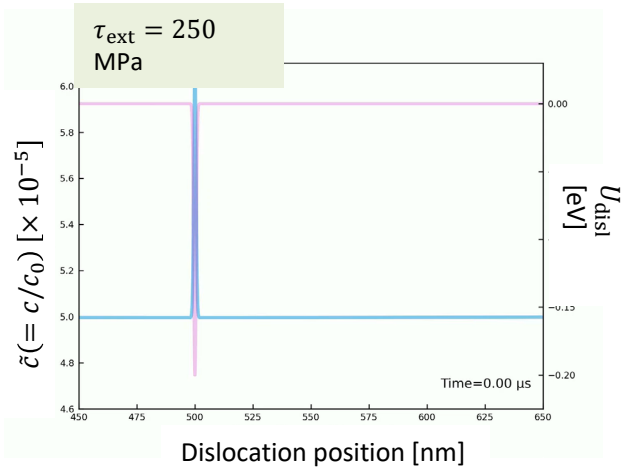

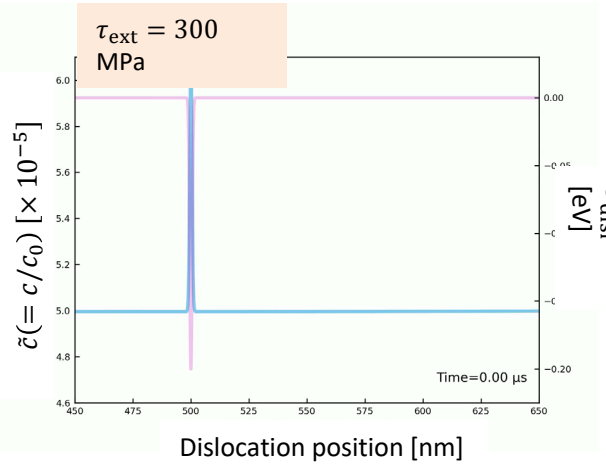

U_{disl} **Dislocation**

$\tilde{c}$ **Dislocation**

Critical stress for H detrapping at 300K τ_c: 250~300 MPa

Kinetics –Hydrogen impacts on defect kinetics
らせん転位ー水素場連成運動の1次元モデルから得られた転位運動加速率

Temperature – Stress – H-concentration dependent acceleration

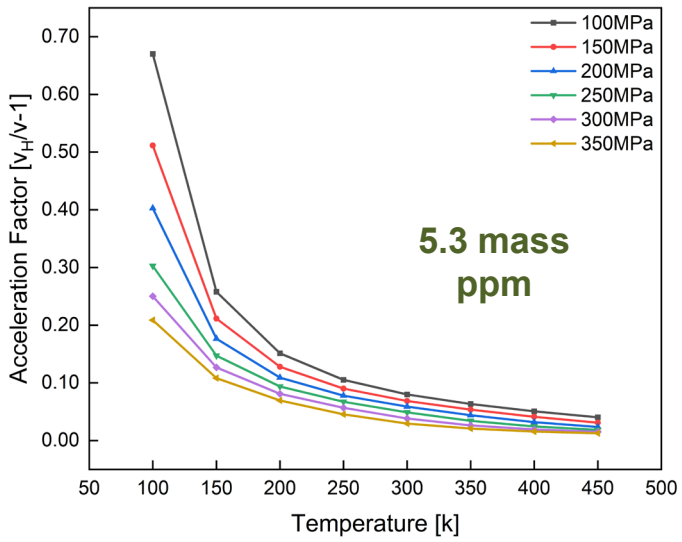

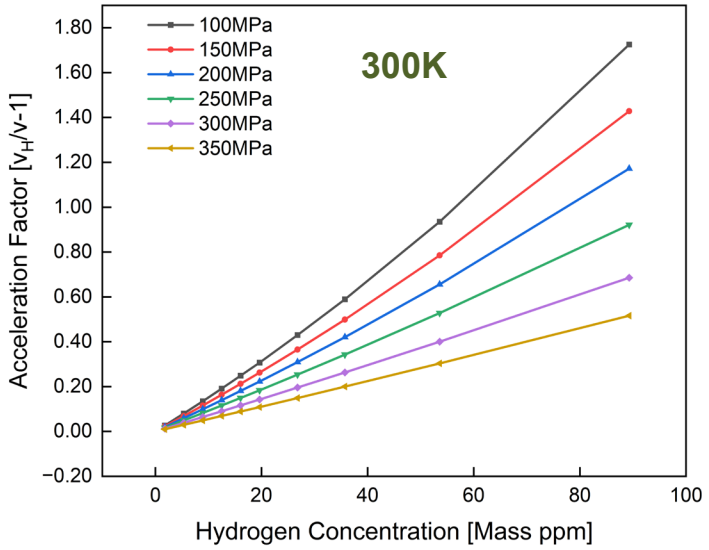

“Hydrogen lubrication effect”

水素環境下における破壊シミュレーション (Σ9粒界モデル) (MD+水素GCMC解析)

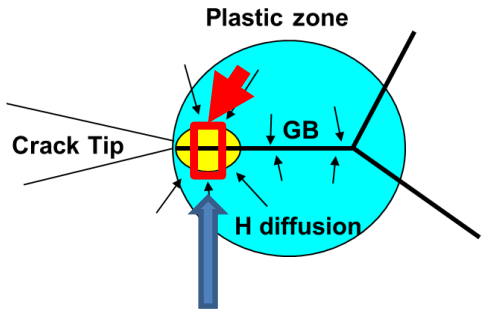

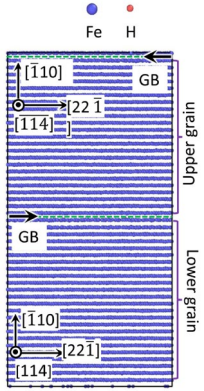

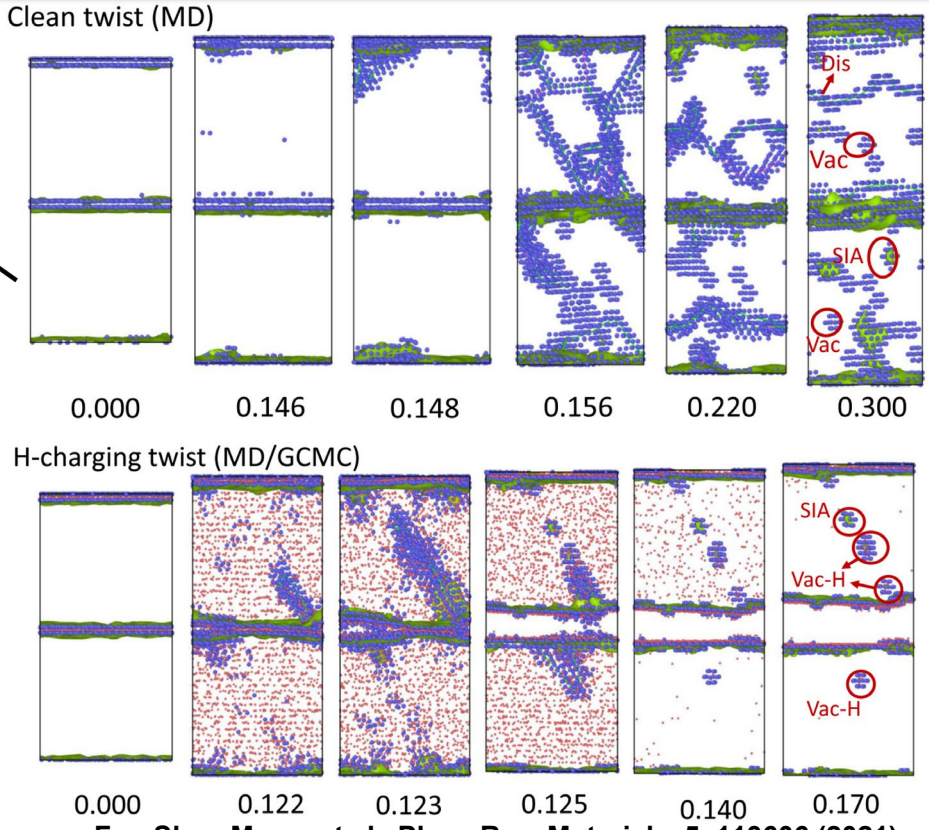

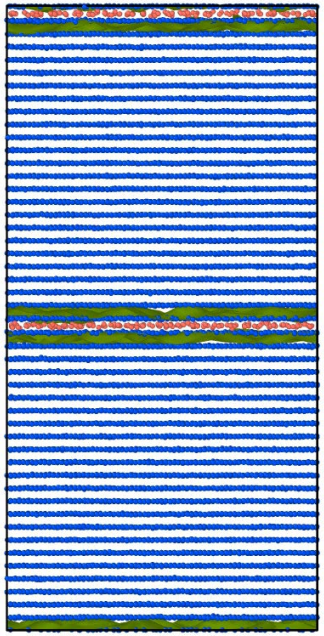

Fan-Shun Meng, et al., Phys. Rev. Materials, 5, 113606 (2021)

Kinetics –Hydrogen impacts on defect kinetics
水素環境下におけるらせん転位の運動の直接分子動力学解析（欠陥生成）

Pure Fe

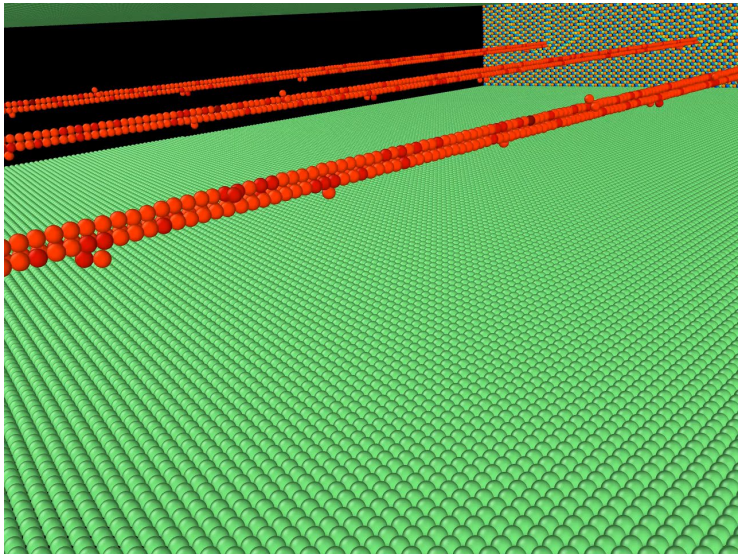

Fe-H

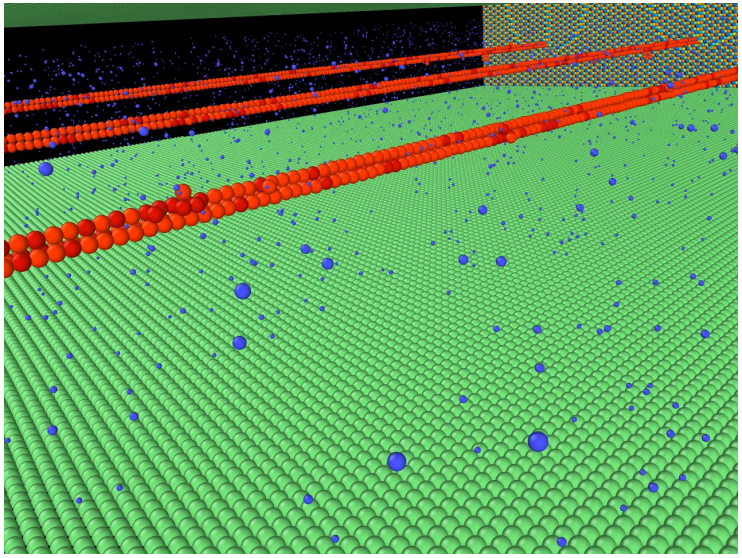

Axis	Orientation	Dimension(Å)
x	$[121]$	111.28
y	$[\bar{1}01]$	80.25(62.13)
z	$[1\bar{1}1]$	647.95(598.61)

- Numbers in parentheses are the model size without vacuum slabs in y and z directions
- Number of atoms: 374784 Fe
- H concentration: ~ 7200 appm
- Temperature: 300K
- Timestep: 0.5 fs
- Strain rate(γ): 4×10^{8} s^{-1}
- The atoms in movies are colored by their ***y*** coordinate to indicate the cross gliding.

Kinetics –Hydrogen impacts on defect kinetics
転位と水素点欠陥複合体との相互作用

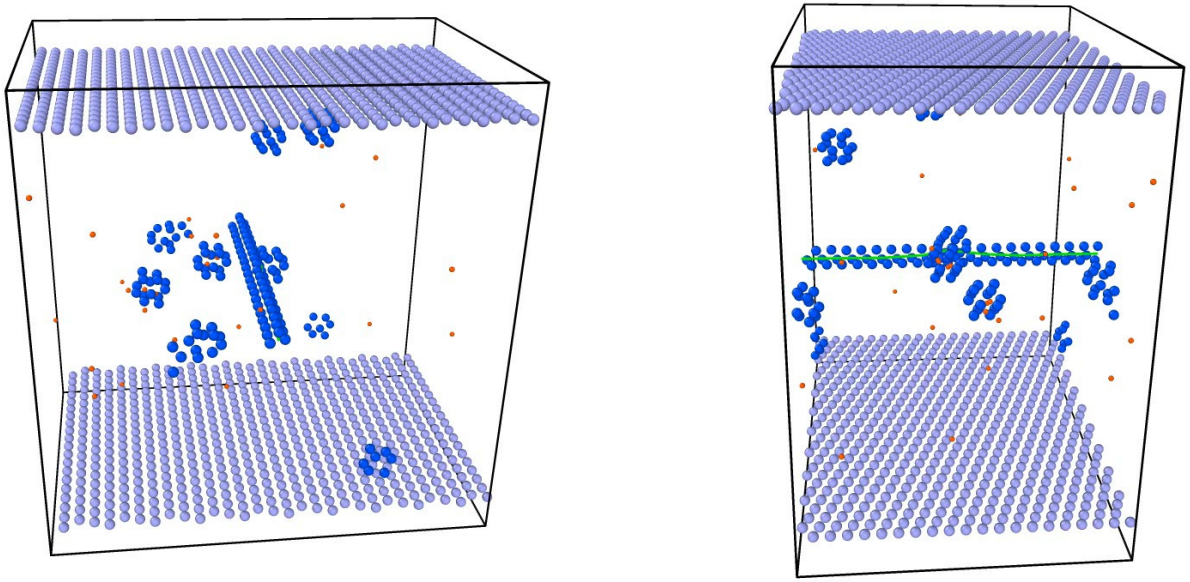

- Hydrogen stabilizes vacancy → more H-vacancy complex exists
- H-vacancy complex and H induce local cross-slip of screw → more vacancies generated
- Dislocation collects vacancies and form large defect (defect precipitation)

内容

- **イントロダクション**　原子論からの材料力学特性のモデリングと材料設計　～マルチスケールの観点から
- **ナノ力学**　原子論からのナノ材料力学の特異性の検討
- **原子論における時間スケール拡張への挑戦**　原子解像度で長時間現象を予測する
- **原子論によるマルチフィジクスへの挑戦**　水素や酸素などの力学特性への影響　～力学・化学・物理
- **材料設計への展開**　強度と延性、靭性を両立した材料設計

強度-延性両立、高靭性化に向けた戦略
- 変形素過程のバトンタッチ -

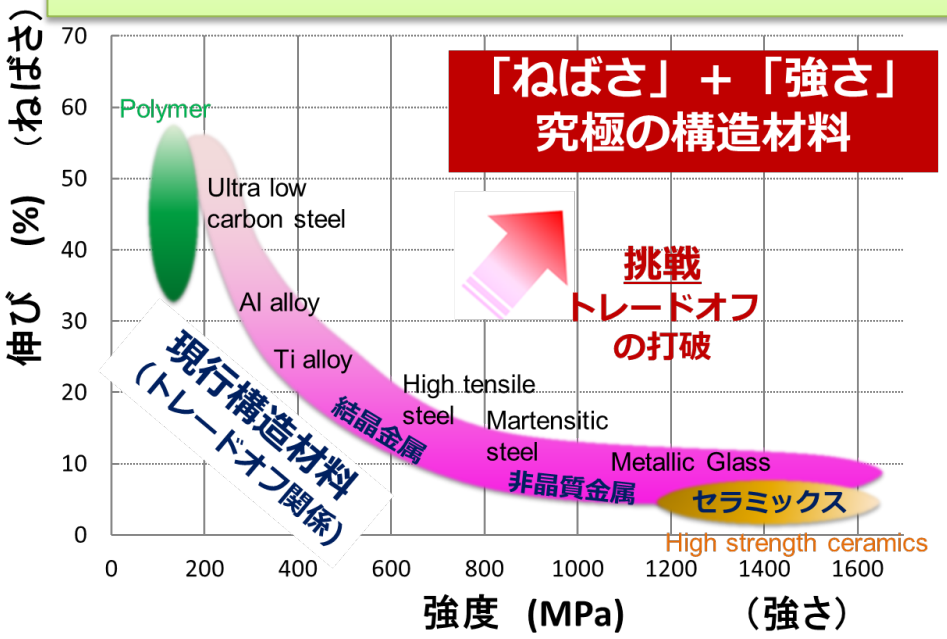

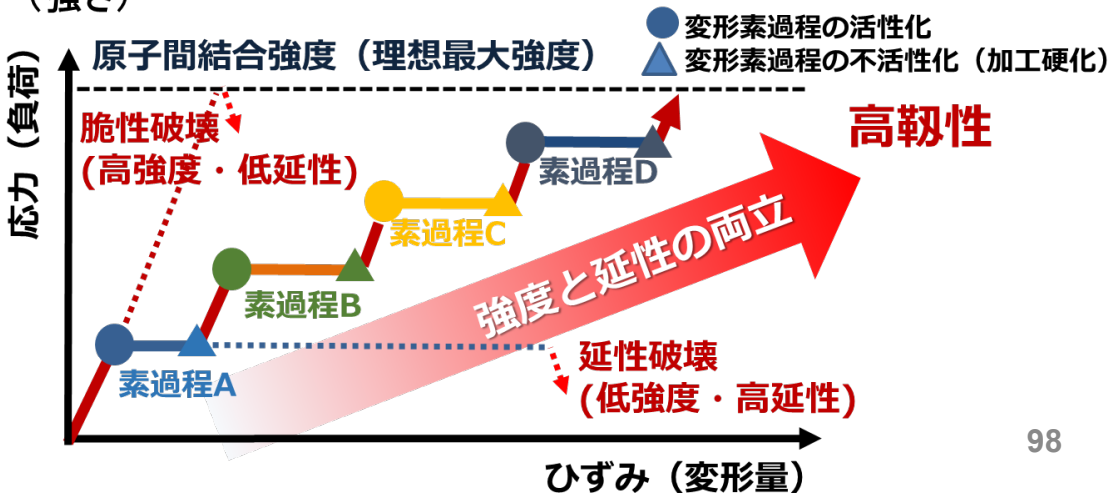

バトンタッチによる強度と延性の両立の例①
- 超微細粒結晶 -

超微細粒純チタン結晶

プラストンの活性化タイミング解析（メカノケミカル反応解析） → 欠陥励起マップ構築（どのプラストンがどの条件下で励起するかのマップ） → 粒径１ミクロンで３種の変形メカニズムのバトンタッチを予測 → 「ねばさ」と「強さ」が共に向上

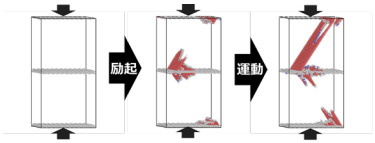

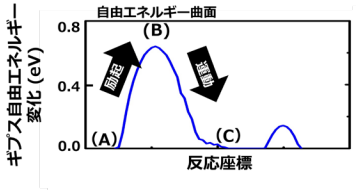

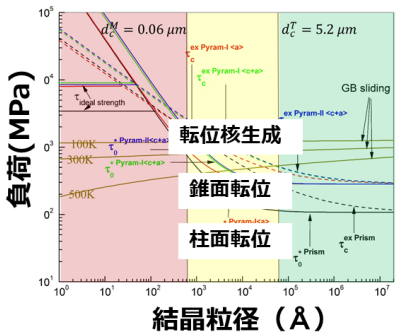

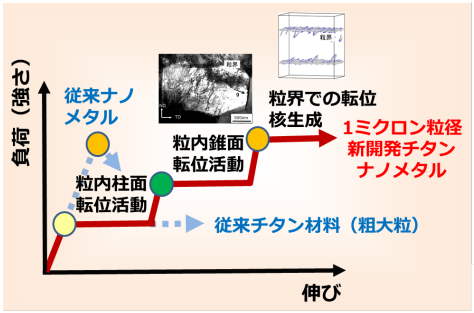

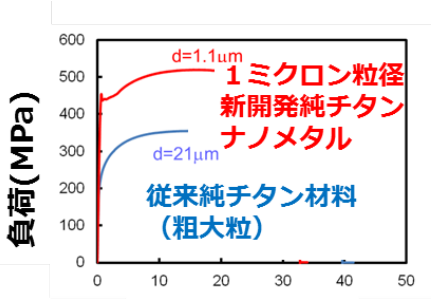

（辻ら）

- 結晶粒径をちょうど１ミクロンに組織制御することで３つの塑性変形過程のバトンタッチを実現し「強度」と「延性」を両立

粒径制御でチタン結晶の持つ潜在能力を極限まで引き出す

バトンタッチによる強度と延性の両立の例②
- ナノ欠陥バブル導入材料 -

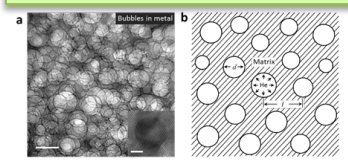

Radiation damage (Cu) (200keV He ion implantation forms 5nm He bubbles)

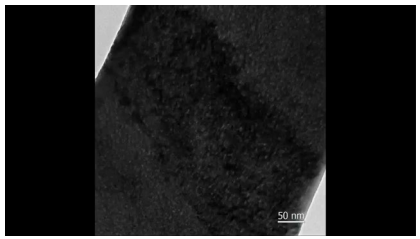

bubble

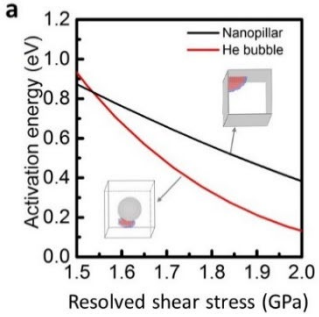

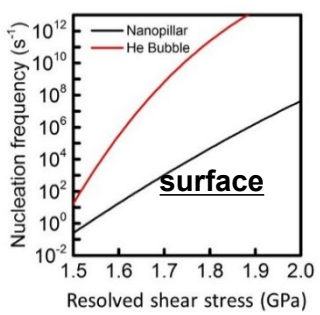

Step (new source)

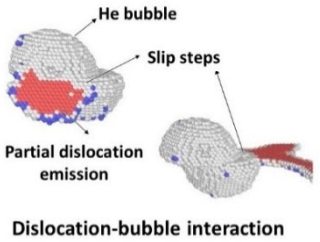

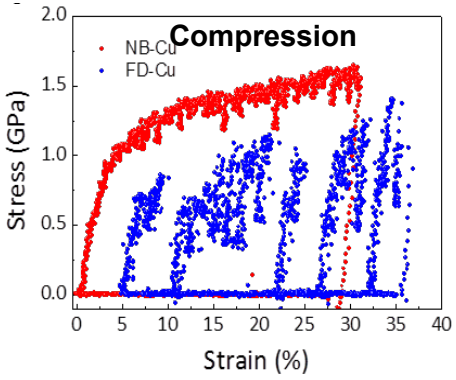

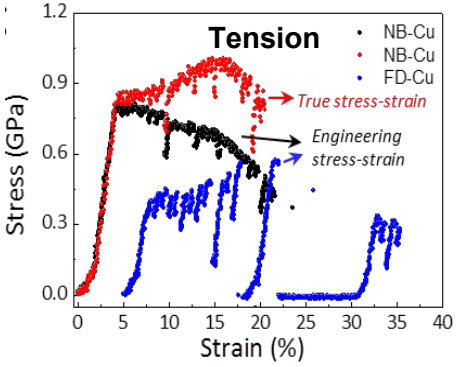

バブル表面から転位発生→バブル転位相互作用→バブル表面に新転位源→転位増殖

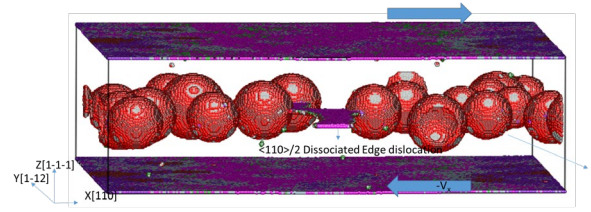

Model size: 67nm× 62nm × 20nm; about 7,000,000 atoms; containing 20 randomly distributed bubbles with average spacing of 15.6 nm.

cutting

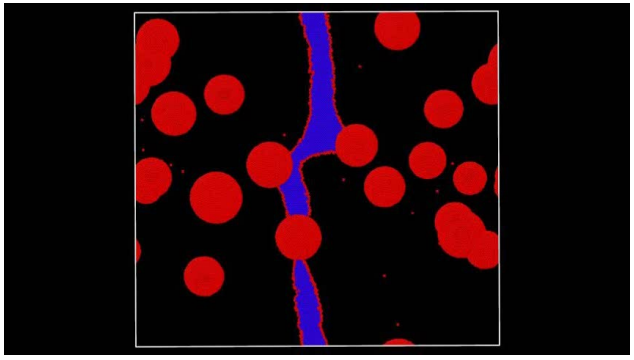

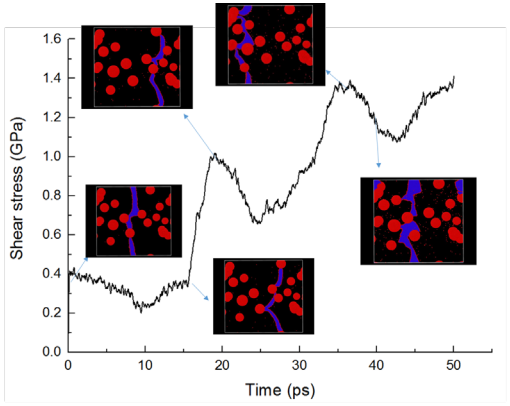

Time evolution of the shear stress and the corresponding dislocation-bubble configurations.

Ming-Shuai Ding, Jun-Ping Du, Liang Wan, Shigenobu Ogata, et al., *Nano Letters* (2016)

バトンタッチによる強度と延性の両立の例③
- ナノCNT複合金属材料 -

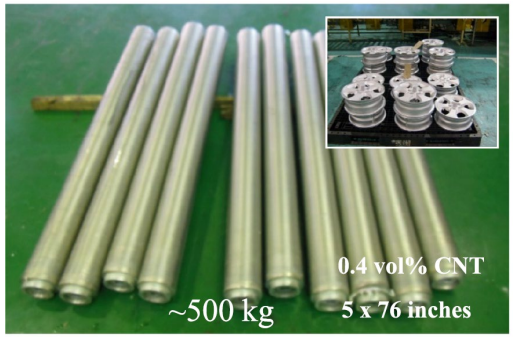

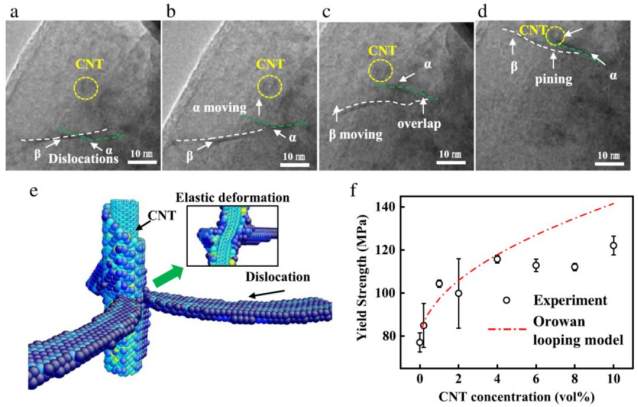

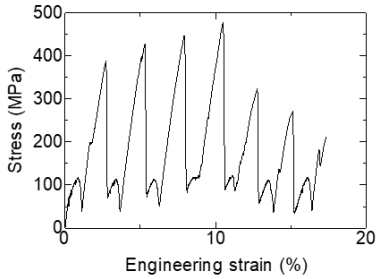

Kang Pyo So, Xiaohui Liu, Hideki Mori, Akihiro Kushima, Jong Gil Park, Hyoung Seop Kim, Shigenobu Ogata, Young Hee Lee, Ju Li, ***Extreme Mechanics Letters*** **(2016) 245**

Dislocation cannot cut CNT and leaves a loop surrounding CNT

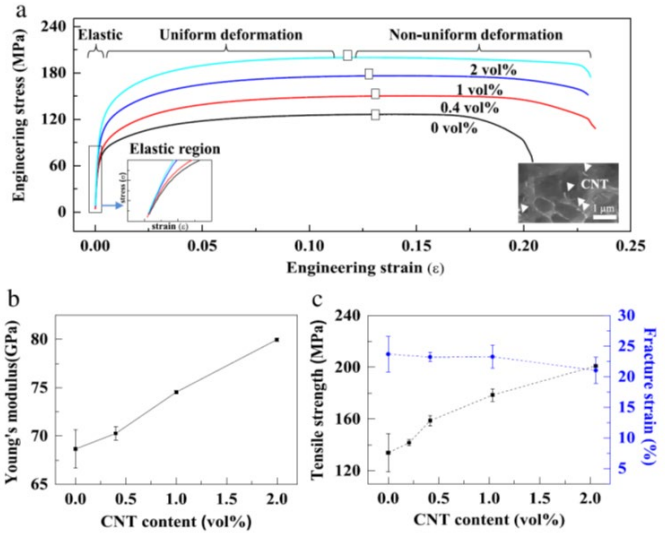

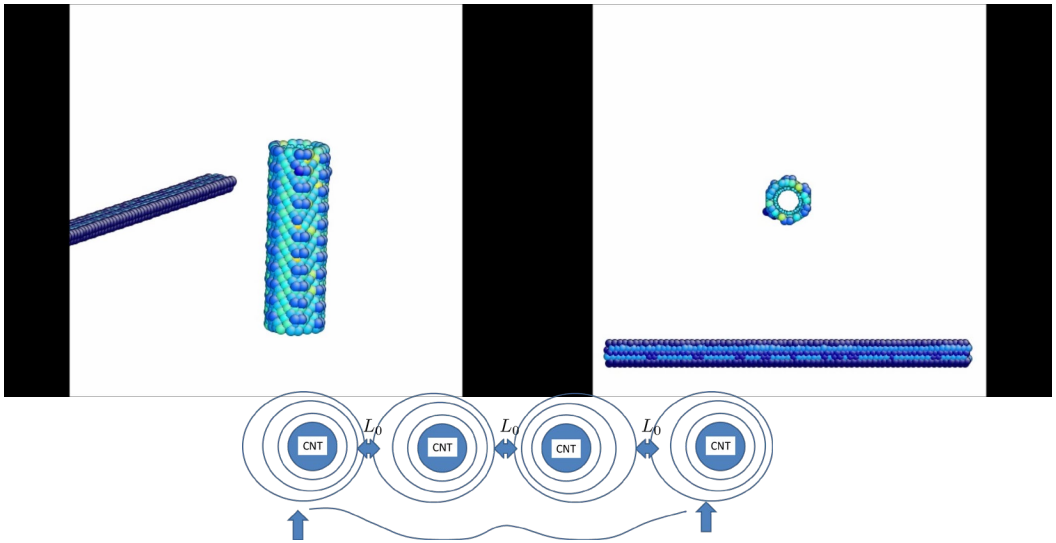

まとめ

- 計算機能力の飛躍的な向上と空間・時間マルチスケール解析手法の発達、特に時間スケールの克服が、これまで不可能であった**原子論からの様々なマクロ力学特性（強度、延性、耐疲労性、耐環境性）の予測や設計**を次第に可能にしつつある。計算科学的アプローチは機械学習との親和性も高く、**AI力学特性設計**への展開が強く期待される。

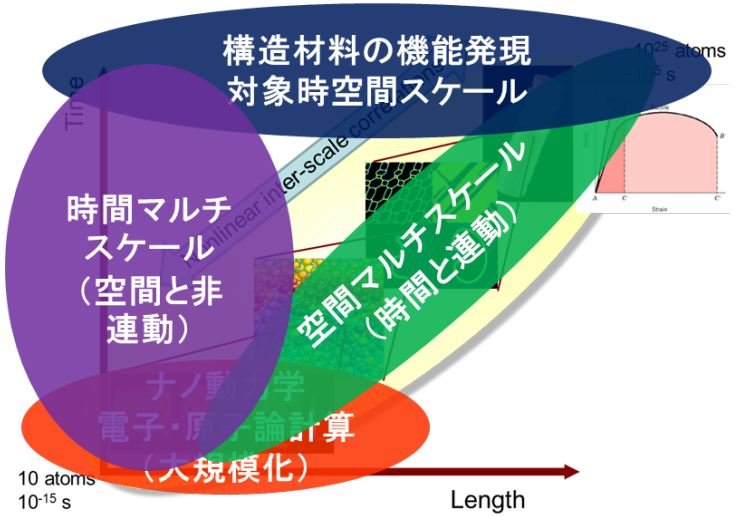

- **イントロダクション**　原子論からの材料力学特性のモデリングと材料設計　～マルチスケールの観点から
- **ナノ力学**　原子論からのナノ材料力学の特異性の検討
- **原子論における時間スケール拡張への挑戦**　原子解像度で長時間現象を予測する
- **原子論によるマルチフィジクスへの挑戦**　水素や酸素などの力学特性への影響　～力学・化学・物理
- **材料設計への展開**　強度と延性、靭性を両立した材料設計